T. L. Harpster
VP-Bell Bend Project-Development:

PPL Bell Bend, LLC
38 Bomboy Lane, Suite 2
Berwick, PA 18603
Tel. 570.802.8111 FAX 570.802.8119
tlharpster@pplweb.com

February 12, 2009

U.S. Nuclear Regulatory Commission
ATTN: Document Control Desk
Washington, DC 20555-0001

ATTN: Michael R. Johnson, Director
Office of New Reactors

BELL BEND NUCLEAR POWER PLANT
SUPPLEMENTAL INFORMATION FOR THE
BELL BEND COLA – FSAR SECTION 2.5.2
BNP-2009-001 Docket No. 52-039

References:

1) BNP-2008-002, T. L. Harpster (PPL Bell Bend, LLC) to U. S. Nuclear Regulatory Commission, "Application for Combined License for the Bell Bend Nuclear Power Plant," dated October 10, 2008

2) BNP-2008-006, T. L. Harpster (PPL Bell Bend, LLC) to U. S. Nuclear Regulatory Commission, "Supplemental Information for the Bell Bend COLA-FSAR Section 2.5," dated November 24, 2008

3) Letter, M. A. Canova (USNRC) to T. L. Harpster (PPL Bell Bend, LLC), "Combined License Application Acceptance Review for Bell Bend Nuclear Power Plant," dated December 19, 2008

PPL Bell Bend, LLC (PPL) submitted an application for a combined license for the Bell Bend Nuclear Power Plant (BBNPP) on October 10, 2008 (Reference 1). Supplemental information required for the staff to complete their acceptance and docketing review of Final Safety Analysis Report (FSAR) Subsections 2.5.1, 2.5.2 and 2.5.3 was submitted to the NRC staff on November 24, 2008 (Reference 2). The NRC subsequently accepted and docketed the COLA for the BBNPP on December 19, 2008 (Reference 3). In its acceptance and docketing letter, the staff requested additional information regarding the Plant Seismic Hazards Analysis (PSHA) conclusions in FSAR Subsection 2.5.2.

The attachment to this letter provides the additional information requested by the staff in the form of a complete replacement of FSAR Subsection 2.5.2, with revisions indicated. This supplement will be incorporated into a future revision of the Bell Bend COLA. Should the staff have any questions or require additional information, please contact Mr. Rocky Sgarro, Manager-Nuclear Regulatory Affairs at 570.802.8102.

I declare under penalty of perjury that the foregoing is true and correct.

Executed on February 12, 2009.

Respectfully,

Terry L. Harpster

D079
4053

Attachment 1: Bell Bend Nuclear Power Plant Supplemental Information for FSAR Section 2.5.2

NRO

cc: (w/ attachment)

Mr. Samuel J. Collins
Regional Administrator
U.S. Nuclear Regulatory Commission
Region I
475 Allendale Road
King of Prussia, PA 19406-1415

bcc: M. Caverly
T. Harpster
G. Kuczynski
V. Lopiano
R. Sgarro
J. Freels
G. Gibson
M. Yox
G. Wrobel

Attachment 1

Bell Bend Nuclear Power Plant Supplemental Information for FSAR Section 2.5.2

2.5.2 Vibratory Ground Motion.

The U.S. EPR FSAR includes the following COL Item for Section 2.5.2:

> A COL applicant that references the U.S. EPR design certification will review and investigate site-specific details of the seismic, geophysical, geological, and geotechnical information to determine the safe shutdown earthquake (SSE) ground motion for the site and compare site-specific ground motion to the Certified Seismic Design Response Spectra (CSDRS) for the U.S. EPR.

This COL Item is addressed as follows:

This section provides a detailed description of the vibratory ground motion assessment that was carried out for the {BBNPP} site, resulting in the development of the {BBNPP} site Safe Shutdown Earthquake (SSE) ground motion response spectra. {Starting points for this site assessment are the United States Geological Service (USGS) documentation of the studies for the 2002 and 2008 National Seismic Hazard maps (USGS, 2002)(USGS, 2008), the EPRI-SOG probabilistic seismic hazard analysis (PSHA) methodology outlined in EPRI NP-4726-A 1988 (EPRI, 1988), and the Early Site Permit (ESP) Application for the Clinton Nuclear Power Plant site (EGC, 2006) submitted to the NRC on April 14, 2006 by Exelon Generation Company (EGC). The following is a review of the approaches outlined in NRC Regulatory Guides 1.165 and 1.208 for conducting the vibratory ground motion studies used for the BBNPP site.

Nuclear Regulatory Commission (NRC) Regulatory Guide 1.208, "A Performance-Based Approach to Define Site-Specific Earthquake Ground Motion," March, 2007, (NRC, 2007a) states in Section B, Discussion:

> "The CEUS is considered to be that part of the United States east of the Rocky Mountain front or east of Longitude 105 West (Refs. 13,14). A Probabilistic Seismic Hazard Analysis (PSHA) in the Central Eastern United States (CEUS) must account for credible alternative seismic sources through the use of a decision tree with appropriate weighting factors that are based on the most up-to-date information and relative confidence in alternative characterizations for each seismic source. Seismic sources identified and characterized by Lawrence Livermore National Laboratory (LLNL) (Refs. 13-15) and the Electric Power Research Institute (EPRI) (Ref. 16, 17) were used for CEUS studies in the past. In addition to the LLNL and EPRI resources, the United States Geological Survey maintains a large database of seismic sources for both the CEUS and the WUS. The characterization of specific seismic sources found in these databases may still represent the latest information available at the time that a PSHA is to be undertaken. However, if more up-to-date information is available, it should be incorporated."

Regulatory Guide 1.165 (NRC, 1997a) provides the framework for assessing the appropriate SSE ground motion levels for new power generating nuclear plants. Regulatory Guide 1.165 also notes that an acceptable starting point for the SSE assessment at sites in the Central and Eastern United States (CEUS) is the PSHA conducted by the Electric Power Research Institute (EPRI) for the Seismicity Owners' Group (SOG) in the 1980s. Regulatory Guide 1.165 further specifies that the adequacy of the EPRI-SOG hazard results must be evaluated in light of more recent data and evolving knowledge pertaining to seismic hazard evaluation in the CEUS.

Reference 16 of the NRC Regulatory Guide 1.208 is Electric Power Research Institute, "Probabilistic Seismic Hazard Evaluations at Nuclear Power Plant Sites in the Central and Eastern United States," NP-4726, All Volumes, 1989-1991. The title and number of the referenced document are not in agreement. The title of EPRI-4726 is "Seismic Hazard Methodology for the Central and Eastern United States." No document could be found that had the title provided by the NRC. In lieu of the reference 16, Section 2.5.2 of this document has used concepts from and interpretations presented in EPRI NP-4726, "Seismic Hazard Methodology for the Central and Eastern United States," (EPRI 1986); EPRI-4726-A, "Seismic Hazard Methodology for the Central and Eastern United States," (EPRI 1988); and EPRI NP-6395-D-1989, (EPRI, 1989a).

As stated in Regulatory Guide 1.208, the PSHA should incorporate the detailed guideline from NUREG/CR-6372 “Recommendations for Probabilistic Seismic Hazard Analysis: Guidance on Uncertainty and Use of Experts” Vol. 1 and 2 (NRC, 1997b). However, RG-1.208 does not limit the procedure to conduct the PSHA to the approach described in EPRI-4926, “Seismic Hazard Methodology for the Central and Eastern United States” (EPRI, 1986). The USGS information is also included in Regulatory Guide 1.208 as a potential starting point. USGS information can be used not only to define seismic sources but also to implement the PSHA procedure. In addition, the PSHA results developed by the USGS (Frankel, 1995) are prescribed in several building codes such as Minimum Design Loads for Buildings and Other Structures (ASCE/SEI 7-05)(ASCE, 2005a), and the International Building Code. These building codes are widely accepted by the engineering community.

Frankel’s smoothed seismicity approach was developed to be applied in the calculation of annual probabilities of exceedance as low as 10E-05. In his original paper, Frankel (Frankel, 1995) shows that his smoothed seismicity methodology reproduces the hazards obtained at 30 nuclear power plants sites following the EPRI methodology. He also shows that at four sites, the PSHA results obtained by his and the EPRI methodologies are very similar down to hazards of 10E-04 to 10E-05.

The USGS and the EPRI PSHA methodologies are essentially the same. Their most noticeable difference is in their approach to calculating the seismicity parameters. Even in this step, both methodologies rely mainly on the historical seismicity, including estimates of incompleteness, and using a Gaussian smoothing procedure. The USGS, as the consultant of the NRC to review the EPRI NP-4726 report expressed several concerns about the EPRI PSHA methodology in calculating the seismicity parameters. However, after discussions among EPRI, USGS, and NRC staffs, they concluded that both the USGS and the EPRI approaches for calculating the seismicity parameters of the source zones provided satisfactory hazard results. Neither approach is superior to the other in performing PSHA especially in the CEUS.

Accordingly, the evaluation of vibratory ground motion made for the BBNPP site addresses seismic hazard update requirements in Regulatory Guide 1.165 (NRC, 1997a) and meets the SSE requirements given in paragraph (d) of 10 CFR 100.23 (CFR, 2007). Following the recommendation of Regulatory Guide 1.165 (NRC, 1997a), the 1989 EPRI study, EPRI NP-6395-D (EPRI, 1989a) provides a basis to start seismic hazard calculations. A Probabilistic Seismic Hazard Analysis (PSHA) determines the annual frequency of exceedance as a function of minimum ground motion. This annual frequency results from the integration of hazard contributions of seismic sources characterized by spatial extent and location, magnitude, frequency recurrence, and propagating the ground motion from the sources to the site. These calculations incorporate parametric variability, including alternative models and parametric distributions, as well as consideration of statistical uncertainties.

Studies were conducted to analyze the sensitivity of the BBNPP seismic hazard to source model parameters, such as maximum magnitude, probability of activity, and geometry. These studies included the following:

1. Five Hundred (500) Mile Sensitivity Study

   This study considered an increased area of influence to update the earthquake catalog, from 200 miles (322 km) to 500 miles (805 km). The purpose of this sensitivity study was to investigate the influence of new earthquake activity from extensive seismic source zones that influence the BBNPP site. Section 2.5.2.1.2 provides a description of the earthquake catalog update, and Section 2.5.2.4.7 provides the sensitivity study results through comparisons of seismicity rates and hazard curves.

2. Charlevoix Sensitivity Study

   In light of recent earthquake activity, specifically the 1988 Saguenay Earthquake, two sensitivity analyses were considered for the Charlevoix seismic zone:

   a) Modification in the geometry of the Charlevoix seismic source zone;

   b) Increase of the maximum magnitude of source zones that included the post-EPRI 1988 Saguenay Earthquake

   Section 2.5.2.2.3.6 presents the nature of the suggested modifications in source models and Section 2.5.2.4.7 provides the results and conclusions of the Charlevoix sensitivity studies.

3. Sensitivity Study on Ramapo Fault System

   A recent publication (Sykes, 2008) postulates the existence of new ramifications of the Ramapo Zone Fault System. A sensitivity analysis is presented to assess the effects of this feature in a quantitative mode. Section 2.5.2.2.3.3 presents the nature of the suggested modifications in source models and Section 2.5.2.4.7 provides the results and conclusions of the Ramapo sensitivity studies.

The following subsections summarize the procedure followed and results from the vibratory ground motion studies that were carried out for the BBNPP site.

1. As a starting step, the EPRI-SOG tectonic interpretations in EPRI NP-4726 (EPRI, 1986) were examined in light of more recent geological, seismological, and geophysical data under the guidance of NRC Regulatory Guide 1.208, (NRC, 2007a). Sections 2.5.2.1 through 2.5.2.3 document this review and update of the EPRI-SOG seismicity, seismic source, and ground motion models.

2. Section 2.5.2.4 develops PSHA parameters at the site assuming the very hard rock foundation conditions implied by currently accepted ground motion attenuation models.

3. Section 2.5.2.5 summarizes information about the seismic wave transmission characteristics of the BBNPP site with reference to more detailed discussion of all engineering aspects of the subsurface in Section 2.5.4.

4. Section 2.5.2.6 describes the development of the horizontal SSE ground motion for the BBNPP site.

The selected SSE ground motion is based on the risk-consistent/performance-based approach of Regulatory Guide 1.208 (NRC, 2007a), with reference to NUREG/CR-6728 (NRC, 2001), NUREG/CR-6769 (NRC, 2002), and ASCE/SEI 43-05 (ASCE, 2005b). Horizontal ground motion amplification factors are developed using site-specific data and estimates of near-surface soil and rock properties. These amplification factors are then used to scale the hard rock spectra to develop Uniform Hazard Spectra accounting for site-specific conditions using Approach 2B of NUREG/CR-6728 (NRC, 2001) and NUREG/CR-6769 (NRC, 2002). Horizontal SSE spectra are developed from these soil Uniform Hazard Response Spectra using the performance-based approach of ASCE/SEI 43-05 (ASCE, 2005b), as implemented in Regulatory Guide 1.208 (NRC, 2007a). The SSE motion is defined at the free ground surface of a hypothetical outcrop at the base of the nuclear island foundation. See Sections 2.5.4 and 2.5.2.5 for further discussion of the subsurface conditions. Section 2.5.2.6 also describes vertical SSE spectra developed by scaling the horizontal SSE by a frequency-dependent vertical-to-horizontal (V/H) factor.

The SSE spectra described herein are considered performance goal-based (risk-informed) site specific safe shutdown earthquake response spectra. As discussed below, the SSE spectra for the BBNPP site have been developed following the graded performance-based, risk-consistent method described in ASCE/SEI Standard 43-05 (ASCE, 2005b). The method specifies the level of conservatism and rigor in the seismic design process such that the performance of structures, systems, and components (SSC) of the plant achieve a uniform seismic safety performance consistent with the NRC's safety goal policy statement.

The SSE spectra, and its specific location at a free ground surface, reflect the seismic hazard in terms of a PSHA and geologic characteristics of the site and represent the site-specific ground motion response spectra (GMRS) of Regulatory Guide 1.208 (NRC, 2007a). These spectra are expected to be modified as appropriate to develop ground motion for design considerations.

The SSE developed in this section meets the requirements of paragraph (d) of 10 CFR 100.23 (CFR, 2007).}

2.5.2.1 Seismicity

{Current probabilistic hazard methodologies consider that the activity in area seismic sources can be adequately represented by the Gutenberg-Richter (G-R) recurrence equation in terms of body wave magnitude, m_b. A quantitative derivation of the G-R parameters is based on historical seismicity, i.e., on catalogs of seismic events. The seismic hazard analysis conducted by EPRI as delineated in NP-6395-D 1989 (EPRI, 1989a) relied, in part, on an analysis of historical seismicity in the Central and Eastern United States (CEUS) to estimate seismicity parameters (rates of activity, a, and slope b-values of the Gutenberg-Richter equation) for individual seismic sources. The historical earthquake catalog used in the EPRI analysis was complete through 1984.

As recognized in NRC Regulatory Guide 1.208 (NRC, 2007a), the United States Geological Survey (USGS) maintains a large database of seismic sources for both the Central and Eastern United States, as part of their efforts to develop National Seismic-Hazard Maps (USGS, 1996)(USGS, 2002)(USGS, 2008). In Open-File Report 96-532, entitled "National Seismic-Hazard Maps: Documentation June 1996 (USGS, 1996) the USGS states that their CEUS catalog was primarily based on a catalog by Seeber (Seeber, 1991), who conducted a refinement of the EPRI 1986 catalog (EPRI, 1986).

Section 2.5.2.1.1 and Section 2.5.2.1.2 are added as a supplement to the U.S. EPR FSAR.}

2.5.2.1.1 Regional Seismicity Catalog

{Many seismic networks record earthquakes in the CEUS. A large effort is continuously made by the USGS to examine and combine available data on historical earthquakes and to develop a homogeneous earthquake catalog that contains all recorded earthquakes for the region. "Homogeneous" means that estimates of m_b for all earthquakes are consistent, duplicate earthquakes have been eliminated, non-earthquakes (e.g., mine blasts and sonic booms) have been eliminated, and significant events in the historical record have not been missed. Thus, the USGS catalog forms a strong basis on which to estimate seismicity parameters. The USGS catalog updated up to 2001 has been used because this is the latest year for which the m_b units were reported. The use of m_b is required in view that the Gutenberg-Richter equation that describes the seismicity in area sources is considered to be valid in m_b units. Table 2.5-1 lists the earthquakes in the USGS Earthquake Catalog for the CEUS with m_b values greater than or equal to 3.0.

2.5.2.1.2 Updated Seismicity Data

Regulatory Guide 1.165 (NRC, 1997a) specifies that earthquakes of a Modified Mercalli Intensity (MMI) greater than or equal to IV or of a magnitude greater than or equal to 3.0 should be listed for seismic sources, "any part of which is within a radius of 200 mi (322 km) of the site (the site region)." The USGS catalog and methodology for determining seismicity parameters consider precisely the minimum magnitude of m_b equal to 3.0.

The USGS updated catalogs are compiled by examining and combining events listed in several CEUS source catalogs (Mueller, 1997). In this effort, the USGS intent is to develop a catalog dominated by entries from the best-researched sources and they use this priority to choose the best location and magnitude from among multiple source catalogs for each earthquake. In addition, the secondary events have been filtered as explained in a recent USGS publication (USGS, 2008). Traditionally, most CEUS earthquake magnitudes are reported as a short-period surface-wave magnitude (m_{bLg}) and the ground-motions used in the hazard analysis are predicted based on m_{bLg}. In most cases a preferred magnitude from a catalog was assumed by the USGS to be equivalent to m_{bLg}, calling it m_b.

The catalog of use is the USGS catalog updated to the year 2007. Recent applications, such as the Clinton ESP (EGC, 2008), conclude that the update in the seismicity from the 1984 EPRI-SOG study do not significantly affect the seismicity parameters, i.e. the slope of the G-R (Gutenberg-Richter) equation (b parameter) and seismic rate (recurrent rate) in their respective regions of study. The same conclusion is reached in relation to the geometry of the seismic sources. The only relevant updates that were identified are the maximum magnitude of the Wabash Valley area source and the introduction of the New Madrid characteristic cluster events. A cluster model is required to represent the events that occurred in the three-series cluster with large magnitude (>7.5M). The seismic parameters related to the New Madrid events are not in agreement with the general G-R equation utilized in the area source hazard computation, and therefore need to be treated separately. The New Madrid events occurred in a cluster of three events. The event shown in the catalog is considered to be the main New Madrid event for the 1811-1812 cluster set. The other two events are considered as the foreshock/aftershock events and are filtered out from the catalog by USGS. This New Madrid event is treated as the New Madrid Characteristic Cluster events in the PSHA since it does not follow the G-R (Gutenberg-Richter) relationship for seismicity rate. Therefore, this 1811-1812 main event (shown in the catalog) is ignored when calculating the seismicity rate for the New Madrid area source.

The 2002 USGS catalog is used to update more current seismicity data required for the PSHA at the BBNPP Plant site. This catalog is a significant update to the EPRI-SOG 1984 seismic catalog. Seismicity recorded up to the year 2007 has been accounted for by adding the only two events within the site region recorded in the period between 2002 and 2007. These two events have been added to the end of Table 2.5-1 and are used in the BBNPP PSHA.

The 2002-2007 update to the catalog does not have a significant effect on the b-parameter, seismic occurrence rate, and/or the entire PSHA study at the BBNPP site. The use of the updated earthquake catalog results in a marginal reduction of the seismic occurrence rates, when compared to the USGS 2002 catalog. The resulting ground motion levels are marginally lower. The USGS 2002 G-R parameters are selected for the BBNPP PSHA since the effect on the seismic hazard of the 2002-2007 update is a marginal reduction in the ground motion levels, which is deemed to be less conservative.

A sensitivity analysis was performed to understand the effects of the 2002-2007 seismicity in an area broader than the 200 mi (322 km) region. For this analysis, an earthquake catalog search for 2002-2007 was performed with the following criteria:

- Use of a 500 mi (805 km) circular area centered at the BBNPP site 16W (41.08(N), -76.16(W)) for the USGS earthquake database; selection of the USGS/NEIC (PDE) '1973 – Present' database for magnitudes from 3.0 to 10.0 between the year 2002 and 2007 (USGS web database: http://neic.usgs.gov/neis/epic/epic_circ.html) (USGS, 2008);

- Use of a rectangular boundary zone with limits from 33.88(N) to 48.27(N) (latitude) and -66.60(W) to -85.70(W) (longitude) for the Advanced National Seismic System (ANSS) earthquake database for magnitude 3.0 to 10.0 between years 2002 to 2007 (ANSS composite web database: http://www.ncedc.org/anss/catalog-search.html) (ANSS, 2008);

- The sensitivity study extended the 2001 catalog to the year 2007. The update methodology adopted the approach described in the USGS open file report 2008-1128 "The 2008 Update of the United States National Seismic Hazard Maps" that USGS uses for catalog updates to 2006 to reduce the additional epistemic uncertainty related to the magnitude conversion. Magnitude may be adopted from the reported values. In addition differences resulting from unit conversion are negligible for small magnitude earthquakes. If more than one magnitude is listed in the original source-catalog record for an earthquake, a preferred magnitude is selected. A preferred magnitude is considered to be one that is closer to m_{bLg} for the specific reported magnitude. For example the local magnitude (ML) may be considered equivalent to m_{bLg};

- For magnitudes less than 5.0, the equivalency between different magnitude scales for different regions are verified using empirical relations. Only about 10 percent of the earthquakes do not have a listed m_{bLg} or m_b (USGS 2008); in these cases, the preferred magnitude is assumed to be m_{bLg}. For the same event, if the magnitude between databases differs, the larger magnitude is selected;

- Consider only those earthquakes within the circular 500 mi (805 km) area.

A search with the criteria listed above returned sixty-six (66) earthquakes recorded between 2002 and 2007. These earthquakes are listed in Table 2.5-62a without reference to their dependent events. These new earthquakes were added to the catalog used in the BBNPP PSHA sensitivity analysis. Table 2.5-62a provides epicenter coordinates, depth of focus, date, origin time, body wave magnitude (m_b) and reference catalog.

As with the 200 mi (322 km) case, this analysis shows that the 2002-2007 update does not have a significant effect on the PSHA study at the BBNPP site. The result is a marginal reduction of ground motion levels, between one and two percent, when compared to the USGS 2002 catalog. Therefore, the more conservative USGS 2002 G-R parameters are selected for use in the BBNPP PSHA. Section 2.5.2.4.7 provides information related to the results of the sensitivity analyses.

Earthquakes outside the region that have significant contribution to the hazard at the BBNPP site have been properly accounted for. Those with significant contribution include the Charlevoix Zone, the New Madrid Fault Zone, and the Charleston Earthquake. These contribute to the low frequency ground motion levels.

Major sources of potential seismic activity such as the New Madrid Seismic Zone (NMSZ) and the Charleston Seismic Zone (CSZ) are located beyond 200 mi (322 km) from the site. However, based on new paleo-seismology data, updated characteristic earthquake models have been recently formulated for the NMSZ and the CSZ. A sensitivity analysis for the BBNPP site using these updated models showed that characteristic earthquake events from both sources are significant contributors to low frequency ground motion at the site. The sensitivity analysis also showed that Charlevoix seismic zone (in Canada) is a contributor to the hazard at low frequencies. Therefore these three sources have been included in the PSHA study for the site.

A PSHA result showed that the New Madrid Seismic Zone (NMSZ) is a contributor to the hazard at the BBNPP site at low frequencies. As such, characterization of this seismic source was added to the PSHA input for BBNPP. After a literature review of the existing NMSZ models, the characteristic earthquake model as described in the Clinton ESP (EGC, 2006) was selected as the input.

The Clinton ESP (EGC, 2006) also documented paleoliquefaction evaluations where evidence of soil liquefaction that occurred in prehistoric times is inferred from features such as sand boils or blows, dikes, and sills. By estimating the date and geographical distribution of these features, it is possible to infer the magnitude of the earthquake that originated the features. Earlier investigations of paleoliquefaction features in the southern Illinois basin and in parts of Indiana, Illinois, and Missouri have identified paleoliquefaction occurrences that could have been caused by Holocene and latest Pleistocene earthquakes with estimated moment magnitudes (M) of 6 to 7.8. Details about the paleoliquefaction reconnaissance carried out for the Clinton ESP Site seismic hazard evaluation are given in Section 2.1.4 and Attachment 1 of Appendix B of the Clinton ESP document (EGC, 2006). These details include a discussion of each of the identified features, pictures of the features, results of radiocarbon dating, and criteria for differentiating seismic versus non-seismic liquefaction features. The Clinton ESP was issued by the NRC in March 2007 (NRC, 2007c).

These paleoliquefaction studies have been utilized for developing improved representations of characteristic earthquakes in the New Madrid Fault System. It was also concluded, from these paleoliquefaction evaluations, that the range of maximum magnitude earthquakes assigned to a random background earthquake in the PSHA for the Clinton ESP site must include events comparable to that estimated for the Springfield, IL earthquake which occurred approximately 22 mi (35 km) northeast of Springfield, IL and 30 mi (48 km) southwest of the Clinton ESP site, that is, M 6.2 to 6.8.5.

The update in the introduction of the New Madrid characteristic cluster events is performed. These updates are adapted to the BBNPP site from the Clinton ESP Application. The updated New Madrid Model is discussed in Section 2.5.2.2.3.1.

Another significant source of severe seismic events in the East Coast of the United States is the Charleston seismic source that is about 620 mi (998 km) from the BBNPP site. Despite this long distance, it was considered that this source could still have some significant contribution to the hazard at the BBNPP site, particularly at low frequency ground motion. Thus, the Charleston seismic source has been included in the present PSHA. Since publication of the EPRI seismic hazard analyses, paleoliquefaction investigations and other studies have impacted the characterization of the geometry, M_{max}, and recurrence in the Charleston seismic source. Paleoliquefaction studies in the area of the 1886 Charleston earthquake date back to a study performed by Cox and Talwani (Cox, 1983) that identified evidence of earthquake induced liquefaction features preserved in the South Carolina Coastal Plain sediments. Following this discovery, USGS conducted intensive studies to identify the spatial extent of paleoliquefaction features. USGS studies led to the discovery of sand blows that predated 1886, hence providing a basis for estimating the recurrence interval of large earthquakes in the Charleston area (Obermeier, 1987). More recent studies and interpretations have led to the refinement of the Charleston source zone parameters (Johnston, 1996; Bakun, 2004; Marple, 2000; Talwani, 2001; USGS, 2002; USGS, 2008). For example, radiocarbon dating techniques in new studies account for the fluctuation of atmospheric C-14 over time while previous studies assumed that the amount of C-14 has remained constant (Talwani, 2001). Based on the new interpretations, alternative geometries have been used for this zone. Marple (Marple, 2000) proposed a postulated East Coast Fault System (ECFS) in the Coastal Plain of the Eastern US and argued that the southern segment of this fault system is probably the source of the 1886 Charleston earthquake. In their 2008 version of National Seismic Hazard Maps, USGS (USGS, 2008) extended the Charleston area source offshore to include the Helena Banks fault zone as a possible source. USGS (USGS, 2008) also define another (elongated) area source which encloses the Woodstock lineament. This area source envelops half of the southern segment of ECFS. These two area sources have equal weights. Bechtel has examined these new data and developed an Updated Charleston Seismic Source (UCSS) model. The UCSS model has been used in development of the FSAR for the Vogtle ESP (SNOC, 2008). The UCSS model as described in the Vogtle ESP (SNOC, 2008) has been adopted here after review and comparison with other models of the Charleston seismic source.

The mean of M_{max} distribution used in the UCSS model (Mw 7.1) is very close to that of USGS (Mw 7.2). The source geometry used by UCSS considers four source zones with different weights. Beside the area of strong shaking during 1886 Charleston earthquake, this source zone combination accounts for the liquefaction features that are distributed far from the epicentral area. It also includes the southern segment of ECFS (Marple, 2000) as a possible source of the 1886 Charleston earthquake with a low weight of 0.1.

The recurrence interval of the Charleston characteristic earthquake in the UCSS model is based on the work of Talwani (Talwani, 2001). While Talwani (Talwani, 2001) argues that only the 2000 year record of paleoliquefaction data is complete, the UCSS model uses a combination of 2000 year and 5000 year records, thereby considering the possibility that the paleoliquefaction features may have been preserved in the 5000 year data. The 5000 year record, however, has a lower weight (0.2) than the 2000 year data (0.8). Based on comparisons between the UCSS model and other Charleston characteristic earthquake models including the USGS (USGS, 2008) model, it is concluded that the UCSS model better addresses the epistemic uncertainty in source zone parameters (including recurrence times) and therefore is used here to characterize the Charleston seismic source. This model is discussed in section 2.5.2.2.3.2. The description of the UCSS model is based on the Vogtle ESP FSAR (SNOC, 2008).

As a result of the investigations performed, relevant updates in maximum magnitude and geometry have been performed for the New Madrid cluster events and the UCSS. These events are distant from the BBNPP site but they still contribute to the hazard at the low frequencies.

The Charlevoix seismic zone is the most seismically active region of Eastern North America. It is located about 60 mi (97 km) downstream from Quebec City. This seismic zone has been the location of numerous small to medium earthquakes as well as five M ≥ 6.0 earthquakes in the last 350 years (Mazzotti, 2005). Among the larger events, only the 1925 earthquake, Ms = 6.2, (Bent, 1992) has been recorded by seismographs. The Canadian Geological Survey (CGS) conducted two field surveys in 1970 and 1974 to define the extensions of the seismic zone. The results of these two surveys delineated an active seismic zone about 20 by 55 mi (32 by 86 km) along the Saint Lawrence River (Earthquakes Canada, 2008). Maximum magnitudes of M ≥ 7.0 have been assigned to this seismic zone (Mazzotti, 2005). All six EPRI teams have considered the Charlevoix seismic zone in their source zone models and assigned mean maximum magnitudes close to or larger than 7.0. This seismic zone is located beyond the 200 mile radius of the Bell Bend site, but a sensitivity analysis showed that it is a contributor to the seismic hazard at the Bell Bend site lower frequencies. Therefore, this seismic source was included in the final PSHA for the BBNPP site.}

2.5.2.2 Geologic and Tectonic Characteristics of Site and Region

{As described in Section 2.5.1, a comprehensive review of available geological, seismological, and geophysical data has been performed for the BBNPP site region and adjoining areas. As discussed in Section 2.5.1.2.5.2, excavation mapping is required during construction and any noted deformational zones will be evaluated and NRC notified when excavations are open for inspection. The seismotectonic characteristics of the region constitute the basis for defining the seismic source zones that affect the BBNPP site.

This section summarizes the geologic structure and activity that could potentially result in seismic-induced vibratory ground motion at the BBNPP site. The summary addresses Regulatory Positions 1 and 2 within Regulatory Guide 1.165 (NRC, 1997a), which requires that investigation of seismic sources to be performed within a 200 mi (322 km) radius of the site. The following sections summarize the seismic source interpretations (EPRI, 1986) that lie at least partially within this radius, relevant post-EPRI seismic source characterization studies and updated interpretations based on new data. The evaluation identified no new information which involved a change to the catalog that could impact the outcome of the PSHA.

Three major updates on seismic sources and characteristic earthquake models include:

The East Coast Fault System (ECFS) represents a new postulated seismic source along the Atlantic Seaboard (Section 2.5.1.1.4.4.1.2). The southern segment of the ECFS has been proposed by Marple (Marple, 2000) as being the source of the 1886 Charleston earthquake;

The average recurrence interval for large magnitude earthquakes in the Charleston characteristic model has been updated to 550 years based on paleoliquefaction data. The Charleston seismic source geometry also has been updated to include the southern segment of the ECFS as a possible source of the 1886 earthquake;

Assessments of magnitude, location, and return periods of large characteristic earthquakes of the New Madrid Seismic Zone (NMSZ) have been updated.

Detailed discussions of the updated source models are presented in the sections 2.5.2.2.3.1 and 2.5.2.2.3.2.

Section 2.5.2.2.1 and Section 2.5.2.2.2 are added as a supplement to the U.S. EPR FSAR.

2.5.2.2.1 Summary of EPRI Seismic Sources

The evaluations of new information examined in previous ESPs (EGC, 2006)(NRC, 2005) concluded that the EPRI-SOG seismic sources remain appropriate for assessing seismic hazards in CEUS. Therefore, the seismic sources defined in the 1989 EPRI/SOG study (EPRI, 1989a) have been adopted for updating the BBNPP site PSHA. However, it is noted that updates and adjustments are required for the maximum magnitude distribution for the area sources and that characteristic earthquake models must be used to properly account for more recent information on the seismic activity in the New Madrid and Charleston seismic zones.

In the 1986 EPRI study (EPRI, 1986), six independent Earth Science Teams (ESTs) evaluated geological, geophysical, and seismological data to develop seismic sources in the CEUS. These sources were used to model the occurrence of future earthquakes and evaluate earthquake hazards at nuclear power plant sites across the CEUS. The six ESTs involved in the EPRI project were: Bechtel Group, Dames & Moore, Law Engineering, Rondout Associates, Weston Geophysical Corporation, and Woodward-Clyde Consultants. Each team produced a report, included in EPRI NP-4726, (EPRI, 1986), that provides detailed descriptions of how they identified and defined seismic sources.

The EPRI/SOG ESTs also determined recurrence parameters and maximum magnitudes for each source in m_b or magnitude units, including their corresponding weights. These models were implemented into a probabilistic seismic hazard analysis (PSHA) reported in EPRI NP-6395-D (EPRI, 1989a). EPRI NP-6452-D (EPRI, 1989b) summarized the parameters used in the final PSHA calculations, and this reference is the primary source for defining the geometry of area seismic sources for the BBNPP PSHA presented herein. For the computation of hazard, some of the 1989 EPRI seismic source parameters were updated, as discussed below.

The following sections list the seismic source interpretations in the 1989 EPRI PSHA study (EPRI, 1989a), relevant post-EPRI seismic source characterization studies, and updated interpretations provided by the more recent data. The summary of seismic sources and parameters was developed from the 1989 EPRI project EPRI NP-6452-D (EPRI, 1989b). The listed area seismic sources are those that at least partially lie within the "site region," i.e. within the circle with a 200-mi (322-km) radius centered at the BBNPP site. The list includes the code used by each team to designate each source, the name of the source, the assigned recurrence parameter b and the assigned maximum magnitude, and weights assigned to each value of the parameter b and of the maximum magnitude.

Figures 2.5-34 through Figure 2.5-39a present the geometry of the seismic sources selected to estimate the hazard at the BBNPP site, including plots of earthquakes with m_b equal to or higher than 3.0 in the updated earthquake catalog, to illustrate the spatial relationships between seismicity and seismic sources. Earthquake epicenters in the updated earthquake catalog include events from the period between 1627 and 2007, as listed in Table 2.5-1. Following the 1989 EPRI study (EPRI, 1989a) and the 1996, 2002 and 2008 USGS studies (USGS, 1996; USGS, 2002; USGS, 2008), the recurrence parameters for area seismic sources were computed for each one-degree latitude and longitude cell that intersects any portion of a seismic source.

The PSHA conducted in the EPRI-SOG study employed three strong ground motion attenuation relationships developed by Boore and Atkinson (Boore, 1987) and McGuire and others (McGuire, 1988) combined with the response spectral shapes by Newmark and Hall (Newmark, 1982) which are based on Western North America earthquake records. More recently-developed ground motion attenuation models (EPRI, 2004) are supported by a better understanding of earthquake generation and indicate that significant differences in the crustal properties between western and eastern North America lead to significant differences in the frequency content of ground motions between the two regions. In addition, the more recent ground motion models include an improved assessment of variability about median estimates, and thus have been used for this evaluation.

2.5.2.2.1.1 Sources Used for EPRI PSHA – Bechtel Group

The seismic sources and recurrence parameters identified by the Bechtel EPRI/SOG EST (EPRI, 1989a) that are within 200 mi (322 km) of the BBNPP site are listed in Table 2.5-3.

Figure 2.5-34 illustrates the locations and geometries of the Bechtel Group seismic sources contributing to 99% of the seismic hazard along with plots of earthquakes with m_b equal to or higher than 3.0 between 1627 and 2007 (within 500 miles (805 km) of the BBNPP site for 2002 – 2007). Figure 2.5-34a shows the same magnitude events within the Bechtel Group seismic source zones for a 50 mi (80 km) radius of the BBNPP site.

2.5.2.2.1.2 Sources Used for EPRI PHSA – Dames & Moore

The seismic sources and recurrence parameters identified by the Dames & Moore EPRI/SOG EST (EPRI, 1989a) that are within 200 mi (322 km) of the BBNPP site are listed in Table 2.5-4.

Figure 2.5-35 illustrates the locations and geometries of the Dames and Moore seismic sources contributing to 99% of the seismic hazard along with plots of earthquakes with m_b equal to or higher than 3.0 between 1627 and 2007 (within 500 miles (805 km) of the BBNPP site for 2002 – 2007). Figure 2.5-35a shows the same magnitude events within the Dames & Moore seismic source zones for a 50 mi (80 km) radius of the BBNPP site.

2.5.2.2.1.3 Sources Used for EPRI PSHA – Law Engineering

The seismic sources and recurrence parameters identified by the Law Engineering EPRI/SOG EST (EPRI, 1989a) that are within 200 mi (322 km) of the BBNPP site are listed in Table 2.5-5.

Figure 2.5-36 illustrates the locations and geometries of Law Engineering seismic sources contributing to 99% of the seismic hazard along with plots of earthquakes with m_b equal to or higher than 3.0 between 1627 and 2007 (within 500 miles (805 km) of the BBNPP site for 2002 – 2007). Figure 2.5-36a shows the same magnitude events within the Law Engineering seismic source zones for a 50 mi (80 km) radius of the BBNPP site.

2.5.2.2.1.4 Sources Used for EPRI PSHA – Rondout Associates

The seismic sources and recurrence parameters identified by the Rondout Associates EPRI/SOG EST (EPRI, 1989a) that are within 200 mi (322 km) of the BBNPP site are listed in Table 2.5-6.

Figure 2.5-37 illustrates the locations and geometries of Rondout seismic sources contributing to 99% of the hazard along with plots of earthquakes with m_b equal to or higher than 3.0 between 1627 and 2007 (within 500 miles (805 km) of the BBNPP site for 2002 – 2007). Figure 2.5-37a shows the same magnitude events within the Rondout Associates seismic source zones for a 50 mi (80 km) radius of the BBNPP site.

2.5.2.2.1.5 Sources Used for EPRI PSHA – Weston Geophysical Consultants

The seismic sources and recurrence parameters identified by the Weston Geophysical EPRI/SOG EST (EPRI, 1989a) that are within 200 mi (322 km) of the BBNPP site are listed in Table 2.5-7.

Figure 2.5-38 illustrates the locations and geometries of Weston seismic sources contributing to 99% of the hazard along with plots of earthquakes with m_b equal to or higher than 3.0 between 1627 and 2007 (within 500 miles (805 km) of the BBNPP site for 2002 – 2007). Figure 2.5-38a shows the same magnitude events within the Weston Geophysical seismic source zones for a 50 mi (80 km) radius of the BBNPP site.

2.5.2.2.1.6 Sources Used for EPRI PSHA – Woodward-Clyde Consultants

The seismic sources and recurrence parameters identified by the Woodward-Clyde Consultants EPRI/SOG EST (EPRI, 1989a) that are within 200 mi (322 km) of the BBNPP site are listed in Table 2.5-8.

Figure 2.5-39 illustrates the locations and geometries of Woodward-Clyde seismic sources contributing to 99% of the hazard along with plots of earthquakes with m_b equal to or higher than 3.0 between 1627 and 2007 (within 500 miles (805 km) of the BBNPP site for 2002 – 2007). Figure 2.5-39a shows the same magnitude events within the Woodward-Clyde seismic source zones for a 50 mi (80 km) radius of the BBNPP site.

2.5.2.2.2 Post-EPRI Seismic Source Characterization Studies

Seismic hazard evaluations more recent than the EPRI/SOG study have identified new information that could affect the assessment of the seismic hazard at the BBNPP site. Specifically, updated data and information can have an impact on:

Characterization of the rate of earthquake occurrences;

Estimates of the maximum magnitude for seismic sources;

Updated earthquake ground motions for the CEUS.

Studies that have used new data and information are described with emphasis on the items relevant for the evaluation of the seismic hazard at the BBNPP site. These descriptions are provided in Section 2.5.2.2.2.1 through Section 2.5.2.2.2.5.

2.5.2.2.2.1 USGS Studies for the United States National Maps

Between 1996 and 2008, the USGS produced updated seismic hazard maps for the United States based on updated seismological, geophysical, and geological information (USGS, 1996)(USGS, 2002)(USGS, 2008). Each map reflects changes to the source models used to construct the previous version of the national seismic hazard maps. Among the most significant modifications to the CEUS portion of the source models are changes in the recurrence, maximum magnitude (M_{max}), and geometry of the Charleston and New Madrid sources. Unlike the EPRI models that incorporate many local sources, the USGS source model in the BBNPP site region (200-mi (322 km) radius) includes only three sources that are important to the site hazard: the Extended Margin background, Stable Craton background, and New Madrid. Except for the New Madrid zone, where earthquake recurrence is modeled as characteristic earthquakes, the hazard for the large background or "maximum magnitude" zones is largely based on historical seismicity and the variation of that seismicity.

Since 1996, the USGS considered the occurrence of large events in the New Madrid as a characteristic rupture model with a characteristic moment magnitude M of 8.0, similar to the estimated magnitudes of the largest events in 1811-12 (USGS, 1996). The geometry of the New Madrid source was modeled as three S-shaped parallel faults encompassing the area of highest historic seismicity. The USGS study used an average recurrence time of 1000 years for the New Madrid characteristic earthquakes.

The 1996 USGS study (USGS, 1996) also recognized that several paleoearthquakes have been identified in the Wabash Valley area. This seismic activity was modeled as an area zone with a maximum magnitude of M 7.5. For background zones, values of the Gutenberg-Richter (G-R) parameter "a" were determined in the 1996 USGS study (USGS, 1996) by counting the number of m_b=3 and larger events within the zone since 1927 and adjusting the rate to equal that since 1976. The area-normalized a-value was then disaggregated into a set of grid cells to calculate the hazard considering the smoothed historic seismicity. The G-R parameter "b" was assigned a value of 0.95, based on calculations for the entire CEUS (USGS, 1996).

Some changes in the 2002 USGS study (USGS, 2002) that most affected the hazard estimates for the BBNPP site were the use of an updated mean recurrence time, characteristic magnitude, and spatial concentration to characterize the New Madrid sources of large earthquakes. A shorter mean recurrence time of 500 years was adopted and logic trees were developed for the characteristic magnitude related to the same configuration of three fictitious fault sources as in the 1996 maps, giving to the central fictitious source twice the weight of each of the faults to the sides. These changes markedly increased the probabilistic ground motions for the 10% probability of exceedance around the New Madrid area, compared to the 1996 results.

The documentation reported by the USGS for its 2008 (USGS, 2008) update of the national seismic hazard maps points out the following changes related to the Central and Eastern U.S.:

Revise catalog and account for magnitude uncertainty

Develop a logic tree for New Madrid (lower recurrence on northern arm and reduced magnitude)

Implement a cluster model for New Madrid earthquakes

Modify hypothetical fault geometry for New Madrid

Develop a logic tree for M_{max} area sources

The USGS basic methodology for hazard estimates in the CEUS for the 2008 hazard maps is similar to that implemented in the 1996 and 2002 maps. Such methodology includes background-seismicity and fault source models (USGS, 1996)(USGS, 2002)(USGS, 2008). Background sources account for random earthquakes that occur off known faults and moderate size earthquakes that occur on modeled faults. The USGS, 2008 background source model (USGS, 2008) is composed of three smoothed gridded seismicity models, a large regional zone model, and local special seismicity-based zones. The gridded seismicity models are based on recorded historical earthquakes and account for the observation that larger earthquakes occur in regions that have experienced previous smaller earthquakes. Large regional zones account for low potential of random seismicity in areas without historical seismicity and establish a floor to the seismic hazard calculations. The special local zones allow for local variability in the G-R seismicity parameters. Fault models account for earthquakes on mapped active faults that have paleoseismic or historical evidence of repeated large earthquakes. One of the four CEUS fault models considered in 2008 by the USGS is the New Madrid Fault System (NMFS).

The USGS gridded seismicity, large regional zone and the local seismicity models require a declustered earthquake catalog for calculation of earthquake rates. The USGS develops these gridded seismicity rates from their seismic catalog for the Central and Eastern United States. The truncated Gutenberg-Richter (Gutenberg, 1944) magnitude-frequency distribution is used to model rates for different sizes of earthquakes in each grid cell or source zone. The USGS estimates completeness levels from the earthquake catalog, and calculates Gutenberg-Richter (G-R) parameters of the magnitude-rate relationship (intercept a and slope b) using a maximum-likelihood method (Weichert, 1980) that accounts for variable completeness. The rates in the gridded cells are spatially smoothed using a two-dimensional Gaussian smoothing operator.

In 2008, the USGS (USGS, 2008) has used five fictitious parallel fault traces, each one having three arms. This is meant to represent the aleatory uncertainty in the locations of future large magnitude earthquakes in New Madrid, in a way similar to the three traces used in their 2002 model. The center of the five traces most closely follows the seismicity pattern and is assigned a weight of 0.7; the traces just outside of the central traces are weighted 0.1 each, and the outer traces are weighted 0.05.

USGS studies have also continuously incorporated developments in ground motion modeling (attenuation equations). In 1996 (USGS, 1996), the USGS adopted attenuation relationships derived for "hard rock conditions" recognizing that most attenuation relations for the CEUS published at that time were based on those site conditions. The USGS noted that it was less problematic to convert these to a firm-rock condition instead of converting them to soil conditions, since there would be less concern over possible non-linearity for the firm-rock site compared to the soil site.

The USGS 2008 study (USGS, 2008) includes several new simulation-based attenuation relations that were not available in 2002. While in 1996 and 2002 the USGS used ground motion models based on a single corner model (USGS, 1996; USGS, 2002), a double corner and hybrid models were incorporated in the 2008 study (USGS, 2008). The following is a list of the eight attenuation relationships used by the USGS in 2008, along with their assigned weights:

Single corner - finite fault

Toro and others (Toro, 1997), weight 0.2

Silva and others (Silva, 2002), constant stress drop with saturation, weight 0.1

Single corner - point source with Moho bounce

USGS (USGS, 1996), weight 0.1

Dynamic corner frequency

Atkinson and Boore (Atkinson, 2006), 140 bar stress drop, weight 0.1

Atkinson and Boore (Atkinson, 2006), 200 bar stress drop, weight 0.1

Full waveform simulation

Somerville and others (Somerville, 2001), for large earthquakes, weight 0.2

Hybrid empirical

Campbell (Campbell, 2003), weight 0.1

Tavakoli and Pezeshk (Tavakoli, 2005), weight 0.1

The 2002 and 2008 USGS efforts (USGS, 2002; USGS, 2008) have produced ground motion maps for a return period of 2475 years for building code applications.

2.5.2.2.2.2 The Lancaster Seismic Zone

The Lancaster seismic zone (LSZ) is located in southeastern Pennsylvania and is known as a post-EPRI study seismic zone located about 55 mi (89 km) south of the BBNPP site (Section 2.5.1.1.4.4.2.10). The largest known earthquake of the LSZ is the January 16, 1994 Cacoosing Valley earthquake of m_{bLg} = 4.6 near Reading Pennsylvania (Seeber, 1998). This event was located about 52 mi (84 km) south of the BBNPP site. The Cacoosing Valley event has been attributed to unloading during a quarry process (Seeber, 1998) but it has not been removed from the standard earthquake catalogs used in PSHA studies. The LSZ is not included in the original EPRI source zone model (EPRI, 1986) as a separate source zone. However, the range of M_{max} values assigned to other EPRI source zones, adequately characterizes the LSZ in terms of the upper bound magnitude (Section 2.5.1.1.4.4.2.10). Therefore no update is required for the EPRI (EPRI, 1986) seismic source zone model within the region of BBNPP site.}

2.5.2.2.3 Updated Interpretations Based on New Data

2.5.2.2.3.1 Updated New Madrid Model

As previously noted, seismologic, geologic, and geophysical studies have associated faults within the New Madrid region with the large-magnitude historical earthquakes that occurred during 1811 and 1812. In particular, paleoliquefaction studies indicate that large-magnitude events have occurred on these faults more frequently than the seismicity rates specified in the EPRI/SOG source characterizations. Thus, the updated seismic source evaluations focus on the characteristic large-magnitude events along the New Madrid Fault System.

<u>Fault Geometry</u>

As reported by the USGS and illustrated on Figure 2.5-74, very significant seismic activity occurs in the area of the New Madrid Fault System (NMFS). The severe 1811 through 1812 earthquakes are thought to have ruptured the Reelfoot Fault and fault segments to the south and the north. The precise locations of these three large events are not entirely known. The only evidence of surface rupture appears along the Reelfoot Fault and earthquake locations are generally constrained only by intensity and paleoseismic data. However, the available information indicates that the seismic activity at the NMFS can be attributed to the following three sources:

New Madrid South (NS) Fault;

New Madrid North (NN) Fault; and

Reelfoot Fault (RF).

The USGS studies for updating the 1996 U.S. national seismic map (USGS, 1996) considered this seismic activity as a "characteristic" rupture model. The USGS 1996 study (USGS, 1996) included a moment magnitude M of 8.0 and a recurrence time of 1000 years for such an event. Later, in the USGS work for the 2002 update of the national seismic hazard map (USGS, 2002), significant changes were introduced in mean recurrence time, characteristic magnitude, and spatial concentration of New Madrid sources of large earthquakes. It was recognized that the locations of these three large events are generally constrained only by intensity (felt) and paleoseismic data and a logic-tree approach was introduced to represent optional interpretations of fault locations and magnitudes of the New Madrid characteristic events. This logic tree was meant to characterize the range of expert opinions on the magnitude of the largest events of the 1811-12 sequence. The 2002 USGS study (USGS, 2002) represented the NMFS as three hypothetical sources: one fault with trace matching the observed microearthquake activity and two adjacent sources situated near the borders of the Reelfoot Rift. Also, a shorter mean return time of 500 years for characteristic earthquakes was considered by the USGS in the development of the 2002 maps (USGS, 2002). The end result was that the probabilistic ground motions for the 10% probability of exceedance level increased markedly around the New Madrid area, compared to the 1996 maps.

It is important to note that in the 1996 and 2002 models, the USGS (USGS, 1996; USGS, 2002) employed a single large earthquake that affects all three of the hypothetical faults, since these source models assumed that all earthquakes were independent.

Very recently, for the 2008 update of the hazard maps (USGS, 2008), the USGS takes into account the uncertainty in the locations of previous earthquakes by using five fictitious parallel fault-traces, similar to those used in the 2002 model (USGS, 2002). The central trace is weighted 0.7, the traces just outside of the central traces are weighted 0.1 each, and the outer traces are weighted 0.05 each. The USGS summarized expert opinions on the magnitudes of the 1811-1812 events, which shows that the estimated magnitudes range from M 7.0 up to M 8.1. Of the three largest New Madrid earthquakes, the one in January 1812 is the most likely to have ruptured the northern arm of the seismic zone (Figure 2.5-74). The three leading sets of magnitude estimates for the New Madrid sequence suggest that the January earthquake was 0.2±0.1 magnitude units smaller than the December shock (Johnston, 1996)(Hough, 2000)(Bakun, 2004).

Based on the updated information, for developing the 2008 maps, the USGS has assigned magnitudes for the northern section of the NMFS that are 0.2 units lower than those assigned for the central and southern sections (USGS, 2008). For the northern arm model the USGS applies the following weighting: M 7.1 (wt 0.15), M 7.3 (wt 0.2), M 7.5 (wt 0.5), and M 7.8 (wt 0.15). The central and southern segments remain characterized as in 2002, i.e., M 7.3 (wt 0.15), M 7.5 (wt 0.2), M 7.7 (wt 0.5), and M 8.0 (wt 0.15).

Regarding large earthquake recurrence for the NMFS, the USGS 2008 study (USGS, 2008) has used paleoliquefaction data indicating a 500 year recurrence. Three large earthquake sequences are recognized from cross-cutting relationships and radiometric dating of sandblows (liquefaction effects). The USGS refers to Tuttle and others (Tuttle, 2002) who have recognized that events about 900 A.D., 1450 A.D., and 1811-1812 A.D. have occurred. These dates agree with a 500-year mean recurrence. However, citing lack of certainty on whether or not the northern portion of the fault system ruptured in the 1450 A.D. sequence, the USGS consider the possibility of 750-year and 500-year recurrences, equally weighted, for the northern arm of New Madrid. The 500 year recurrence for the southern and central sections remained unchanged in view that Tuttle and others (Tuttle, 2002) published evidence that all three of the sequences affected those arms.

Another relevant modification made by the USGS in their 2008 New Madrid source modeling (USGS, 2008) is that in addition to an unclustered model, as used in the 1996 and 2002 studies, a clustered large earthquake model was included. A clustered model postulates that the 1811-1812 earthquakes involved a sequence of three large earthquakes. This hypothesis is supported by geologic data of Tuttle and others (Tuttle, 2002) showing evidence that pre-historic earthquakes on the NMFS typically occur in sequences of three large earthquakes similar to those observed in 1811-1812. The relevance of this consideration is that a particular site will have a larger probability of exceeding a ground motion level if it is affected by three dependent events rather than one independent event.

The USGS 2008 study assigns equal weight to a clustered model for the NMFS characteristic earthquake and to a 2002-type unclustered source model. In addition, a more extensive logic tree was used to represent the rates and location of seismic activity at the NMFS.

The recent ESP submitted by Exelon for the Clinton site (EGC, 2006) also recognizes that seismologic, geologic, and geophysical studies have associated faults within the New Madrid region with the large-magnitude historical earthquakes that occurred during 1811 and 1812. The Clinton site was included in the 1989 EPRI/SOG study; however, the Clinton ESP notes that paleoliquefaction studies indicate that large-magnitude events have occurred on the NMFS more frequently than the seismicity rates specified in the EPRI/SOG source characterizations.

Thus, Exelon decided to update the seismic source evaluations for the Clinton site focusing on the characteristic large-magnitude events along New Madrid. To this end, Exelon supported a vast paleoseismicity investigation to develop an improved model for the characteristic events at the NMFS. This investigation provides the most complete available representation of New Madrid characteristic events, particularly regarding the development of logic trees for representing various rupture scenarios and optional recurrence models. Details of the Clinton ESP characterization of the NMFS are presented in subsequent sections of this document. Due to its proximity to the Clinton site, Exelon conducted comprehensive studies for characterizing the seismic activity in the NMSZ as presented in the 2006 Clinton ESP application (EGC, 2006). The Exelon efforts included a thorough review of the technical literature as well as paleoliquefaction studies to identify the fault source geometry and to estimate recurrence parameters in the NMSZ. It was recognized that paleoliquefaction studies indicate that clustered large-magnitude earthquakes have occurred in this zone which can be properly modeled as characteristic events. Recent work for characterizing seismic activity at the NMSZ has also been conducted by the USGS for the 2008 update of the National Seismic Hazard Maps (USGS, 2008). The USGS also considers a temporal clustering model for the large NMSZ earthquakes and has developed a logic tree for representing these events. A detailed review of the Exelon and the 2008 USGS characteristic earthquake models for the NMSZ was conducted. Estimates of the locations, potential magnitudes, and recurrence of the characteristic events are similar in both models, even though the Exelon model is appreciably more detailed. The main difference is that the USGS also considers an un-clustered model giving only 50% weight to their clustered model while the Exelon model incorporates only the clustered model with a 100% weight. Thus the Exelon approach is appreciably more conservative and it is considered that this level of conservatism is adequate for assessing the seismic hazard for critical facilities such as nuclear power plants. The Exelon model for the NMSZ has also been adopted by EPRI in the 2004 update of the seismic hazard for nuclear power plant sites in the CEUS.

Based on the Clinton ESP (EGC, 2006), the logic tree used to represent the uncertainty in the model for the NMFS characteristic events is shown on Figure 2.5-42. The first two levels of the logic tree take into account the uncertainty in the location and extent of the faults that can rupture in an earthquake sequence, by considering alternative geometries for the NS, RF and NN Faults. The considered fault locations are displayed on Figure 2.5-74. Distances to the BBNPP site for the various options are listed in Table 2.5-9.

For the New Madrid South fault arm, two alternatives are considered:

1. Blytheville arch/Bootheel lineament (BA/BL); weight 0.6, length 82 mi (132 km), and

2. Blytheville arch/Blytheville fault (BA/BFZ); weight 0.4, length 71 mi (115 km).

Two alternative total lengths are considered for the New Madrid North fault arm:

1. With a weight of 0.7, rupture of the NN 37-mi (60-km) segment, and

2. The 60 mi (97 km) length including the NN and NNE is given a 0.3 weight.

Two possible alternatives are considered for the Reelfoot arm:

1. A full length segment including the northwest part, with weight 0.7, and

2. A central segment, excluding the northwest part, with 0.3 weight.

New Madrid Characteristic Earthquake Magnitude

Table 2.5-10 contains expected moment magnitudes for characteristic earthquake ruptures for each fault within the New Madrid Fault System along with their corresponding weights. As considered in the Clinton ESP, the size of the next characteristic earthquake is assumed to vary randomly about the expected value following a uniform distribution over a range of ±0.25 moment magnitude units, to represent the aleatory variability in the size of individual characteristic earthquakes.

For the Clinton ESP, constraints on recurrence of characteristic NMFS events were derived from paleoliquefaction and paleoseismic investigations of the Reelfoot fault scarp and associated fold. It was concluded that the NMFS has generated temporally clustered large earthquakes in AD 900±100, AD 1450±150 years and in 1811 to 1812; the time between clustered events may be from 200 to 800 years, with an estimated average of 500 years. Thus, a quantitative assessment of the uncertainty in the dates for prehistoric New Madrid earthquakes was developed, using a Monte Carlo simulation of constraints on the possible dates for the prehistoric earthquakes. The time intervals between these simulated dates were then fit with poissonian and renewal recurrence models. Table 2.5-10 lists the discrete distribution for equivalent annual frequency for characteristic New Madrid earthquakes. In this table, for Model A, all ruptures are similar in size to the 1811 and 1812 earthquakes. In Model B, 1/3 of the sequences consider a smaller (lower magnitude) rupture of the New Madrid North fault and 1/3 of the sequences assume a smaller rupture of the New Madrid South fault. The difference in magnitude from the 1811and 1812 ruptures was set to be no more than 1/2 magnitude unit, and no magnitude ruptures are considered to be less than M 7. Model A and Model B were assigned weights of 2/3 and 1/3, respectively.

New Madrid Characteristic Earthquake Recurrence

The recurrence estimates, based on the poissonian and renewal models, used to represent the occurrence of characteristic New Madrid earthquakes in the Clinton ESP have been used herein, as well as their corresponding weights, as summarized in Table 2.5-10. Since the site is affected by three dependent events, the frequency of exceedance, $v(z)$, of a spectral value z from a characteristic earthquake sequence is where:

$$v(z)_{characteristic} = \lambda_{rate\ of\ cluster}(1-(1-P_1)(1-P_2)(1-P_3))$$

$v(z)_{characteristic}$ is the probability of exceeding ground motion z,

$\lambda_{rate\ of\ cluster}$ is the equivalent mean annual rate of occurrence of the event cluster, and

P1, P2, and P3 are the probabilities of exceeding the ground motion level z, when an earthquake of specified magnitude and distance occurs.

The values and weights for the rate of cluster are included in Table 2.5-10.

New Madrid Characteristic Earthquake Ground Motion Assessment

Consistent with the hazard calculation for area sources, the contribution of the New Madrid characteristic events was conducted using the CEUS ground motions developed by EPRI

(EPRI, 2004). Figure 2.5-75 shows the logic tree structure defined by EPRI to represent the uncertainty in the median ground motion equation and in the aleatory variability about the median. As noted in the previous sections for area sources, the EPRI 2004 Report defines four clusters of median ground motion models to represent the alternative modeling approaches. All four clusters have been used for assessing the hazard from the New Madrid characteristic earthquakes, as illustrated on Figure 2.5-75. The rift option was selected for the fourth cluster, instead of the non-rift option that is used for area sources.

The three branches of the second level of the logic tree on Figure 2.5-75 represent the epistemic uncertainty in the median attenuation relationship for each cluster. The branches incorporate a three-point discrete distribution with weights of 0.63, 0.185 and 0.185 for the median, the 5th and the 95th percentiles, respectively. The third branching level addresses the uncertainty in the model for the aleatory variability in ground motions about the median attenuation relationship. Models 1A and 1B, as well as their weights, are those proposed by Abrahamson (EPRI, 2006a)(EPRI, 2006b) to account for inter-event and intra-event variability for events with distances longer than 12.4 mi (20 km) (termed s1 by Abrahamson). The additional standard deviation, s2, developed by Abrahamson to incorporate additional variability at short distances, is not applicable for the distances between the BBNPP site and any of the arms of the New Madrid faults.

The EPRI 2004 ground motion attenuation relationships use either the closest distance to the rupture plane or closest distance to the surface projection of the rupture plane (Joyner-Boore distance). Thus, the EPRI 2004 document also presents adjustments for use when the hazard integration is conducted based on point-source distances. These adjustments were unnecessary in the hazard calculations due to the New Madrid characteristic events, since the specific closest or Joyner-Boore distance was calculated for each fault arm, for input to the EPRI ground motion models.

2.5.2.2.3.2 Updated Charleston Seismic Source (UCSS) Model

Results of several post-EPRI studies have demonstrated that the parameters of the Charleston seismic source need to be updated. These parameters include the geometry, the maximum magnitude and the recurrence of characteristic events. Recent models of the Charleston characteristic earthquake are significantly different from the 1986 EPRI characterizations. The most recent and detailed study of the Charleston characteristic events has been conducted for the Vogtle ESP (SNOC, 2008) producing the so-called Updated Charleston Seismic Source (UCSS) Model. The present PSHA for the BBNPP has adopted the UCSS model that was developed for the Vogtle ESP (SNOC, 2008) and was also used in the seismic hazard studies that support the recent FSAR for the CCNPP Unit 3 (UniStar Nuclear, 2007). The following description of the UCSS model is based on Section 2.5.2 of the CCNPP Unit 3 FSAR. The information with the largest relevance for the BBNPP site is the assessment of characteristic magnitude. The exact location is less important in view of the large distance, more that 500 mi (805 km), to the BBNPP site. The selection of the UCSS model has been based on the review of current literature related to the geometry (Marple, 2000; USGS 2002; USGS 2008), maximum magnitude (Johnston, 1996; Bakun 2004; USGS 2008), and recurrence intervals (Obermeier, 1987; Talwani, 2001). Based on this literature review (including the UCSS model), it was concluded that the UCSS model better captures the epistemic uncertainty in recurrence intervals and source zone geometries. The mean of maximum magnitude distribution is very similar to other models. For this reason, the UCSS model was selected as the preferred model to characterize the characteristic earthquake for the Charleston seismic source.

UCSS Geometry

The UCSS model includes four mutually exclusive source zone geometries (A, B, B', and C; Figure 2.5-82). These geometries have been defined based on the current understanding of geologic and tectonic features and shaking intensity in the region affected by the 1886 Charleston earthquake; on the distribution of seismicity; and on the geographic distribution, age, and density of liquefaction features associated with both the 1886 and prehistoric earthquakes. These features indicate that most of the evidence related to the Charleston source is concentrated in the Charleston area and is not widely distributed throughout South Carolina.

Geometry A

Geometry A is a northeast-oriented area centered at the 1886 Charleston meizoseismal area (Figure 2.5-82). This geometry encompasses the 1886 earthquake MMI X isoseismal (Bollinger, 1977), most identified Charleston area tectonic features and inferred fault structures and the majority of reported 1886 liquefaction features. Geometry A excludes outlying liquefaction features, because liquefaction occurs as a result of strong ground shaking that may extend well beyond the aerial extent of the tectonic source.

Existing evidence indicates that the seismic source for the 1886 Charleston earthquake was located in a relatively restricted zone defined by Geometry A. This zone envelops the local tectonic features, the area of ongoing concentrated seismicity, the area of high density liquefaction features, and the meizoseismal area of the 1886 earthquake. These observations suggest that future earthquakes with magnitudes comparable to the 1886 Charleston earthquake will likely occur within the area of Geometry A. Thus, a weight of 0.7 has been assigned to Geometry A (Figure 2.5-83).

Geometries B, B', C

Geometries B, B', and C are defined to capture the possibility that future earthquakes may not be restricted to Geometry A. The distribution of liquefaction features along the entire coast of South Carolina suggests that the Charleston source could extend beyond Geometry A. Therefore, Geometries B and B' represent larger source zones, while Geometry C represents the southern segment of the hypothesized East Coast Fault System source zone. Geometry B' is a subset of B and defines the onshore coastal area as a source thus restricting the earthquakes in such onshore regions.

Geometry B - Coastal and Offshore Zone

Geometry B is a coast-parallel source including Geometry A in its entirety and elongated to the northeast and southwest to capture more distant liquefaction features in coastal South Carolina. The source also extends to the southeast region to include the offshore Helena Banks fault zone. This geometry is assigned a weight of 0.1.

Geometry B' - Coastal Zone

Geometry B' is a coast-parallel source that also incorporates all of Geometry A, as well as the majority of reported paleoliquefaction features. However, it does not include the Helena Banks Fault Zone. A weight of 0.1 has been assigned to this geometry.

Geometry C - East Coast Fault System (ECFS South Segment)

Geometry C envelops the southern segment of the proposed East Coast Fault System (Marple, 2000) as a possible source for the 1886 Charleston earthquake. A weight of 0.1 has been assigned to geometry C.

<u>UCSS Maximum Magnitude Return Period</u>

Based on currently available data and interpretations regarding modern M_{max} estimates (Table 2.5-18), the UCSS model modifies the USGS magnitude distribution (USGS, 2002) to include a total of five discrete magnitude values each separated by 0.2 M units (Figure 2.5-83). The UCSS M_{max} distribution includes a discrete value of M 6.9 to represent the Bakun best estimate of the 1886 Charleston earthquake magnitude, as well as a lower value of M 6.7 to capture a low probability that the 1886 earthquake was smaller than the Bakun mean estimate of M 6.9 (Bakun, 2004).

The UCSS magnitudes and weights are as follows:

M	Weight
6.7	0.10
6.9	0.25
7.1	0.30
7.3	0.25
7.5	0.10

This, results in a weighted mean Maximum magnitude of M 7.1 for the UCSS. This is slightly lower than the mean magnitude of M 7.2 in the USGS model (USGS, 2002).

The UCSS model incorporates geologic data to characterize the return period of M_{max} earthquakes. Identifying and dating paleoliquefaction data provides a basis for estimating the recurrence of large earthquakes. Recent estimates of M_{max} recurrence intervals are significantly shorter than estimates in the EPRI models. Details regarding the processing, aging, and completeness of Charleston paleoliquefaction data can be found in Talwani (Talwani, 2001) and the CCNPP Unit 3 FSAR (UniStar Nuclear, 2007).

Records along two different time intervals (2000 yr and 5000 yr) are used in the UCSS model. Return periods derived from recorded paleoliquefaction features assume that these features were produced by large M_{max} events and that both the 2000-year and 5000-yr records are complete.

The UCSS model calculates two average recurrence intervals covering two different time intervals, which are used as two recurrence branches on the logic tree (Figure 2.5-83). The first average recurrence interval is based on four events that occurred in the past 2000 years. The second average recurrence interval is based on events that occurred within the last 5000 years. The 2000 and 5000 records have been assigned weights of 0.8 and 0.2, respectively.

2.5.2.2.3.3 The Ramapo Fault

Reactivation of the Ramapo Fault during the Quaternary period has not been demonstrated. Results of core analyses in six localities of Ramapo and other basin-border faults showed that the most recent slip was extensional at each locality. The extensional tectonic episode did not extend beyond the Mesozoic and there is no evidence of post-Jurassic displacement (Sykes, 2008).

There is an apparent discrepancy between the distribution of earthquakes in the Ramapo Seismic zone and the lack of displacement in the last 150 Ma in the localities where the cores have been taken (Sykes, 2008). As a possible explanation for this discrepancy, it is assumed that earthquakes may originate from other preexisting faults which may or may not strike similar to the Ramapo fault. The term "Ramapo Seismic Zone" (RSZ) is used for the seismically active 7.5 mi (12 km) wide eastern area of the Reading Prong (Sykes, 2008). Since post 1974 earthquakes have been located with higher accuracy, this 7.5 km (12 km) width cannot be attributed to location errors. Therefore, it is concluded that more than one fault must be involved in generating the earthquakes (Sykes, 2008). This instrumental data suggests that activity in the Manhattan prong cuts off abruptly along a nearly vertical, northwest-striking boundary that extends from Stamford, Connecticut, to Peekskill, New York. The Peekskill-Stamford boundary is considered a newly identified feature (Sykes, 2008). It was possible to identify it after accurate locations and depths of earthquakes, especially those east of the Hudson River, however, became available with the installation of a seismic station near the New York–Connecticut border in 1971.

It is not clear which faults are active. The seismicity data used and processed cannot be solely used to delineate a single fault or multiple faults. Geologic evidence of Holocene fault movements is also very hard to be found in the study area. It is not possible to conclude that the Ramapo fault is an active feature. Therefore, even though it cannot be ruled out as a possible source for some of the observed earthquakes, the cause of the earthquakes is still unknown. This is a conclusion that has been reached by most previous studies (Kafka, 1985).

Recent research (Sykes 2008) has extrapolated the Gutenberg-Richter (GR) recurrence law for the earthquakes to magnitudes 6 and 7 and obtained the repeat times of 670 and 3400 years respectively. This has been done based on the observed seismicity of the whole study area and not just the Ramapo fault. It is not clear which magnitude will probably represent the maximum magnitude for the area or for the Ramapo fault assuming that it is active. The largest observed earthquake in the area is the 1884 (offshore) New York earthquake with m_{bLg} = 5.25. Based on the observed seismicity a maximum magnitude of 6 or slightly higher is adequate.

The EPRI seismic source model does not consider the Ramapo fault system as a separate seismic source. For the BBNPP PSHA, the maximum magnitudes of the EPRI seismic source zones (that encompass the Ramapo seismic zone) range from 5.3 to 7.1. These values have been presented in different logic trees by six EPRI teams and adequately characterize the upper level seismicity.

Even though a larger source zone (currently used in the BBNPP PSHA) tends to diffuse the hazard, this would only have an effect if the RSZ was located closer to the site. Based on the available data and information the current PSHA results adequately reflect the hazard at the BBNPP site from the Ramapo fault zone. The Ramapo fault is located 82-93 mi (132-150 km) away from the BBNPP site. Some branches of the Ramapo fault system (not the Ramapo fault itself) may extend into southeastern Pennsylvania. Those branches have similar distances from the site. Assuming the Ramapo fault is an active source (with M_{max}~6.0), would still not produce significant ground motion at the site because of the relatively large distance. A sensitivity analysis is performed as follows to support this conclusion.

As previously mentioned, the largest known event in the study area of Sykes et al. (1998) is an earthquake of m_{bLg} 5.25 which occurred offshore of New York City in 1884. From the extrapolation of the frequency-magnitude relationship for the study area, Sykes predicts return periods of 670 and 3500 years for events with magnitudes equal to and larger than 6.0 and 7.0, respectively. It is not clear how far the extrapolation should go, which translates into how large M_{max} should be. A maximum magnitude of 6.0 or slightly larger is adequate based on the maximum observed earthquake. Assuming a maximum magnitude of M 6.0 for the RSZ, it is possible to compare this value with the maximum magnitude distribution of the EPRI-SOG source zones. Table 2.5-62f shows the maximum magnitude distribution for the EPRI-SOG source zones that encompass the RSZ.

Figure 2.5-86i shows the study area of Sykes et al., (2008). Events are from the USGS 2002 catalog and are supplemented by PDE events up to the end of 2007. The PDE catalog does not include all the events with magnitudes less than 3. Approximate boundaries of RSZ are shown by the dashed lines. The arrows denote northwest-striking seismic boundary between Stamford, CT and Peekskill, NY (Sykes et al., 2008).Only the Bechtel Source Zone 13 and Weston Source Zone 21 have maximum magnitudes below the assumed maximum magnitude for the RSZ (M 6.0). All other EPRI-SOG source zones in Table 2.5-62f have higher mean values than M 6.0. It should be noted that the RSZ is a small part of a larger area in the Sykes et al. (2008) study. Most studied events (especially the larger shocks) are not located in the RSZ zone. Therefore, considering a maximum magnitude of M 6.0 is adequate for the RSZ. Furthermore, it can be seen that the maximum magnitudes in Table 2.5-62f can adequately characterize the upper bound magnitude in the Sykes et al. (2008) study area and not just the RSZ zone. The only exception would be the Weston mean value.

As a sensitivity analysis case, the contribution of the RSZ and the Greater New York City-Philadelphia area (as defined in Sykes et al. (2008)) to the hazard has been further investigated by considering them as "stand-alone" seismic source zones. The study area of Sykes et al. (2008) is referred to as the NY-Ph seismic zone. Since recent fault displacements in the area have not been observed, area source zones are used to characterize the seismicity. Two cases are considered:

(a) Ramapo Seismic Zone

A narrow seismic zone has been drawn around the RSZ area as defined by Sykes et al. (2008). The selected area is somewhat broader than the RSZ in the 2008 Sykes paper. A reliable estimate of the b value cannot be obtained; therefore, a regional b value for the Central and Eastern United States (CEUS) of 0.95 is utilized. The completeness periods obtained in the Sykes et al. (2008) paper are very similar to the completeness periods used in USGS hazard maps for the CEUS. These analyses used the USGS completeness periods for the CEUS and the EPRI (2004) attenuation relationships for hazard contribution of RSZ. Based on above discussions, a maximum magnitude of M 6.0 was used for this zone. All other inputs are also the same as the ones used for hazard calculation at the Bell Bend site.

(b) NY-Ph study area

The study area with coordinates (40° N-42° N and 73.5° W-75.5° W) has been used to define the larger source zone without any change. A b value of 0.85 from the seismicity of this region has been derived. This is higher than the value of 0.7 derived by Sykes et al. (2008) but this value is preferable since it is based on the analysis with the current catalog. The maximum magnitude for this zone is M 6.0 as previously discussed. As in the case for the RSZ, all other inputs remain unchanged.

The results of the previous two cases are reported in Section 2.5.2.4.7.

2.5.2.2.3.4 The St. Lawrence Zone

Recent research has been performed in the southeastern corner of Lake Ontario and the western Lake Ontario in a search for evidence of neotectonic faulting (Wallach, 2002). In the Rochester Basin, vertical separations of layers of unconsolidated sediments and the underlying Paleozoic bedrock had been recognized. It may be possible to interpret that the observed displacements of the units are due to the recent tectonic faulting (Wallach 2002). However, such interpretation remains uncertain. Finding Quaternary faulting in Eastern North America (ENA) will continue to be difficult. Evidently, more rigorous study and work is needed in the study area to favor or to refute these interpretations.

In addition, historical seismicity, including instrumentally recorded data, show significant seismic activity in 3 areas of the St. Lawrence Seismic Zone (LSZ): (1) the Lower St. Lawrence Seismic Zone, (2) the Charlevoix Seismic Zone, and (3) the area of the 1944 Cornwall-Messana earthquake. The study region in the Lake Ontario south of Cornwell has not experienced high seismicity. According to the Earthquakes Canada website the region of southern Great Lakes has a low to moderate level of seismicity compared to more active zones to the east in general and to Charlevoix in specific. A map of seismicity on the website shows even fewer events for the Lake Ontario (Earthquakes Canada, 2008). It may be argued that the seismicity history is short but other zones in the Saint Lawrence Seismic Zone show high levels of activities in the same short period of time. According to the same website, on average, 2 to 3 magnitude 2.5 and larger earthquakes have been recorded in the southern Great Lakes region in the past 30 years. It is postulated that (Wallach, 2002):

"Because earthquakes of M ~ 5.5-7.0 have been spatially related to the Saint Lawrence fault zone northeast of study area, similar sized earthquakes might reasonably be expected beneath Lake Ontario".

In order to further investigate on previous postulate, different studies conducted to refine the location of earthquakes in Eastern North America (ENA) in order to correlate the epicenters with existing geologic structures and lineaments were reviewed. Some of these studies have focused on the earthquakes of the Eastern Great Lakes (Dineva et al., 2004; Ebel and Tuttle, 2002; Seeber and Armbruster, 1993; Mohajer, 1993). The study area is characterized by Paleozoic sedimentary rocks lying on Precambrian basement (Seeber and Armbruster, 1993). Among geologic structures and proposed lineaments that transect the area, only a few seem to correlate with the observed clusters of seismicity. For example, seismicity in the Attica seismic zone has been associated with the Clarendon-Linden fault but even in this case the association is not absolute. The Eastern Great Lakes Basin (EGLB) is an area of low to moderate seismicity and the largest recorded earthquake in this area had a magnitude of less than about 5.5. Some of the mentioned studies have discussed the possibility of future large earthquakes in this area of low seismicity but none provided quantitative results (Ebel and Tuttle, 2002; Seeber and Armbruster, 1993).

Seeber and Armbruster (1993) argue that occurrence of a large earthquake can significantly change the pattern of seismicity and, therefore, favor the models which consider temporal changes in seismicity. This means that present areas of low seismicity may experience large earthquakes in the future. Armbruster and Seeber (1993) note that lack of evidence for substantial accumulated neotectonic displacements on structures such as the Clarendon Linden fault does not necessarily rule out the possibility of large earthquakes from such structures. Assuming that many such structures may exist in the study area, it would follow that large earthquakes may happen everywhere in ENA.

Time dependent models of seismicity are not well constrained except for special cases. Therefore, most seismic hazard studies are based on the assumption of stationary seismicity. As Seeber and Armbruster state "seismicity is still the main observable which can offer insight into intracratonic neotectonics and a basis for hazard assessment" (Seeber and Armbruster, 1993). In this case, the areas with low level of seismic activity are the areas with low levels of seismic hazard and this is confirmed by the seismic hazard maps. Unless strong geologic evidence indicates otherwise, observed patterns of seismicity will be the main basis for estimating recurrence parameters in seismic hazards. The geologic evidence should provide quantitative results as input for seismic hazard evaluations. Current available geologic data cannot constrain upper bound magnitude in the study area and most parts of ENA. Seismicity data, although limited, are used in many practices of seismic hazard assessment for this purpose. Some have adopted the approach in which data from similar tectonic environments supplement the limited existing data.

Ebel and Tuttle (2002) present a summary of seismicity and its relation to stress and geologic structures in EGLB and characterize it as an area with a lower rate of earthquake activity in comparison to the New Madrid, Charlevoix, and Saint Lawrence Valley seismic zones.

Ebel and Tuttle (2002) show seismicity rates per 100 years as contour plots for ENA. The plots clearly shows low levels of activity in Lakes Ontario and Erie compared to other active seismic zones of ENA. Ebel and Tuttle (2002) mention that 4 paleoseismology studies in the EGLB have not found evidence of large ($M > 6$) earthquakes during recent geologic times. The low seismicity rates may represent a long-term behavior of the region and potential large earthquakes ($M > 6$) in the region may have long recurrence intervals of > 12000 years (Ebel and Tuttle, 2002).

The 2005 version of Canadian National Seismic Hazard Maps (2% in 50 yrs) shows that Lake Erie and Lake Ontario are areas of low to moderate hazard. The maps are for firm ground or soil class C of the National Building Code of Canada (NBCC). The 2008 version of USGS National Seismic Hazard Maps (2% in 50 years) for site class BC conform to the Canadian maps with somewhat lower hazard values for the study area.

The studies provided by Wallach (2002) do not provide any quantitative results or descriptions of tectonic features that could be used for quantitative analyses. The author claims that earthquakes up to magnitude 7 might reasonably be expected beneath Lake Ontario and implies that seismic hazards in the area of this lake might be comparable with that of seismically active areas of the St. Lawrence seismic zone. There is no direct geologic evidence to support this conclusion. Seismicity in the area obviously shows much lower activity levels compared with Charlevoix and other active areas of the St. Lawrence seismic zone. Assuming upper bound magnitudes of 7 or larger for the area would be an overestimation of this parameter while the maximum recorded event had a magnitude of $M < 5.5$. There is not sufficient evidence that could support the westward extension of the seismic zone. The lower St. Lawrence Zone and the Charlevoix zone are properly accounted for by the BBNPP PSHA.

2.5.2.2.3.5 The New England Seismic Source Zone and the Cape Ann Earthquake

The area of seismic activity of the New England region in northeastern United States is called the New England seismic zone. The seismic zone has experienced small to moderate historical seismicity. The 1755, M 5.9, Cape Ann earthquake (Ebel, 2006) is an example of the moderate historical events in this seismic zone. There is no evidence that earthquakes with magnitudes M 7.0 or larger may have happened in this seismic zone. The estimated magnitude of the 1638 New Hampshire earthquake (Estimated M=6.5-7.0) (Ebel, 1996) is also uncertain. The Weston Observatory of Boston College has operated a seismic network to monitor the earthquake activity in the New England seismic zone and adjacent areas. The seismic network can provide more accurate earthquake locations that can be used to explore the possibility of correlation between the epicenters and known tectonic and geologic features. Moderate magnitude events (M=6.0) from this seismic zone (which is located beyond the 200 mile radius) will not result in significant ground motion levels at the BBNPP site.

The Cape Ann, Massachusetts earthquake of 1755 was felt over an extensive area along the East Coast around the New England Region. The most likely location of its epicenter is 25 mi (40 km) East North East of Cape Ann, Massachusetts (Ebel, 2006). The estimated moment magnitude is M 5.9 and it is believed that peak ground accelerations were as high as 0.08 to 0.12 g in some soil locations. Due to the large distance and moderate (estimated) magnitude for this event, it is concluded that such earthquakes would not significantly affect the seismic hazard at the BBNPP site.

Recent research (Ebel, 2006) aims at refining the earthquake location and providing estimates of ground motion levels at a few locations using different methods for the 1755 earthquake. Three different methods have been used to estimate ground motion from the 1755 earthquake (Ebel, 2006): (1) using attenuation equations for CEUS assuming a magnitude and distance for the earthquakes; (2) MMI to ground motion conversions; and (3) estimates from chimney and unreinforced masonry damage. Ground motion estimates from the three methods have been given for PGA and 0.3 sec spectral acceleration assuming 5% damping for soil and rock sites at several locations.

The most distant location (Ebel, 2006) analysis of ground motion using attenuation relationships is New Haven, CT with an estimated distance of 175 mi (282 km) from the epicenter. The most conservative estimates for PGA and SA (0.3 sec) among all possibilities are 0.01g and 0.014g respectively. The soil acceleration for the same hazard level is 0.21 g. The Bell Bend site is located at a larger distance from the proposed epicenter of the 1755 event. The PSHA of the BBNPP site results in a uniform hard rock PGA of 0.1 g for 1E-4 hazard level.

The Cape Ann earthquake and associated seismic area do not have a significant contribution to the seismic hazard at the BBNPP site. The Cape Ann earthquakes are included in the PSHA in the USGS 2002 catalog and as part of the Law Engineering EST EPRI source zones.

Another earthquake of interest is M 5.6, 1727 Newbury event. The estimated magnitude for the 1727 event is M 5.6 (Ebel, 2000), which is a moderate event. This event is distant from the BBNPP site and would not have a significant contribution to the hazard.

Significant zones of seismicity in New England are located at large distances (beyond 250 miles (402 km)) from the BBNPP site. The area has not experienced the occurrence of large earthquakes. The contribution from this seismic zone will be much less than NY-Ph because of the large distance from the site. In the initial hazard calculation for the Bell Bend site, some EPRI sources were considered that covered parts of seismicity in the New England Seismic zone. These sources had negligible contribution to the hazard at the site. Records of historical seismicity do not indicate the possibility of earthquakes with M ≥ 7.0. There is also no geologic evidence of active or potentially active structures capable of producing such earthquakes. Examples of some EPRI source zones that cover parts of seismicity in the New England region are listed below. The mean maximum magnitude for each source is also given.

Bechtel:

Source zones 5 (M 6.2), 8 (M 6.2), 9 (M 6.2), and BZ8 (M 6.2)

Dames and Moore:

Source zones 2 (M 6.7), 56 (M 6.6), and 61 (M 6.2)

Source zone 53 has already been included

Law Engineering:

Source zones 24 (M 5.6), and 102 (M 5.7)

Rondout Associates:

Source zones 40 (M 6.8), and 43 (M 6.5)

Weston Geophysical:

Source zones 13 (M 6.0), and 14 (M 6.0)

All teams (except LAW Engineering) used maximum magnitude distributions with mean value around 6.0 or higher. This is adequate for many zones in New England. It is important to note that post-EPRI data do not imply any need for defining new seismic zones. The question is whether the maximum magnitudes are needed to be updated. The 1755 Cape Ann earthquake had an estimated magnitude of M 5.9. The 1638 New Hampshire earthquake might have had a magnitude larger than 6.0. This does not justify update of the M_{max} for the whole New England region. Regardless, increasing the EPRI M_{max} values for seismic sources in the New England region by 0.5 units would have a negligible effect on the hazard values at the BBNPP site due to the large distance from the site. Sensitivity analyses performed for the Ramapo Fault System (Section 2.5.2.4.7.3), which is closer to the BBNPP site clearly indicate that quantitative sensitivity on the New England Seismic Source Zone would not affect the PSHA results.

2.5.2.2.3.6 Charlevoix

As previously discussed, the Charlevoix seismic zone is the most seismically active region of Eastern North America. It is located about 60 mi (97 km) downstream from Quebec City. All six

EPRI teams have considered the Charlevoix seismic zone in their source zone models and assigned maximum magnitudes close to or larger than 7.0. This seismic zone is located beyond the 200 mile radius of the BBNPP site, but a sensitivity analysis showed that it is a contributor to the seismic hazard at Bell Bend site lower frequencies.

Section 2.5.2.4.2 provides a discussion on related to the Gutenberg-Richter b parameter update from the original EPRI-SOG work. The BBNPP evaluation considered that an update is required to the b value of this zone. Values of b for the Charlevoix seismic zone were computed using the USGS 2001 (USGS, 2002) catalog and source zone geometries of Dames and Moore and Woodward-Clyde and a value of 0.7 was obtained in both cases. This is consistent with the b value obtained by other EPRI EST teams. Therefore, the b value for the Charlevoix seismic zone for those two teams was changed to 0.7. A b value of 0.7 is slightly more conservative than 0.79. Due to the long distance of the Charlevoix seismic zone from the BBNPP site, the new b value equal to 0.7 does not have a significant impact on the PSHA results.

An event of interest near the Charlevoix Zone is the November 25, 1988 Saguenay, Quebec earthquake, which occurred 22 mi (35 km) south of Chicoutimi, Quebec and 47 mi (75 km) north (northwest) of the Charlevoix seismic zone (Earthquakes Canada, 2008). The earthquake had an estimated magnitude of 5.9 in both body wave and moment magnitude units (m_b 5.9, M 5.9). A depth of 18 mi (29 km) was estimated for the earthquake. This earthquake was located outside the Charlevoix seismic zone and, according to Earthquakes Canada, it occurred in a relatively aseismic region. The earthquake was felt over a wide area with a maximum epicentral intensity of VII-VIII. The maximum recorded accelerations on rock were 0.156 g on the horizontal component (at 40 mi (64 km) distance) and 0.102 g on the vertical component (at 27 mi (43 km) distance).

The epicenter of Saguenay earthquake (48.12 N, 71.18 W) was located about 540 mi (870 km) from the BBNPP site. According the intensity map of Earthquakes Canada website, this event was felt with intensity III (MMI scale) in Pennsylvania.

The Saguenay earthquake epicenter is outside all defined areas of Charlevoix seismic zone for all 6 ESTs. The maximum magnitude estimates for the zone that contain the 1988 earthquake may have been underestimated by the EPRI teams. Since there has been no significant seismicity in the epicentral area of 1988 prior to the Saguenay earthquakes, most ESTs have defined small source zones for the Charlevoix based on the well defined area of significant seismicity. Weston has defined an alternative zone to consider the probability that some events outside Charlevoix may indeed belong to this zone. Rondout Associates defined a larger zone for Charlevoix and the 1988 is outside but very close to the western edge of this zone. The following are two cases suggested for the EPRI source zone model:

1. Define a broader Charlevoix seismic zone to cover the epicentral area of the 1988 earthquake. For all 6 ESTs, the geometry of the Charlevoix source zone was modified as shown in the Figures 2.5-86j through 2.5-86o. The parameter b and maximum magnitude distribution remained as used in the base case analysis. Since the Mmax of the existing EPRI/SOG source zones for Charlevoix is about M 7.0 or more, no increase in this value is required because the magnitude of the 1988 earthquake is only M 5.9. The b values used in the base case PSHA do not need to be changed. This was verified by adding the 1988 earthquake to the catalog for Charlevoix events and deriving the b value. The b value remains unchanged. Furthermore, additional earthquakes with epicenters within 625 (1000km) miles radius in the period of 2002-2007 were added to the USGS 2002 catalog and were considered in the evaluation of the impact of the

modification of the EPRI source zone model. The radius was selected to incorporate events as far as the Saguenay location. These events are shown in Figures 2.5-86j through 2.5-86o.

2. Increase the maximum magnitude distribution (Table 2.5-62d) of the current source zones that contain the epicenter of the 1988 earthquake. New earthquakes in the period 2002-2007 inside the 625 mile (1000 km, approximately) radius were updated into the USGS 2002 catalog. The b value and maximum magnitude distribution for the other zones remain without changes. The following adjustments were incorporated as an update sensitivity to the EPRI source zone model:

   - For the Bechtel EST, the Saguenay Earthquake is outside Source Zone 3 (Charlevoix/La Malbaie) and Source Zone 2 (St. Lawrence), but is located inside the Background Zone 7 (BZ7, Figure 2.5-86p). The seismic parameter b and maximum magnitude for BZ7 remains unchanged.

   - For the Dames and Moore EST, the Charlevoix Source Zone (Zone 59, Figure 2.5-86q) does not include the Saguenay Earthquake, but this event is inside Source Zone 72 (Eastern Canada Province). Consequently, Zone 72 was defined using the maximum distribution indicated in Table 2.5-62d and a parameter b=1.04.

   - For the Law Engineering Team EST, a new seismic zone (Zone 109, Figure 2.5-86r) was defined in the EPRI source model by using the magnitude distribution indicated in Table 2.5-62d. A parameter b=0.970 was considered.

   - For the Rondout and Weston Geophysical Source Zones ESTs, the Saguenay Earthquake is not inside the Charlevoix Zone. Source Zones 50-1 and 18 were incorporated and assigned a b value of 1.01 and 0.90, respectively (Figures 2.5-86s and 2.5-86t).

   - For the Woodward and Clyde Source Zones, the 1988 event is outside Zone 12 (Charlevoix). Because there is not a source zone which includes this event, a new source zone was defined in order to include this earthquake (Figure 2.5-86u). The new source zone was defined with a b value of 0.90 and a maximum magnitude distribution as indicated in Table 2.5-62d.

2.5.2.3 Correlation of Earthquake Activity with Seismic Sources

{Following Regulatory Guide 1.165 (NRC, 1997a) and 10 CFR 100.23 (CFR, 2007), a PSHA was conducted to determine the SSE and to account for uncertainties in the seismological and geological evaluations for the BBNPP site. The probabilistic approach was based on the PSHA conducted by the EPRI for CEUS in the mid to late 1980s (EPRI, 1989a) with changes to incorporate updated data. Expert opinion was incorporated following a Senior Seismic Hazard Analysis Committee (SSHAC) approach (NRC, 1997b).

The location of earthquakes was accounted for by an updated USGS catalog (USGS, 2002), covering events between 1627 and 2007. The updated catalog has been adopted for assessing the BBNPP site seismic hazard. This update is a refinement of the EPRI SOG catalog that listed earthquakes between 1627 and 1984 (EPRI, 1988). Figure 2.5-34 through Figure 2.5-39a show the distribution of earthquake epicenters from both the EPRI (EPRI, 1986) and updated 2001 USGS (USGS, 2002) earthquake catalogs in comparison to the seismic sources identified by each of the EPRI ESTs. These figures include updates for seismic activity in the zones for 2002 – 2007 out to a radius of 500 mi (805 km) from the BBNPP site. The comparison of earthquake distributions from both earthquake catalogs supports the following conclusions:

- The updated catalog does not show any earthquakes within the site region that can be associated with a known geologic or tectonic structure.
- The updated catalog does not show a unique cluster of seismicity that would suggest a new seismic source outside of the EPRI seismic source model (EPRI, 1986).
- The updated catalog does not show a pattern of seismicity that would require significant revision to the EPRI seismic source geometry.
- Two events were added to the 2001 USGS catalog in the period of 2002-2007. This update does not impact the result of the PSHA.}

2.5.2.4 Probabilistic Seismic Hazard Analysis and Controlling Earthquake

{Sections 2.5.2.4.1 through 2.5.2.4.6 are added as a supplement to the U.S. EPR FSAR.

2.5.2.4.1 1989 EPRI Probabilistic Seismic Hazard Analysis

The seismic hazard for the BBNPP was calculated using the original EPRI EST teams area sources, plus the New Madrid and Charleston characteristic earthquakes, and with the updated ground motion model and aleatory uncertainty model. This calculation was first made for hard rock conditions, and these results were then modified to account for local site conditions.

The analysis of seismic hazard consists of calculating annual frequencies of exceeding different amplitudes of ground motion, for all combinations of seismic sources, seismicity parameters, maximum magnitudes, ground motion equations, and ground motion aleatory uncertainties. This calculation is made separately for the New Madrid zone, for the Charleston zone and for the seismic sources defined by each of the six EPRI EST teams and results in a family of seismic hazard curves. The alternative assumptions on seismic sources, seismicity parameters, maximum magnitudes, ground motion equations, and ground motion aleatory uncertainties are weighted, resulting in a combined weight associated with each hazard curve. From the family of hazard curves and their weights, the mean hazard (and the distribution of hazard) can be calculated.

The quantification of the Probabilistic Seismic Hazard at hard rock utilized Rizzo's in-house software, ProHazard. This code uses the definition of site area seismic sources, the seismic potential of these sources in terms of generating future earthquakes, and the ground motion models, to estimate the annual exceedance probabilities for various levels of spectral accelerations at different spectral frequencies.

The technical methodology utilized in ProHazard follows the approach implemented in the 1989 Electric Power Research Institute study for Nuclear Power Plant Sites in the Central and Eastern United States (EPRI, 1989). This methodology is generally based on the early work of Cornell (Cornell, 1968) (Cornell, 1971) and integrates the product of the conditional probability that a ground motion measure will be exceeded given the earthquake magnitude and distance, and the probability distribution of magnitude and distance over all sources that can significantly contribute to the site seismic ground motion. This is expressed as:

$$v(z) = \sum \alpha_n(m_o) \int f(m) [\int f(r|m) P(Z > z|m,r) dr] dm$$

where:

Z is the peak ground acceleration or the spectral pseudo-acceleration at prescribed natural frequencies,

P(Z>z|m,r) is the conditional probability that Z will exceed a value z, given the earthquake magnitude, m, and distance, r,

f(m) and f(r) are the probability density functions for magnitude and distance, and

$\alpha_n(m_o)$ is the number of earthquakes per year above a prescribed minimum magnitude m_o, in the n-th seismic source.

The integration over magnitude is performed from m_o to an upper bound magnitude m_u, and the integration over distance is performed usually over a prescribed radius from the site, typically larger than 186 mi (300 km). The probability density function for distance assumes that earthquakes can occur randomly over the source areas or faults. The functions f(m) and $\alpha(m_o)$ define the recurrence relationships for the respective source zones.

The conditional probability in the above equation represents the random uncertainties in the natural phenomenon (aleatory). Additionally, ProHazard addresses epistemic uncertainties in sources and recurrence parameters and the ground motion attenuation resulting from limitations in the available data and alternative interpretations of this data. Alternative assumptions on seismic sources, seismicity parameters, maximum magnitudes, ground motion equations, and ground motion aleatory uncertainties are weighted, resulting in a combined weight associated with each hazard curve. The mean hazard and the distribution of hazard (i.e., median and fractiles) are obtained from the resulting family of hazard curves and the associated weights.

The attenuation relationships developed in 2004 by EPRI (EPRI, 2004) for the CEUS have been implemented in ProHazard. This model was the outcome of several workshops that convened a panel of six ground motion experts who developed a consensus-based ground motion model consisting of weighting of several attenuation relationships. The ground motion model relates spectral accelerations at frequencies of 100 Hz (equivalent to peak ground acceleration (PGA)), 25 Hz, 10 Hz, 5 Hz, 2.5 Hz, 1 Hz, and 0.5 Hz for generic hard rock conditions to moment magnitude at and distance to a given source. Epistemic uncertainty is represented using multiple ground motion equations and multiple estimates of aleatory uncertainty (sigma), all with associated weights. Further, EPRI (EPRI, 2006) corrects the excessive aleatory uncertainties in the 2004 study, particularly for low frequencies.

The above uncertainties are implemented in the ProHazard analysis utilizing the logic tree formalism. The logic trees represent discrete alternatives of models and model parameters and assign relative weights to the alternatives. These weights were developed from statistical analysis of the data and represent the best judgment of experts. Thus, several analyses reflecting various scenarios quantitatively assess the modeling uncertainties.

ProHazard has been subjected to the verification and validation procedures stipulated in Rizzo's Quality Assurance Manual. Computer software control for ProHazard has been done according to Rizzo's Quality Assurance Manual. The Quality Assurance Manual addresses software activities including software acquisition and development, tracking installation of design and analysis software on individual computers, program verification and validation, in-use testing, software usage, change control, configuration control, error notice documentation and distribution, software maintenance, virus protection, software retirement, records and monitoring.

The method used to verify and validate the capabilities of ProHazard are in accordance with methods accepted by the NRC and as described in EPRI NP-4726 (EPRI, 1986). Validation test problems are selected for testing specific combination of analysis capabilities of the ProHazard. The problems are modeled and analyzed using ProHazard. The analysis results obtained from ProHazard are then compared with the benchmark solutions from published technical literatures.

2.5.2.4.2 Effects of New Regional Earthquake Catalog

A sensitivity study was done in order to determine if the activity rates have changed. Seismicity rates in the EPRI study (EPRI, 1986) were based on an earthquake catalog that extended through 1984. The USGS 2001 catalog (USGS, 2002) has 17 more years of data and it was updated to include seismicity data up through the year 2007. Using the USGS 2001 catalog and completeness periods the b values for some of the EPRI source zones were computed and compared to the b values obtained by EPRI teams. The differences between the two sets of b values are small and can be attributed to using different catalogs and different completeness periods. For example, the EPRI b value for Rondout source zone 31 is 0.96 while the estimated b value using USGS 2001 catalog is 1.02. For many of the source zones the differences are less than 0.05. Therefore, the EPRI b values do not need any update with exception of the Charlevoix seismic zone. Except for the Dames and Moore and Woodward-Clyde teams, other EPRI EST teams have derived a b value between 0.70 and 0.79 for the Charlevoix seismic zone. The USGS used a b value of 0.76 (USGS, 1996) (USGS, 2002) (USGS, 2008) for this source zone based on the work of Adams and others in the Geological Survey of Canada. Values of b for the Charlevoix seismic zone were computed using the USGS 2001 (USGS, 2002) catalog and source zone geometries of Dames and Moore and Woodward-Clyde and a value of 0.7 was obtained in both cases. This is consistent with the b value obtained by other EPRI EST teams. Therefore, the b value for the Charlevoix seismic zone for those two teams was changed to 0.7. A b value of 0.7 is slightly more conservative than 0.79. However, considering the long distance of the Charlevoix seismic zone from the BBNPP site, the new b value equal to 0.7 does not have a significant impact on the PSHA results. No other changes in EPRI seismicity parameters are required.

2.5.2.4.3 New Maximum Magnitude Information

The upper magnitude, M_{max}, utilized in the magnitude recurrence equation could significantly affect the low probability seismic hazard, in particular from the near field events. In the 1989 EPRI/SOG (EPRI, 1989a) study, each EST developed alternative values of M_{max} for each seismic source in a body wave (mb) unit. More recent studies (USGS, 2008; Bakun, 2004), however, have revised M_{max} for the Charleston, New Madrid, and local sources. In addition, it has been recognized that large historical events have occurred at the New Madrid and the Charleston fault systems that cannot be adequately modeled by the G-R equation. Instead, the concept of characteristic earthquakes (Schwartz, 1984; Youngs, 1985) has been introduced to more appropriately represent the seismic activity at New Madrid and Charleston. Thus, characteristic events have been adopted in the calculation of the hazard at the BBNPP site. Moment magnitudes M between 7 and 8.1 were considered for the New Madrid source and between 6.5 and 6.7 for the Charleston source. Tables 2.5-3 through Table 2.5-8 list revised maximum magnitudes and their corresponding weights for the seismic sources selected for the BBNPP site PSHA.

The EPRI/SOG ESTs defined the maximum magnitude for each of their seismic sources using either body wave magnitude, m_b, or seismic moment magnitude, M. Furthermore, the G-R parameters a and b are derived in terms of m_b, while the equations for ground motion models are functions of M. Therefore, conversions from body wave magnitude into moment magnitude are required. The three magnitude-conversion relationships shown in Table 2.5-2 were used in the BBNPP PSHA and the three of them were assigned equal weight.

2.5.2.4.4 New Seismic Source Characterizations

New characteristic earthquake New Madrid and Charleston source models have been adopted to reflect updated estimates of the possible geometries and maximum magnitude at both fault zones. The Gutenberg-Richter (G-R) equation (Gutenberg, 1944) has been used to describe recurrence in area seismic sources. This equation was truncated at the maximum magnitude, M_{max}. The a and b parameters characterizing the potential of area seismic sources have been updated as well as their maximum earthquake magnitude. As noted before, each EPRI EST (EPRI, 1989a) developed G-R parameters a and b for each of their seismic sources, identifying their selected smoothing options and their corresponding weights. Smoothing allows incorporation of the variation of the G-R parameters a and b within the seismic source. For the BBNPP PSHA, the smoothing approach developed by USGS (USGS, 2002) (USGS, 2008) has been used. This approach considers only the variation of the intercept parameter a for prescribed constant values of the slope parameter b. The constant values of b have been taken as the averages of the b-values adopted for each seismic source by each EPRI EST (EPRI, 1989a), along with the corresponding weights for each smoothing option. Tables 2.5-3 through Table 2.5-8 present the values of the average seismic parameter b used as input to the BBNPP PSHA.

Four smoothing options are considered for characterizing the recurrence parameter a in the USGS 2008 approach. Each of the first three smoothing options is based on an incompleteness period, a minimum incompleteness magnitude, and a smoothing correlation distance. The fourth option is considered only for the background seismic source since it has negligible effect on main sources such as New Madrid or Charleston that have a much smaller area than the background source. The information for each model is listed in Table 2.5-16.

2.5.2.4.5 New Ground Motion Models

Once the earthquake sources are defined, attenuation relations relate the source characteristics of the earthquake and propagation path of the seismic waves to the ground motion at a site. Predicted ground motions are typically quantified in terms of a median value (a function of magnitude, distance, site condition, and other factors) and a probability density function of peak horizontal ground acceleration or spectral accelerations.

The estimation of strong ground motion for specified magnitude, distance, and site conditions in the CEUS is difficult due to the paucity of physical data. Most of the available data correspond to M < 5.8 and distances exceeding about 31 mi (50 km). Considerable effort has been directed to developing appropriate attenuation relations for the CEUS conditions. In general, the attenuation relationships utilize standard forms to regress on recorded data in the region, augmented by data from other similar tectonic regimes and stochastic time histories tied to source types and styles of faulting.

Since publication of the 1989 EPRI study (EPRI, 1989a), much work has been done to evaluate strong earthquake ground motion in the CEUS. In 2004, EPRI completed a study on strong ground motion prediction in the CEUS following the SSHAC (NRC, 1997b) guidelines for a Level III Analysis. A panel of six ground motion Experts was reconvened during several workshops to provide advice to a Technical Integrator (TI) on the adequacy of available CEUS ground motion relationships. On this basis, the TI developed a representation of the current scientific understanding on the subject, consisting of "clusters" of ground motion relationships with associated weights to represent the uncertainty in predicting the median ground motion, in terms of moment magnitude. Each cluster corresponds to relationships based on a similar approach for ground motion modeling. The uncertainty in the median model for each ground motion cluster is defined by two additional models: one representing the 5^{th} percentile of the median uncertainty distribution and the other corresponding to the 95^{th} percentile.

Epistemic uncertainty is modeled using multiple ground motion equations and multiple estimates of aleatory uncertainty (sigma), all with associated weights. Different sets of equations are recommended for sources that represent rifted versus non-rifted parts of the earth's crust. Equations are available for spectral frequencies of 100 Hz (equivalent to PGA), 25 Hz, 10 Hz, 5 Hz, 2.5 Hz, 1 Hz, and 0.5 Hz, and these equations apply to hard rock conditions, i.e., rock with a shear wave velocity of 9200 ft/sec (2804 m/sec).

EPRI has published updated estimates of aleatory uncertainty (EPRI, 2006a). This update reflected the observation that sources of the aleatory uncertainties in the original EPRI attenuation study (EPRI, 2004) were probably too large, resulting in over-estimates of seismic hazard. The 2006 EPRI study (EPRI, 2006a) recommends a revised set of aleatory uncertainties (sigmas) with weights that can be used to replace the original aleatory uncertainties published in the 2004 EPRI study (EPRI, 2004).

In accordance with Regulatory Guide 1.208 (NRC, 2007a), the hazard curves from the PSHA have to be defined for generic hard rock conditions as defined in the development of the attenuation equations. The 2004 EPRI ground motion models correspond to a shear wave velocity (V_s) of 9200 ft/sec (2804 m/sec). These EPRI 2004 equations have been adopted for median ground motion estimates, and the Abrahamson log-sigma model (EPRI, 2006a) is used to incorporate aleatory variability. Within this context, Figure 2.5-76 shows the logic tree for general area sources such as background or local source, and Figure 2.5-75 shows the logic tree for non-general sources such as New Madrid and Charleston. Adopting the EPRI 2004 ground motion model implies that the seismic hazard is calculated at the location where the rock reaches a V_s of 9200 ft/sec (2804 m/sec).

EPRI TR-1014381 (EPRI, 2006a) was used in lieu of the Regulatory Guide 1.208 cited document, i.e. EPRI Report 1013105 (EPRI, 2006b). EPRI Report 1013105 (EPRI, 2006b) was an Update Report while EPRI TR-1014381 (EPRI, 2006a) is the final report. For the purposes of revised estimates of aleatory uncertainty in the CEUS, there is no technical difference between the documents. The "Recommended CEUS Sigma" values and "Conclusions" of both reports are identical.

Earthquakes occurring within the area seismic sources were treated as point sources. Thus, the adjustments to the ground motion equations developed in EPRI (EPRI, 2004) to account for this point-source representation were incorporated in the hazard calculations.

2.5.2.4.6 Updated EPRI Probabilistic Seismic Hazard Analysis Deaggregation, and 1 Hz, 2.5 Hz, and 10 Hz Spectral Accelerations

Figures 2.5-67 through Figure 2.5-73 and Tables 2.5-19 through 2.5-25 present the resulting updated probabilistic seismic hazard hard rock curves for the seven spectral ordinates (100 Hz (equivalent to PGA), 25 Hz, 10 Hz, 5.0 Hz, 2.5 Hz, 1.0 Hz, and 0.5 Hz). The mean and fractile (5%, 16%, 50% (median), 84% and 95%) hazard curves are indicated.

Figure 2.5-43 shows mean and median uniform hazard spectra for 10^{-4}, 10^{-5}, and 10^{-6} annual frequencies of exceedance from these calculations at seven structural frequencies. Numerical values of these spectra are documented in Table 2.5-14.

The mean rock hazard has been de-aggregated for the 10^{-4}, 10^{-5} and 10^{-6} levels of probability of exceedance. The magnitude and distance bins for the de-aggregation table were taken from Regulatory Guide 1.208 (NRC, 2007a). The results have been plotted in Figures 2.5-44 through Figure 2.5-47, Figure 2.5-85 and Figure 2.5-86, for the required low frequency (1 and 2.5 Hz), the high frequency (5 and 10 Hz) ranges, and for the 10^{-4} ,10^{-5} , and 10^{-6} levels of probability of exceedance, respectively. These figures depict the percent contribution of each magnitude-distance bin to the total hazard.

Approach 2B of NUREG/CR-6728 (NRC, 2001) was used to derive the controlling events at the BBNPP site. First, the controlling events were identified using the de-aggregation results. Table 2.5-11 lists the de-aggregated controlling events. Each de-aggregated earthquake (DE) is prescribed as a pair of distance and its associated contribution to a high frequency (HF) or low frequency (LF) response. DEL indicates the low end of the distance range, while DEM and DEH refer to the middle and high ends, respectively. Using the magnitude-distance pairs for each sub-controlling event, DEL, DEM, and DEH, the CEUS single corner spectral shapes from NUREG/CR-6728 (NRC, 2001) were adopted to develop the corresponding spectral shapes. Then, the response spectra of each sub-controlling event were scaled to match the rock UHRS at 1.75 or 7.5 Hz for low frequency and high frequency events (Reference Events, REF), respectively. The resulting scaled response spectra are presented on Figure 2.5-77 and Figure 2.5-78 for hazard levels of 10^{-4} and 10^{-5}, respectively.

The de-aggregation of the total hazard clearly reveals that the nearby area sources largely govern the hazard at the BBNPP site. The influence of local earthquakes is more appreciable in the HF motion. Each of the controlling earthquakes (DEL, DEM, and DEH) of both LF and HF was taken as input for the seismic site amplification analyses as described in the following section. For each sub-controlling event, all selected time histories have been scaled and modified to match their calculated response spectra with the target scaled response spectrum. Figure 2.5-79 compares the target response spectrum with the response spectra of selected time histories, after performing the spectral matching for the 10^{-4} hazard low frequency controlling event of the sub-controlling DEL and DEH.

2.5.2.4.7 Results of Sensitivity Studies

The following subsections provide results and conclusions of the sensitivity studies performed for the BBNPP site:

2.5.2.4.7.1 Five Hundred (500) Mile Catalog Update

Figures 2.5-86a through 2.5-86f show the 2002-2007 events in the 500-mile (805 km) radius centered at the Bell Bend site. Events prior to 2002 are omitted for clarity purposes. These figures show that each of these new events was considered in its corresponding source zone by each independent Earth Science Team (EST). The figures show the seismic source zones that are either partially or totally within the 500 mile (805 km) radius and contribute to 99% of the hazard at the site.

The 500 mi (805 km) sensitivity study results show marginal reduction of ground motion levels, between 0.3 and 2.7%, when compared to the base case PSHA calculation. It is, therefore, concluded that the base case provides adequate estimation of the hazard at the BBNPP site. Table 2.5-62b compares the Uniform Hazard Response Spectra (UHRS) at hard rock conditions between cases considering the updated catalog and the base case analysis. The result is a marginal reduction of ground motion levels, between one and two percent. The more conservative USGS 2002 Guttenberg-Richter b parameters were selected and used in this study. Consequently, this analysis shows that the 2002-2007 extended catalog does not have a significant effect on the PSHA at the BBNPP site due to the decrement of the seismicity rates. As an example, Figure 2.5-86g provides a comparison of the seismicity rates, for the Bechtel EST team and the Source Zone 3 (Charlevoix) and Background Zone. Figure 2.5-86h provides a comparison of the mean hazard curves for Peak Ground Acceleration (PGA).

2.5.2.4.7.2 Charlevoix Sensitivity Study

Table 2.5-62c compares the Uniform Hazard Response Spectra (UHRS) at hard rock conditions between cases considering the original EPRI/SOG base case analysis and the updated Charlevoix geometry for Case 1 of the Charlevoix sensitivity study.

Table 2.5-62e shows a comparison between the Uniform Hazard Response Spectra obtained with the Charlevoix sensitivity analysis Case 2 and those calculated with the EPRI/SOG base case geometry.

Both cases show that no significant changes in the PSHA results occurred. Both cases provide practically equal results which is attributed to the large distance (540 mi (870 km)) between the Charlevoix zone and the site. The differences with the base case are mainly due to the 2002-2007 seismicity update for a larger influence region of 625 miles (1006 km). Figure 2.5-86v compares the seismic hazard curves. Figure 2.5-86w provides the seismicity rates for the Charlevoix zone from three of ESTs. The change in the seismicity rates is marginal and, thus, the sensitivity study performed does not affect the PSHA results for the BBNPP site.

Ramapo Fault Sensitivity Studies

Results of the sensitivity analyses are shown in Figure 2.5-86x. Contribution of the RSZ to the hazard at 0.1 g ground motion level is not significant. The total hazard curves and values at the Bell Bend site already include the seismicity from the RSZ and NY-Ph. However, the seismicity has been taken into account by using the source models of EPRI and not using the specified RSZ and NY-Ph zones. At 0.1 g the contribution from RSZ is about 0.8 % and from NY-Ph less than 7%. The contribution from both zones is accounted for in the BBNPP PSHA. Seismicity rates are provided for the isolated zone by Figure 2.5-86y. The final EPRI seismic source zones that contribute to 99% of the seismic hazard at the Bell Bend site all include the area of the RSZ and NY-Ph. As was shown earlier, the maximum magnitude of EPRI zones are not underestimated. The definition of new zones or modification of existing ones will not lead to significant changes in the seismic hazard at the BBNPP site. This sensitivity analysis was performed to address the Sykes, 2008 publication in the Bulletin of the Seismological Society of America (BSSA).

2.5.2.5 Seismic Wave Transmission Characteristics of the Site

{The uniform hazard spectra developed through Section 2.5.2.4 and displayed on Figure 2.5-43 are defined on hard rock (shear-wave velocity of 9200 ft/sec (2804 m/sec)). Rock layers with shear-wave velocities of such value are located at depths between 190 ft (57.9 m) below the foundation level at the BBNPP site. To determine the SSE at the ground surface, it is necessary to adjust the uniform hazard spectra for amplification or de-amplification as the vibratory ground motion propagates through the soil media. As mentioned above, the adjustment was made by conducting Site Response Analyses following Approach 2B described in NUREG/CR-6728 (NRC, 2001). These analyses consist in defining the shear wave velocity and material damping characteristics in the soil and rock profile between the ground surface and the depth of hard rock. Then uni-dimensional site analyses are conducted using equivalent linear procedure (Schnabel, 1972). The results are used to derive site amplification factors for modifying the response spectra at rock on account of the seismic wave transmission characteristics of the soil layers. This section describes the various steps involved in the calculation and application of the site amplification factors. The seismic wave transmission characteristics and effects of this thick soil column on hard rock ground motions are described in this section.

Section 2.5.2.5.1 is added as a supplement to the U.S. EPR FSAR.

2.5.2.5.1 Development of Site Amplification Functions

2.5.2.5.1.1 Methodology

The calculation of site amplification factors is performed in the following 4 steps:

1. Develop a best estimate soil and rock column in which mean low-strain shear wave velocities and material damping values, and strain-dependencies of these properties, are estimated for relevant layers from the surface to the hard rock horizon. At the BBNPP site, hard rock (V_s = 9200 ft/sec (2804 m/sec)) is at sloping depths between 190 ft (57.9 m) and 237 ft (72.2 m);

2. Develop a probabilistic model that describes the uncertainties in the above properties, locations of layer boundaries, and correlation between the velocities in adjacent layers, and generate a set of 60 artificial "randomized" profiles;

3. For each of the sub-controlling earthquakes (DEL, DEM, and DEH) of 10^{-4} and 10^{-5} annual frequencies of exceedance for both LF and HF earthquakes, use the corresponding controlling time histories for input into dynamic response analysis as the outcrop motion at the hard rock elevation;

4. Use an equivalent-linear time-history site-response formulation to calculate the dynamic response of the site for each of the 60 artificial profiles, and calculate the mean of site

response. This step is repeated for each de-aggregated earthquake of the four input motions (10^{-4} and 10^{-5} annual frequencies, HF and LF events).

These steps are described in the following subsections. The calculation of site effects was performed with an in-house version of the computer program SHAKE (Schnabell, 1972). This program computes the response in a system of viscous-elastic, horizontally layered, soil units, overlying a uniform half-space, subjected to transient, vertical travelling shear waves.

The analytical method implemented in SHAKE is based on the solution of the wave equation and the Fast Fourier Transform algorithm. The nonlinearity of the shear modulus and damping is accounted for by the use of equivalent linear soil properties within an iterative procedure to obtain values for modulus and damping compatible with the effective strains in each layer. Therefore, for any set of layer properties, SHAKE performs a linear analysis.

The motion used as basis for the analysis (i.e., the motion that is considered to be known) can be applied to any layer in the system. An iterative procedure is used to account for the nonlinear behavior of the soils. The object motion can be specified at the top of any sub-layer within the soil profile or at the corresponding outcrop.

It is noted that the solution of a particular problem requires use of realistic ground motions (loading), modeling site dynamics (response), and the interpretation and prediction of soil behavior subject to dynamic loading (analysis). To facilitate conducting and verifying these tasks, modifications incorporated in Rizzo's in-house version include the following:

- The number of sub-layers was increased to up to 500 to allow a more accurate representation of deeper and/or softer soil deposits;
- Modulus reduction and damping relationships can be specified by the user, up to 13 different curves;
- User specified periods are allowed for calculating spectral ordinates;
- The code can accept input data to generate random soil/rock columns by utilizing best estimates of the mean and the standard deviation along with prescribed probabilistic distributions for material properties (stiffness, mass and damping) and for layer thickness.

Computer software control for SHAKE has been done according to Rizzo's Quality Assurance Manual. The Quality Assurance Manual addresses software activities including software acquisition and development, tracking installation of design and analysis software on individual computers, program verification and validation, in-use testing, software usage, change control, configuration control, error notice documentation and distribution, software maintenance, virus protection, software retirement, records and monitoring.

To verify and validate the reliability and functionality of the Rizzo's in-house version of SHAKE, six validation problems are chosen. Each function in the program is verified at least once by the sample problems. One of the sample problem intents to verify the capability of the number of soil layers of 500 in the in-house version. The results calculated by the program are compared to analytical solutions from public sources. The validation and verification presents a good agreement between SHAKE computational solution and analytical solution for each sample problem.

2.5.2.5.1.2 Base Case Soil/Rock BBNPP and Uncertainties

Development of a best estimate soil/rock column is described in detail in Section 2.5.4. Summaries of the low strain shear wave velocity, material damping, and strain-dependent properties of the base case materials are provided below in this section. These parameters are used in the site response analyses.

The total depth of approximately 386 ft (117.7 m) of the BBNPP site was investigated using test borings and geophysical methods. The geotechnical investigation is described in detail in Section 2.5.4.

The layers in the 386 ft (117.7 m) of the site consist of the following stratigraphic units:

- Overburden Soils:
  - Glacial Overburdens
- Rock Formations:
  - Mahantango Shale

A layer of concrete with an average thickness of 10 ft (3 m) below the center line of the planned nuclear reactor facility will be built on top of the Mahantango Shale. This concrete layer is placed between the power block basemat and the bedrock. Section 2.5.4 provides detailed contour information related to the position of the bedrock below the power block's footprint.

The compressional and shear-wave velocities are taken from geophysical field tests using two different techniques:

1. Four sets of downhole tests,
2. Four sets of suspension logging tests

Of the eight geophysical measurements, two borings, G301 and B301, provide the deeper site-specific geophysical information collected during the geotechnical investigation. P-S Suspension and downhole tests were performed down to a depth of approximately 400 ft (122 m) (GeoVision, 2008; NGA, 2008). These two locations are at the center line of the projected containment footprint.

The downhole profiles consist of average compressional and shear-wave velocities for thicknesses varying from 13 ft (4 m) to 120 ft (36.6 m). The suspension logging profiles provide detailed discrete compressional and shear-wave velocities for thickness of approximate 1.5 ft (0.5 m).

Resonant Column and Torsional Shear Laboratory Tests were performed on soil and backfill samples. The complete set of results from these tests is reported in Section 2.5.4.2.3. Generic cohesionless soil curves (EPRI, 1993) were adopted to describe the strain dependencies of shear modulus and damping for the backfill based on available results from the site investigation. As required by Regulatory Guide 1.208 (NRC, 2007a) the damping curves for soils were truncated at 15 percent for the site response analysis.

In these areas, there are numerous records of deep gamma ray surveys and geologic columns with lithologic descriptions. The analysis of shear wave velocities at depths beyond the reach of the boring exploration program became irrelevant since the 9200 ft/sec (2804 m/sec) horizon was clearly encountered by the geophysical exploration program.

The Mahantango Formation reached such shear wave velocity above a depth of 350 ft (107m). Past reports place the total thickness of the Mahantango Formation at approximately 1,500 ft (457 m) (Inners, 1978).

The geologic column at the site is an extension of the Mahantango Shale, which is a dark gray to black formation, with few to no fractures. Some distinctive features are the presence of calcareous zones, the presence of thin pyrite lenses that increase in abundance with depth, and the presence of calcite veins perpendicular to the bedding plane that are micro-faulted. The upper surface of the Mahantango Formation shows the effects of solution and weathering in a few areas, but it is predominantly very competent and indurated.

For the Site Response Analyses, the concrete and Mahantango Shale is assumed to behave linearly during earthquake shaking. "Free-Free" Direct arrival tests were performed on undisturbed rock samples by the University of Texas. The "Free-Free" Direct arrival test results are provided in Table 2.5-42. The tests provided material velocity and damping values associated with shear-waves as well as those associated with compressional waves.

The average of the laboratory test results for damping for the Mahantango Shale is 0.86 percent. Lower values, 0.8 and 0.7 percent, are conservatively used for the analysis. The Mahantango Shale has a very high Rock Quality Designation (RQD) and as a rock mass is capable of transmitting shear waves very efficiently with small amounts of damping. Therefore, the lower reported laboratory values are selected for the analysis. The RQD of the Mahantango Shale is reported in the field boring logs.

2.5.2.5.1.3 Site Properties Representing Uncertainties and Correlations

To account for variations in shear-wave velocity across the site, 60 artificial profiles were generated using the stochastic model developed by Toro (Toro, 1996), with the approximation of the standard deviation of ln V_s as the coefficient of variation of V_s (Ang and Tang, 1975). These artificial profiles represent the soil column from the top of the ground surface to the top of bedrock with a shear-wave velocity of 9,200 ft/s (2804 m/sec). The model uses as inputs the following quantities:

- The best estimate of the shear-wave velocity profile and other soil properties described above;
- The coefficient of variation of the shear wave velocity as a function of depth, developed using available site data (refer to Section 2.5.4);
- Correlation coefficients between V_s in adjacent layers, determined using correlation results for the USGS site characterization category (Toro, 1996);

- The probabilistic characterization of layer thickness as a function of depth, computed assuming a normal distribution;

- The depth to bedrock, which is randomized assuming a normal distribution to account for epistemic uncertainty in the bedrock-depth data described in Section 2.5.4.

Figure 2.5-50 shows the best estimate V_s value and corresponding coefficient of variation as a function of depth of the downhole tests and suspension logging tests at different boreholes.

The coefficient of variation of shear wave velocities calculated from the best estimate soil/rock column is used as the standard deviation of $\ln(V_s)$ as a function of depth. Figure 2.5-51 shows the coefficient of variation of shear-wave velocity, which were used to generate multiple profiles. The correlation coefficients between shear wave velocities in adjacent layers were determined using USGS empirical relationships.

The randomly generated thicknesses of layer were computed assuming a normal distribution using the coefficient of variation of 0.10 to 0.15 for thickness of each layer. For consistency with the site-specific data, the generated ln-velocities and the generated thicknesses were truncated at ±2s according to the recommendations of Toro (Toro, 1996).

Figure 2.5-52 illustrates the V_s profiles generated for profiles 1 through 60, using the median, logarithmic standard deviation, and correlation models described. These profiles include uncertainty in depth to bedrock. In total, 60 profiles were generated. Figure 2.5-53 compares the mean of these 60 V_s profiles to the best estimate V_s profile described in the previous section, indicating very good agreement. This figure also shows the ±1 standard deviation values of the 60 profiles, reflecting the coefficient of variations indicated on Figure 2.5-51.

Mean values of shear stiffness (G/G_{MAX}) and damping for each geologic unit are described in Section 2.5.4. Uncertainties in the properties for each soil unit are characterized using the values obtained by Costantino (Costantino, 1996). Figure 2.5-54 and Figure 2.5-55 illustrate the shear stiffness and damping curves generated for backfill, although that is not present in the Best Estimate soil column model. Stiffness and damping of soils depend on the strain level during ground shaking. However, for significantly stiff materials such as concrete and the Mahantango Shale, these properties are independent of the strain level during earthquake ground motion. Both properties retain their "low-strain" values. These values are also subject to the random variation procedure.

This set of 60 profiles, consisting of V_s versus depth, depth to bedrock, stiffness, and damping, are used to calculate and quantify site response and its uncertainty, as described in the following sections.

2.5.2.5.1.4 Development of Smooth Uniform Hazard, Controlling, and Reference Response Spectra

In order to derive smooth spectra corresponding to the 10^{-4} and 10^{-5} amplitudes, the magnitude and distance pairs of both controlling and reference earthquakes summarized in Table 2.5-11 were used as described below.

The magnitudes and distances were applied to spectral shape equations from NUREG/CR-6728 (NRC, 2001) to determine realistic spectral shapes for the four representative earthquakes (at spectral frequency 0.5, 1.75, 7.5, and 25 Hz) of 10^{-4} and 10^{-5} events.

For smooth Uniform Hazard Response Spectra (UHRS), the 25 Hz smooth shapes were utilized and scaled to the Uniform Hazard Spectra mean values for 10^{-4} or 10^{-5} between 25 Hz and 100 Hz. The 7.5 Hz smooth shapes were utilized and scaled to the Uniform Hazard Spectra mean values for 10^{-4} or 10^{-5} between 5 Hz and 10 Hz. The 1.75 Hz smooth shapes were utilized and scaled to the Uniform Hazard Spectra mean values for 10^{-4} or 10^{-5} between 0.5 Hz and 2.5 Hz. Below 0.5 Hz, the 0.5 Hz smooth shapes were scaled and utilized without any modification. The smooth UHRS are presented in Table 2.5-61, and in Figure 2.5-48 for 10^{-4}, 10^{-5}, and 10^{-6}.

For the reference response spectra, the HF reference spectra shapes for 10^{-4} or 10^{-5} at the spectral frequency above 5 Hz were the same as the smooth UHRS. The spectral shape at 7.5 Hz was extrapolated from 5 Hz without regard to Uniform Hazard Spectra amplitudes at lower frequencies. The LF reference spectra shapes were scaled to the smooth UHRS values for 10^{-4} or 10^{-5} for frequency less than 2.5 Hz. Above 2.5 Hz, the spectral shape was extrapolated from 2.5 Hz, without regard to Uniform Hazard Spectra amplitudes at higher frequencies by using the smooth spectral shape at frequency of 1.75 Hz.

Creation of smooth 10^{-4} and 10^{-5} reference spectra (REF) in this way ensures that the HF spectra match the 10^{-4} and 10^{-5} Uniform Hazard Spectra values at high frequencies (5 Hz and above), and ensures that the LF spectra match the 10^{-4} and 10^{-5} Uniform Hazard Spectra values at low frequencies (2.5 Hz and below). In between calculated values, the spectra have smooth and realistic shapes that reflect the magnitudes and distances dominating the seismic hazard, as reflected in Table 2.5-12. The smooth reference spectra are presented in Figure 2.5-80 and Figure 2.5-81. For controlling response spectra, the smooth spectra shapes for 10^{-4} and 10^{-5} events, LH and HF, and sub-event, DEL, DEM, and DEH were developed directly from the NUREG/CR-6728 using the magnitudes and distances in Table 2.5-11 without any modification. These smooth spectra then scaled to match the smooth UHRS at 1.75 Hz for LF events and at 7.5 Hz for HF events. The smooth controlling response spectra are presented on Figure 2.5-77 and Figure 2.5-78.

2.5.2.5.1.5 Controlling Time Histories

Four initial time histories were selected from the rock time histories database from NUREG/CR-6728 (NRC, 2001) for sub-controlling earthquakes (DEL, DEM, and DEH) for the 10^{-4} and 10^{-5} levels and for both LF and HF events according to their deaggregated magnitudes and distances. These time histories were then modified according to the spectral matching criteria set for time histories in Appendix F of Regulatory Guide 1.208 (NRC, 2007a) to match their target smooth controlling response spectra. The selected time histories are listed in Table 2.5-17.

2.5.2.5.1.6 Site Response Analysis

The site response analysis performed for the BBNPP site used a time history-based procedure in conjunction with the following assumptions:

- Vertically-propagating shear waves are the dominant contributor to site response.
- An equivalent-linear formulation of soil nonlinearity is appropriate for the characterization of site response.

Sixty response analyses were performed using the program SHAKE (Schnabel, 1972) to calculate the site amplification function for each de-aggregation earthquake. The 60 randomized velocity profiles were paired with the 60 sets of randomized modulus reduction and damping curves (one profile with one set of modulus). Sixty response analyses were performed using the program SHAKE (Schnabel, 1972) as modified by Rizzo to calculate the site amplification function for each de-aggregation earthquake. The 60 randomized velocity profiles were paired with the 60 sets of randomized modulus reduction and damping curves (one profile with one set of modulus reduction and damping curves) to define 60 soil columns, each characterized by a set of shear wave velocities, modulus reduction curves, and material damping curves. Each of the four scaled time histories corresponding to a de-aggregated earthquake was used to compute the response of fifteen profile-soil property curve sets.

For each analysis, the response spectrum for the computed motion at the top of the concrete was divided, frequency by frequency, by the response spectrum for the input motion at the hard rock to obtain a site amplification function. The arithmetic mean of these 60 individual response spectral ratios was taken as the mean site amplification function for each de-aggregated earthquake.

The following figures and table describe the site amplification factors for the high and low frequencies and 10^{-4} and 10^{-5} input motions:

- Figure 2.5-56: mean site amplification factor and coefficient of variation at the top of concrete for 10^{-4} HF DEM input motion;
- Figure 2.5-57: maximum strains vs. depth for 10^{-4} HF DEM input motion;
- Figure 2.5-58: mean site amplification factor and coefficient of variation at the top of concrete for 10^{-4} LF DEM input motion;
- Figure 2.5-59: maximum strains vs. depth for 10^{-4} LF DEM input motion;
- Figure 2.5-60: mean site amplification factor and coefficient of variation at the top of concrete for 10^{-5} HF DEM input motion;
- Figure 2.5-61: maximum strains vs. depth for 10^{-5} HF DEM input motion
- Figure 2.5-62: mean site amplification factor and coefficient of variation at the top of concrete for 10^{-5} LF DEM input motion; and
- Figure 2.5-63: maximum strains vs. depth for 10^{-5} LF DEM input motion.
- Table 2.5-13: amplification factors for 10^{-4} and 10^{-5} input motions and HF and LF rock spectra}

2.5.2.6 Ground Motion Response Spectra

The U.S. EPR FSAR includes the following COL Item in Section 2.5.2.6:

> A COL applicant that references the U.S. EPR design certification will verify that the site-specific seismic parameters are enveloped by the CSDRS (anchored at 0.3 g PGA) and the 10 generic soil profiles discussed in Section 2.5.2 and Section 3.7.1 and summarized in Table 3.7.1-6.

This COL Item is addressed as follows:

This section and Section 3.7.1 describe the reconciliation of the site-specific parameters for the {BBNPP} and demonstrates that these parameters are enveloped by the Certified Seismic Design Response Spectra (CSDRS), anchored at 0.3 g PGA, and the 10 generic soil profiles used in the design of the U.S. EPR.

Table 5.0-1 of the U.S. EPR FSAR identifies shear wave velocity as a required parameter to be enveloped, defined as "Minimum shear wave velocity of 1000 feet per second (Low strain best estimate average value at bottom of basemat)."

{Figure 2.5-84 compares the 10 generic soil profile cases used for the U.S. EPR and the best estimate shear wave velocity profile that was adopted for the BBNPP site.

Reconciliation of the BBNPP site-specific seismic parameters with the U.S. EPR certified seismic design response spectra (CSDRS) and the 10 generic soil profiles used for the U.S. EPR is addressed in Section 3.7.1. The evaluation guidelines in U.S. EPR FSAR Section 2.5.2.6 are used to perform the reconciliation.

The steps and conclusions of the seismic parameter reconciliation are summarized below. Summaries of select U.S. EPR structures, systems, and components evaluations which confirm they are adequate for the BBNPP site are also provided as required by seismic reconciliation Step 9.

The seismic reconciliation steps and conclusions:

1. Step 1 of the U.S. EPR FSAR Section 2.5.2.6 seismic reconciliation guidelines is confirmation that the peak ground acceleration for the ground motion response spectrum (GMRS) is less than 0.3g. The BBNPP site-specific GMRS are described in Section 3.7.1. The peak ground acceleration for the BBNPP site-specific GMRS is confirmed to be less than 0.3g.

2. Step 2 of the U.S. EPR FSAR Section 2.5.2.6 seismic reconciliation guidelines is confirmation that the low strain, best estimate value of the shear wave velocity at the bottom of the foundation basemat of the NI Common Basemat Structures is 1000 fps, or greater. The low strain, best estimate value of the BBNPP site-specific shear wave velocity at the bottom of the foundation basemat of the NI Common Basemat Structures is confirmed to be greater than 1000 fps.

3. Step 3 of the U.S. EPR FSAR Section 2.5.2.6 seismic reconciliation guidelines is confirmation that the foundation input response spectra (FIRS) are enveloped by the certified seismic design response spectra (CSDRS). Comparison of the BBNPP site-specific GMRS/FIRS with the U.S. EPR CSDRS is described in Section 3.7.1. The site-specific horizontal and vertical GMRS/FIRS exceed the envelope of the U.S. EPR CSDRS ground motions, primarily in the high frequency region. The BBNPP design ground motion response spectra are as described in Section 3.7.1, instead of the CSDRS, because the GMRS/FIRS exceed the CSDRS. This represents a departure from the U.S. EPR FSAR, as described in Section 3.7.1.

4. Step 4 of the U.S. EPR FSAR Section 2.5.2.6 seismic reconciliation guidelines is confirmation that the site-specific soil profile is laterally uniform. Horizontal soil layering is confirmed for the BBNPP site-specific soil profile.

5. Step 5 of the U.S. EPR FSAR Section 2.5.2.6 seismic reconciliation guidelines is confirmation that the idealized site soil profile is similar to or bounded by the 10 generic soil profiles used for the U.S. EPR. The BBNPP idealized site soil profile is described in Section 3.7.1. The BBNPP idealized site soil profile is not considered bounded by the U.S. EPR 10 generic soil profiles. This represents a departure from the U.S. EPR FSAR, as described in Section 3.7.1.

6. Step 6 of the U.S. EPR FSAR Section 2.5.2.6 seismic reconciliation guidelines is confirmation that the conditions of Steps 1 through 5 are met. The conditions of Steps 3 and 5 are not met for the BBNPP site because the BBNPP site-specific GMRS/FIRS exceed the envelope of the U.S. EPR CSDRS and the BBNPP site-specific idealized site soil profile is not bounded by the 10 generic soil profiles used for the U.S. EPR. Because the conditions of Steps 3 and 5 are not met for the BBNPP site, seismic reconciliation guideline Step 7 is performed.

7. Step 7 of the U.S. EPR FSAR Section 2.5.2.6 seismic reconciliation guidelines is performance of intermediate-level studies, such as evaluation of the site-specific motion at the top the of the basemat, to demonstrate that the site is bounded by the design of the U.S. EPR. BBNPP site-specific response spectra are developed for the NI Common Basemat Structures basemat and the footprints of the EPGB and ESWB and are compared to the corresponding U.S. EPR design certification spectra. The BBNPP site-specific spectra exceed the envelope of the U.S. EPR certified design spectra; therefore, seismic reconciliation guideline Step 8 is performed.

8. Step 8 of the U.S. EPR FSAR Section 2.5.2.6 seismic reconciliation guidelines is performance of site-specific soil-structure interaction (SSI) analyses, development of in-structure response spectra (ISRS), and confirmation that the BBNPP site-specific ISRS do not exceed the ISRS for the U.S. EPR design certification by more than 10% at the key building locations. BBNPP site-specific SSI analyses are performed and site-specific ISRS are developed for comparison to the U.S. EPR design certification ISRS. The U.S. EPR design certification SSI analysis methodology is used to perform the site-specific SSI analyses, except as noted in Sections 3.7.1 and 3.7.2. Performance of the SSI analyses and comparison of the BBNPP site-specific ISRS with the U.S. EPR design certification ISRS is described in Section 3.7.1. The BBNPP site-specific ISRS exceed the envelope of the U.S. EPR certified design ISRS by more than 10% at some of the specified key building locations. This represents a departure from the U.S. EPR FSAR, as described in Section 3.7.1. Therefore, seismic reconciliation guideline Step 9 is performed.

9. Step 9 of the U.S. EPR FSAR Section 2.5.2.6 seismic reconciliation guidelines is performance of additional evaluations to confirm that safety-related structures, systems, and components of the U.S. EPR at the building locations where BBNPP site-specific ISRS exceed the ISRS for the U.S. EPR design certification by more than 10% are not affected. These evaluations, summarized below, confirm that the safety-related structures, systems and components of the U.S. EPR are not affected.

The BBNPP average shear wave velocity profile shown in the above figure is for soils below elevation +638 ft (195 m) (bottom of the basemat). Soils such as Glacial Overburdens will not be used for support of foundations of the BBNPP Nuclear Island. Therefore, shear wave velocity measurements in the BBNPP site soils above elevation +638 ft (195 m) regardless of value, are excluded from this evaluation as they lie above the basemat. Results from the above figure indicate that:

1. The BBNPP average shear wave velocity profile is bounded by the 10 generic profiles used for the U.S. EPR.

2. The BBNPP average shear wave velocity profile offers a shear wave velocity at the bottom of the basemat (approximate elevation +638 ft (195 m)(or depth = 0 in the above figure)) of 7,240 ft/sec (2,207 m/sec).

3. The minimum shear wave velocity from the BBNPP average shear wave velocity profile is 6,800 ft/sec (2,073 m/sec).

On the above basis, it is concluded that the BBNPP site shear wave velocity profile is bounded by the 10 generic soil profiles used for the U.S. EPR and meets the minimum 1,000 ft/sec (305 m/sec) criterion identified in the U.S. EPR FSAR.}

As described in Section 2.5.2.4, the end results of the site response analysis are weighted average site amplification factors. In this section, these factors are used to develop the ground motion response spectra (GMRS) by modifying the spectra at rock. The GMRS was developed in accordance with the performance-based approach described in Regulatory Position 5 of Regulatory Guide 1.208 (NRC, 2007a).

The Safe Shutdown Earthquake (SSE) ground motion was developed starting from the 10^{-4} and 10^{-5} rock Uniform Hazard Spectra. At high frequencies, the appropriate (10^{-4} or 10^{-5}) HF mean amplification factor was applied to the 10^{-4} or 10^{-5} HF smooth rock spectrum, to calculate site spectral amplitudes for 10^{-4} and 10^{-5} annual frequencies of exceedance. At low frequencies, a similar technique was used with the LF mean amplification factors. At intermediate frequencies, the larger of the HF and LF site spectral amplitudes was used.

{Figure 2.5-64 illustrates the resulting site spectra. At high frequencies, the HF spectral amplitudes are always greater, and at low frequencies, the LF spectral amplitudes are always greater.

This procedure implements Approach 2B in NUREG/CR-6728 (NRC, 2001) and NUREG/CR-6769 (NRC, 2002), where in the rock Uniform Hazard Spectra (for example, at 10^{-4}) is multiplied by a mean amplification factor at each frequency to estimate the 10^{-4} site Uniform Hazard Spectra. Note that the amplification factors plotted on Figure 2.5-56, Figure 2.5-58, Figure 2.5-60, and Figure 2.5-62 are logarithmic mean amplification factors, which correspond approximately to the median. The amplification factors used to prepare Figure 2.5-64 are arithmetic mean amplification factors, which are slightly higher than the median.

The low-frequency character of the spectra on Figure 2.5-64 reflects the low-frequency amplification of the site, as shown in the amplification factors of Figure 2.5-56, Figure 2.5-58, Figure 2.5-60, and Figure 2.5-62. That is, there is a fundamental site resonance at about 0.22 Hz, with a dip in site response at about 0.4 Hz, and this dip occurs for all 60 of the site profiles that were used to characterize the site profile. As a result, there is a dip in the site spectra for 10^{-4} and 10^{-5} at 0.4 Hz that reflects the site characteristics.

The ASCE (ASCE, 2005b) performance-based approach was used to derive an SSE from the 10^{-4} and 10^{-5} site spectra. The SSE spectrum is derived at each structural frequency as follows:

$$A_R = SA(10^{-5})/SA(10^{-4})$$

$$DF = 0.6\ A_R^{0.8}$$

$$SSE = \max(SA(10^{-4})\times\max(1.0, DF), 0.45\times SA(10^{-5}))$$

The last term in the above equation was not published in this form in ASCE (ASCE, 2005) but is a supplemental modified form, as presented in NRC Regulatory Guide 1.208 (NRC, 2007a). The resulting horizontal SSE spectrum is plotted in Figure 2.5-65.

A vertical SSE spectrum was constructed from the horizontal SSE spectrum following the approach described in NUREG/CR-6728 (NRC, 2001) by deriving vertical-to-horizontal (V/H) ratios and applying them to the horizontal SSE. As background and for comparison purposes, V/H ratios were obtained by the following methods:

The vertical SSE spectrum was constructed from the horizontal Design Response Spectrum (DRS) using vertical to horizontal (V/H) response spectral ratios appropriate for the BBNPP site. The V/H ratios are developed following the approach described in NUREG/CR-6728 (NRC, 2001). Figure 2.5-66 shows the V/H ratios recommended for CEUS rock sites as a function of spectral frequency and the level of peak ground acceleration (PGA) for the horizontal component. Figure 2.5-66 shows the weighted average of these V/H ratios based on the PGA for the de-aggregated earthquakes (DEs) that make up the high-frequency (HF) and low-frequency (LF) mean 10^{-4} reference earthquakes (REs). The weights assigned to the DE are listed in Table 2.5-11. The weighted V/H ratios are essentially the same for the HF and LF mean 10^{-4} DE.

The EPRI 2004 ground motion model for CEUS is defined at the hard rock or at the elevation that the shear wave velocity in the material is approximately 9200 ft/sec (2804 m/sec). Only the horizontal component of the ground motion is defined in this ground motion model, not the vertical component. Consequently, the PSHA is done at the hard rock level for the horizontal ground motion component. The site response analysis is performed to bring the ground motion from the hard rock elevation to the ground surface or top of competent material to define the GMRS according to Regulatory Guide 1.208 (NRC, 2007a). The end result of the site response analysis is the horizontal ground motion at free field or top of competent material. In order to define the vertical ground motion component, Regulatory Guide 1.208 (NRC, 2007a) Section C5.2 permits using the procedure described in NUREG/CR-6728 (NRC, 2001) for the CEUS soil site. The procedure begins by calculating the V/H ratio of the rock site in the CEUS via the set of equations provided in NUREG/CR-6728 (NRC, 2001). The transfer function calculated from the ratio of V/H ratio of the soil site with respect to the V/H ratio of the rock site in the WUS soil site is applied the V/H ratio of the rock site in the CEUS to obtain V/H ratio for the soil site in the CEUS. The Clinton ESP (EGC, 2006) also performed the GMRS calculation according to this procedure. The Clinton ESP application has been accepted by the NRC (NRC, 2007c).

The vertical DRS is obtained by scaling the horizontal DRS by the soil V/H ratios shown on Figure 2.5-66. A smooth spectrum enveloping the vertical DRS was then constructed. The resulting vertical SSE is shown on Figure 2.5-65 and is tabulated in Table 2.5-12 along with the horizontal SSE spectrum.

Refer to Sections 3.7.1 and 3.7.2 for a description of the soil-structure interaction analyses performed for the U.S. EPR design certification.}

CAV Filtering In Surface Ground Motions

The use of a lower bound magnitude in the calculation of the probabilistic seismic hazard could result into some excessive conservatism as a consequence of including the effects of non-damaging earthquakes. The reason is that, according to probabilistic methodologies and current attenuation equations, small magnitude near site events could occur very frequently having a significant contribution to the integrated hazard. However, it has been found that facilities designed and built with sound engineering practices do not suffer damage from this type of events (EPRI, 1988a). Examining this issue, the Cumulative Absolute Velocity (CAV) was proposed as a parameter for quantifying the damage potential associated to an earthquake record (EPRI, 1988). For a given accelerogram, a(t), the CAV is calculated with the following equation:

$$CAV = \Sigma i\ H(pga_i - 0.025g) \int_i | a(t) |\ dt$$

pga is peak ground acceleration

g is gravity

H(x) is the Heaviside function (unity for x>0 and 0 otherwise)

It should be noted that the surface ground motion a(t) is used to calculate the CAV. It has been observed that no damage occurs on well designed and built structures when the CAV is equal to or lower than 0.16g-sec (EPRI, 2006).

Recently, EPRI (EPRI, 2006) has published methodologies for incorporating the CAV filter into seismic hazard calculations. The most direct method consists in including the probability of exceeding the 0.16g-sec threshold into the integral to calculate the hazard. This, however, would require that site effects be included in the hazard integration, for instance, in the attenuation equations. In addition, the computation time would be significantly increased. Thus, EPRI (EPRI, 2006) has also developed a more efficient method for applying the minimum as a post-processing procedure to the hazard calculation. EPRI TR-1014099 (EPRI, 2006) was used in lieu of the Regulatory Guide 1.208 (NRC, 2007a) cited document (EPRI Report 1012965). EPRI Report 1012965 was an update report for CAV research while EPRI TR-1014099 (EPRI, 2006) is the final report. For the purposes of revised calculation of the CAV in the CEUS, there is no technical difference between the documents. The methodologies of calculation of the CAV of both reports are identical. This approach uses the hazard curve and the de-aggregation obtained in the PHSA at rock to calculate the rate of occurrence, $\nu(z_k, i, j)$, of the spectral acceleration around a small acceleration range close to z_k, due to a magnitude-distance pair (Mi, Rj). Equations developed by EPRI to estimate the CAV in terms of M and peak ground acceleration (PGA) can then be used to calculate the probability that P(CAV > 0.16) for the corresponding Mi, Rj pair, and the filtered hazard $\nu'(S)$ is calculated as follows:

$$\nu'(S > z) = \Sigma i\ \Sigma j\ \Sigma k\ \nu(z_k, i, j)\ P(CAV > 0.16)$$

The CAV filtering is implemented by first breaking the hazard curve at rock into rates of occurrence of scenario earthquakes (M, R, PGA). We can then compute the probability that this scenario will lead to a CAV value greater than 0.16g-sec. This probability is then multiplied by the rate of the scenario, and the sum of the filtered rates furnishes the CAV filtered hazard. The spectral value can be related to a corresponding PGA using the uniform hazard spectrum shape at the corresponding exceedance rate.

Following details presented in EPRI (EPRI, 2006), the CAV filtering was incorporated as a post-processing application into the hazard calculation at the BBNPP site. Very modest reductions in spectral values were obtained, particularly for the 10^{-5} hazard. The explanation is that after applying the site amplification factors, the PGA values corresponding to this hazard level are relatively high (about 0.4g) and, consequently, almost certainly damaging. In fact, CAV reductions on the GMRS were negligible.

2.5.2.7 Conclusions

{This section is added as a supplement to the U.S. EPR FSAR.

An updated evaluation of the vibratory ground motion has been conducted for the BBNPP site. A Probabilistic Seismic Hazard Analysis (PSHA) was selected as the appropriate basis for evaluating the vibratory ground motion accounting for all credible alternative seismic sources. The alternative seismic sources identified by the Electric Power Research Institute (EPRI) for the Central and Eastern United States (CEUS), Seismic Hazard Methodology for the Central and Eastern United States (EPRI, 1986) issued in 1986 are still considered to constitute an adequate definition of seismic area sources. However, updated information available from databases maintained by the United States Geological Survey has been used to determine recurrence parameters. Since the New Madrid Fault System (NMFS) and the Charleston Seismic Source (CSS) have some contribution to the seismic hazard at the BBNPP site, updated logic-tree representations of the clustered characteristic earthquakes at the NMFS and the un-clustered CSS have been incorporated into the PSHA. The NMFS characterization is provided by Exelon in the Clinton ESP application (EGC, 2006) and the CSS characterization is the one presented in the CCNPP Unit 3 FSAR (UniStar Nuclear, 2007). Both characterizations have been verified with USGS modeling of the New Madrid and Charleston Faults. The PSHA for the BBNPP site makes use of a decision tree approach with appropriate weighting factors that are based on the most up-to-date information and relative confidence in alternative characterizations for each area and characteristic seismic source.

The guidance of Regulatory Guide 1.208, "A Performance -Based Approach to Define the Site-Specific Earthquake Ground Motion," (NRC, 2007a) was used to develop the Ground Motion Response Spectra (GMRS) at the BBNPP site. This GMRS adequately represents the regional and local seismic hazards and accurately includes the effects of the local soils at the BBNPP site.

It is concluded that the performance-based approach outlined in Regulatory Guide 1.208 (NRC, 2007a) constitutes an advancement over the solely hazard-based reference probability approach recommended in Regulatory Guide 1.165 (NRC, 1997a) and used it where appropriate in the determination of the GMRS. The performance-based approach uses not only the seismic hazard characterization of the site from the PSHA but also basic seismic fragility SSC modeling in order to define a ground motion that directly targets a structural performance frequency value. It is concluded that the application for the BBNPP site is acceptable from a geologic and seismologic standpoint and meets the requirements of 10 CFR 100.23(d) (CFR, 2007). Deviations from the NRC guidance in Regulatory Guide 1.165 (NRC, 1997a), Regulatory Guide 1.208 (NRC, 2007a), or review criteria in Standard Review Plan 2.5.2 (NRC, 2007b) have been identified and acceptable alternatives, including technical justification, have been provided.}

2.5.2.8 References

{This section is added as a supplement to the U.S. EPR FSAR.

Abrahamson, 1997. Empirical Response Spectral Attenuation Relations for Shallow Crustal Earthquakes. N. A. Abrahamson and W. J. Silva. Seismological Research Letters, Volume 68, Number 1, 1997.

Ang and Tang, 1975. Probabilistic Concepts in Engineering Planning and Design, Volume 1, A.H. Ang and W.H. Tang, John Wiley and Sons, New York, 1975.

Atkinson, 2006. Earthquake Ground-Motion Prediction Equations for Eastern North America," G. M. Atkinson and D. M. Boore, Seismological Society of America, Bulletin, Volume 96, Number 6, pp. 2181-2205, 2006.

ASCE, 2005a. Minimum Design Loads for Buildings and Other Structures, ASCE/SEI 7-05, American Society for Civil Engineers/Structural Engineering Institute, 2005.

ASCE, 2005b. Seismic Design Criteria for Structures, Systems, and Components in Nuclear Facilities, ASCE/SEI 43-05, American Society for Civil Engineers/Structural Engineering Institute, 2005.

ANSS, 2008, ANSS web database, http://www.ncedc.org/anss/catalog-search.html, last accessed November 2008.

Bakun, 2004. Magnitudes and Locations of the 1811-1812 New Madrid, Missouri, and the 1886 Charleston, South Carolina, Earthquakes, W. H. Bakun and M. G. Hopper, Seismological Society of America, Bulletin, Volume 94, Number 1, pp. 64-75, 2004.

Bent, 1992, A re-examination of the 1925 Charlevoix, Bent, A. L., Bulletin of the Seismological Society of America, Vol. 82, No. 5, 2097-2113.

Bollinger, 1977. Reinterpretation of the Intensity Data for the 1886 Charleston, South Carolina, Earthquake in Studies Related to the Charleston, South Carolina, Earthquake of 1886 -A Preliminary Report, in D. W. Rankin, Editor, G. A. Bollinger, U. S. Geological Survey Professional Paper 1028, pp. 17-32, 1977.

Boore, 1987. Stochastic Prediction of Ground Motion Response Parameters at Hard-Rock Sites in Eastern North America, D.M. Boore and G.M. Atkinson, Bulletin Seismological Society of America, Volume 77, Number 2, pp. 440-467, 1987.

Campbell, 2003. Updated Near-Source Ground-Motion (Attenuation) Relations for the Horizontal and Vertical Components of Peak Ground Acceleration and Acceleration Response Spectra. K. W. Campbell, and Y. Bozorgnia. Bulletin of the Seismological Society of America. Volume 93, No. 1. pp. 314-331. 2003.

CFR, 2007. Title 10, Code of Federal Regulations, Part 100.23(d), Geologic and Seismic Siting Factors, 2007.

Cornell, 1968. Engineering Seismic Risk Analysis, C.A. Cornel, Bulletin of Seismological Society of America, Volume 58, pp, 1583-1606, 1968.

Cornell, 1971. Probabilistic Analysis of Damage to Structure Under Seismic Loads, C.A. Cornel, Dynamic Waves in Civil Engineering, Chapter 27, edited by D.A. Howells, I.P Haigh, and C. Taylor, 1971.

Costantino, 1996. Recommendations for Uncertainty Estimates in Shear Modulus Reduction and Hysteretic Damping Relationships, C. J. Costantino, 1996, Published as an appendix in "Description and validation of the stochastic ground motion model," W.J. Silva, N. Abrahamson, G. Toro and C. Costantino, 1997, Report Submitted to Brookhaven National Laboratory, Associated Universities, Inc. Upton, New York 11973, Contract No. 770573.

Cox, 1983. Paleoseismic Studies in the 1886 Charleston Earthquake Meizoseismal Area, Geological Society of America Abstracts with Programs, J. Cox and P. Talwani, 1983.

Dineva, 2004, Seismicity of the Southern Great Lakes: Revised Earthquake Hypocenters and possible tectonic controls, Bulletin of the Seismological Society of America, Dineva S., D. Eaton, and R. Mereu, 94, 1902-1918.

Earthquakes Canada, 2008,
http://earthquakescanada.nrcan.gc.ca/zones/eastern_e.php#SGLSZ, last accessed Nov. 2008.

Ebel, 1996. The Seventeenth Century Seismicity of Northeastern North America, John E. Ebel, Seismological Research Letters, Volume 67, Number 3, p. 51-68, 1996.

Ebel, 2002, Earthquakes in the Eastern Great lakes basin from a regional perspective, Tectonophysics, Ebel J. E., and M. Tuttle (2002). 353, 17-30.

Ebel, 2006. The Cape Ann, Massachusetts Earthquake of 1755: A 250th Anniversary Perspective, John E. Ebel, Seismological Research Letters, Volume 77, Number 1, p. 74-86, 1996.

EGC, 2006. Submittal of Revision 4 to Exelon Generation Company's Early Site Permit Application for Clinton, Including Administrative Information, Emergency Plan, Site Redress Plan, Environmental Report and Site Safety Analysis Report, April 14, 2006.

EPRI, 1986. Seismic Hazard Methodology for the Central and Eastern United States, NP-4726, Volumes 1-10, Electric Power Research Institute, July 1986.

EPRI, 1988. Seismic Hazard Methodology for the Central and Eastern United States, NP-4726-A, Revision 1, Volume 1, Part 2, Electric Power Research Institute, 1988.

EPRI, 1988a. A Criterion for Determining Exceedance of the Operating Basis Earthquake, NP-5930, Electric Power Research Institute, 1988.

EPRI, 1989a. Probabilistic Seismic Hazard Evaluations at Nuclear Power Plant Sites in the Central and Eastern United States: Resolution of the Charleston Earthquake Issue, NP-6395-D, Electric Power Research Institute, 1989.

EPRI, 1989b. EQHAZARD Primer, NP-6452-D, Electric Power Research Institute, June 1989.

EPRI, 1993. Guidelines for Determining Design Basic Ground Motions, TR-102293, Volume 1, Electric Power Research Institute, 1993.

EPRI, 2004. CEUS Ground Motion Project Final Report, TR-1009684 2004, Electric Power Research Institute, December 2004.

EPRI, 2006. Program on Technology Innovation: Use of Cumulative Absolute Velocity (CAV) in Determining Effects of Small Magnitude Earthquakes on Seismic Hazard Analyses, Report 1014099, Electric Power Research Institute, Palo Alto, CA, and U.S. Department of Energy, Germantown, MD, 2006.

EPRI, 2006a. Program on Technology Innovation: Truncation of the Lognormal Distribution and Value of the Standard Deviation for Ground Motion Models in the Central and Eastern United States, TR-1014381, Electric Power Research Institute, August 2006.

EPRI, 2006b. Program on Technology Innovation: Truncation of the Lognormal Distribution and Value of the Standard Deviation for Ground Motion Models in the Central and Eastern United States, Technical Update 1013105, Electric Power Research Institute, February 2006.

Frankel, 1995. Mapping Seismic Hazard in the Central and Eastern United States, A.D. Frankel, Seismological Research Letters, Volume 66, Number 4, pp. 8-21, 1995.

GeoVision, 2008. Report Revision B, Boring Geophysical Logging, Borings B301, G-301, G302, and G-303, Berwick Unit 1 COL Project, GEOvision Geophysical Services, 2008.

Gutenberg, 1944. Frequency of earthquakes in California. B. Gutenberg, and C. F. Richter, Bulletin of the Seismological Society of America, Volume 34, p. 185-188, 1944.

Hough, 2000. On the Modified Mercalli intensities and magnitudes of the 1811-1812 New Madrid earthquakes. S. E. Hough, Armbruster, J.G., Seeber, L., and Hough, J.F Journal of Geophysical Research, Volume 105, Number B10, pp. 23,839-23,864, 2000.

Inners, 1978. Geology and Mineral Resources of the Berwick Quadrangle, Luzerne and Columbia Counties, Pennsylvania, Pennsylvania Geological Survey, Fourth Series, pp. 1-34, J.D. Inners, 1978.

Johnston, 1996. Seismic Moment Assessment of Earthquake in Stable Continental Regions - III. New Madrid 1811-1812, Charleston 1886 and Lisbon 1755, A. C. Johnston, Geophysical Journal International, Volume 126, pp. 314-344, 1996.

Kafka, 1985, Earthquake activity in the Greater New York City area: magnitudes, seismicity, and geologic structures, Kafka, A. L., E. A. Schlesinger-Miller, and N. L. Barstow (1985), Bulletin of the Seismological Society of America, 75 (5), 1285-1300.

Marple, 2000. Evidence of a buried fault system in the Coastal Plain of the Carolinas and Virginia- Implications for neotectonics in the southeastern United States, R. Marple and P. Talwani, Geological Society of America Bulletin, Volume 112, Number 2., pp. 200-220, 2000.

Mazzotti, 2005, GPS crustal strain, postglacial rebound, and seismc hazard in eastern North America: The Saint Lawrence Valley example, Mazzotti, S., T. S. James, J. Henton, and J. Adamas, Journal of Geophysical Research, Vol. 110, B11301, doi:10.1029/2004JB003590.

McGuire, 1988. Engineering Model of Earthquake Ground Motion for Eastern North America, Electric Power Research Institute Technical Report NP-6074, R. K. McGuire, G.R. Toro and W.J. Silva, 1988.

Mueller, 1997. Preparation of Earthquake Catalogs for the National Seismic-Hazard Maps: Contiguous 48 States, C. M. Mueller, C., M. Hopper, and A. Frankel, U.S. Geological Survey Open-File Report 97-464, 1997.

Mohajer, 1993, Seismicity and seismotectonics of the western Lake Ontario region, Géographie physique et Quaternaire, Mohajer, A. A., 1993, Vol. 47, 353-362.

Newmark, 1982. Earthquake Spectra and Design, N. M. Newmark and W.J. Hall, Earthquake Engineering Research Institute, Berkeley, California, 1982.

NGA, 2008. Final Report Revision 0, Susquehanna Unit 3 Nuclear Power Plant Downhole Seismic Velocity Survey, Berwick, Pennsylvania, Northwest Geophysical Associates, Inc., 2008.

NRC, 1997a. Identification and Characterization of Seismic Sources and Determination of Safe Shutdown Earthquake Ground Motion, Regulatory Guide 1.165, U. S. Nuclear Regulatory Commission, March 1997.

NRC, 1997b. Recommendations for Probabilistic Seismic Hazard Analysis: Guidance on Uncertainty and Use of Experts, Prepared by Senior Seismic Hazard Analysis Committee (SSHAC), NUREG/CR-6372, U. S. Nuclear Regulatory Commission, 1997.

NRC, 2001. Technical Basis for Revision of Regulatory Guidance on Design Ground Motions, Hazard- and Risk-Consistent Ground Motion Spectra Guidelines, NUREG/CR-6728, U. S. Nuclear Regulatory Commission, 2001.

NRC, 2002. Technical Basis for Revision of Regulatory Guidance on Design Ground Motions: Development of Hazard- & Risk-Consistent Seismic Spectra for Two Sites, NUREG/CR-6769, U. S. Nuclear Regulatory Commission, 2002.

NRC, 2005. Safety Evaluation Report for an Early Site Permit (ESP) at the North Anna ESP Site, NUREG-1835, U. S. Nuclear Regulatory Commission, September 2005.

NRC, 2007a. A Performance-Based Approach to Define the Site-Specific Earthquake Ground Motion, Regulatory Guide 1.208, U. S. Nuclear Regulatory Commission, March 2007.

NRC, 2007b. Vibratory Ground Motion, Standard Review Plan, NUREG-0800, Section 2.5.2, Revision 4, U.S. Nuclear Regulatory Commission, March 2007.

NRC, 2007c. Issuance of Early Site Permit for Exelon Generation Company, LLC (ESP-001), Letter from D.B. Matthews (NRC) to M.C. Kray (Exelon Nuclear), March 15, 2007.

Obermeier, 1987. Earthquake Induced Liquefaction Features in the Coastal South Carolina Region, U.S. Geological Survey Open File Report 87-504, S.F. Obermeier, R.E. Weems, R.B. Jacobson, 1987.

Scharnberger, 2006, Earthquake hazard in Pennsylvania, Pennsylvania Geological Survey, S.C. Scharnberger, Pennsylvania Geological Survey, Educational Series 10.

Schnabel, 1972. SHAKE - A Computer Program for Earthquake Response Analysis of Horizontally Layered Sites, P.B. Schnabel, J. Lysmer and H.B. Seed, Report No. EERC 72-12, University of California, Berkeley, 1972.

Schwartz, 1984. Fault Behavior and Characteristic Earthquakes: Examples from the Wasatch and San Andreas Fault Zones, Journal of Geophysical Research, D.P. Schwartz and K.J. Coppersmith, Volume 89, Number B7, pp 5681-5698, 1984.

Seeber, 1991. The NCEER-91 earthquake catalog: improved intensity-based magnitudes and recurrence relations for U.S. earthquakes east of New Madrid, L. Seeber and J. G. Armbruster National Center for Earthquake Engineering Research, NCEER-91-0021, 1991.

Seeber, 1993, Natural and induced seismicity in the Lake Erie-Lake Ontario region: reactivation of ancient faults with little neotectonic displacement, Géographie physique et Quaternaire, Seeber, L., and J. G. Armbruster, Vol 47, 363-378.

Seeber, 1998. The 1994 Cacoosing Valley earthquakes near Reading, Pennsylvania: A shallow rupture triggered by quarry unloading, L. Seeber, J. G. Armbruster, W.Y. Kim, N. Barstow, and C. Scharnberger, Journal of Geophysical Research, Volume 103, Number B10, pp. 24,505-24,521, 1998.

Silva, 2002. Development of regional hard rock attenuation relations for central and eastern North America, W. Silva, N. Gregor and R. Darragh, Pacific Engineering Analysis, El Cerrito, CA, 2002.

SNOC, 2008. Early Site Permits - Southern Nuclear Operating Company Application for the Vogtle ESP Site, Revision 4, Southern Nuclear Operating Company, 2008.

Somerville, 2001. Ground-Motion Attenuation Relations for the Central and Eastern United States, P. G. Somerville, N. Collins, N. A. Abrahamson, R. Graves and C. K. Saikia, Report to the USGS, NEHRP External Research Program, Award No. 99-HQ-GR-0098, 2001.

Sykes, 2008. Observations and Tectonic Setting of Historic and Instrumentally Located Earthquakes in the Greater New York City – Philadelphia Area, Lynn R. Sykes, John G. Armbruster, Won-Young Kim, and Leonardo Seeber, Bulletin of the Seismological Society of America, Volume 98, Number 4, p. 1696-1719, 2008.

Talwani, 2001. Recurrence rates of Large Earthquakes in the South Carolina Coastal Plain Based on Paleoliquefaction Data, P. Talwani and W. T. Schaeffer, Journal of Geophysical Research, Volume 106, Number B4, pp. 6621-6642, 2001.

Tavakoli, 2005. Empirical-stochastic ground-motion prediction for eastern North America, B. Tavakoli, B. and S. Pezeshk, Bulletin of the Seismological Society of America, Volume 95, pp. 2283-2296, 2005.

Toro, 1996. Probabilistic Models of Site Velocity Profiles for Generic and Site-Specific Ground Motion Amplification Studies, G. R. Toro, Published as an appendix in W. J. Silva, N. Abrahamson, G. Toro and C. Costantino, 1997, Description and validation of the stochastic ground motion model, Report Submitted to Brookhaven National Laboratory, Associated Universities, Inc. Upton, New York 11973, Contract No. 770573, 1996.

Toro, 1997. Model of Strong Ground Motions from Earthquakes in Central and Eastern North America: Best Estimates and Uncertainties, G. R. Toro, N. A. Abrahamson, and J. F. Schneider, Seismological Research Letters, Volume 68, Number 1, pp. 41-57, 1997.

Tuttle, 2002. The Earthquake Potential of the New Madrid Seismic Zone, M. P. Tuttle, E.S. Schweig, J.D. Sims, R.H. Lafferty, L.W. Wolf, and M.C. Haynes, Bulletin of the Seismological Society of America, Vol. 92, No. 6, pp. 2080-2089, 2002.

UniStar Nuclear, 2007. Calvert Cliffs Nuclear Power Plant Unit 3, Combined License Application, Revision 0, Part 2 Final Safety Analysis Report, Section 2.5.2, Vibratory Ground Motion, UniStar Nuclear, 2007.

USGS, 1996. National seismic-hazard maps: documentation, U. S Geological Survey, Open-File Report 96-532, A. Frankel, T. Barnhard, D. Perkins, E. V. Leyendecker, N. Dickman, S. Hanson, and M. Hopper, 1996.

USGS, 2002. Documentation for the 2002 Update of the National Seismic Hazard Maps, U.S. Geological Survey Open-File Report 02-420, A. D. Frankel, M. D. Petersen, C. S. Mueller, K. M Haller, R. L. Wheeler, E. V. Leyendecker, R. L. Wesson, S. C. Harmsen, C. H. Cramer, D. M. Perkins, and K. S. Rukstales, 2002.

USGS, 2008. Documentation for the 2008 update of the United States National Seismic Hazard Maps: U.S. Geological Survey Open-File Report 2008-1128, M. D. Peterson, A. D. Frankel, S. C. Harmsen, C. S. Muller, K. M. Haller, R. L. Wheeler, R. L. Wesson, Y. Zeng, O.S. Boyd, D. M. Perkins, N. Luco, E. H. Field, C. J. Wills, and K. S. Rukstales, 2008.

USGS, 2008, USGS web database: http://neic.usgs.gov/neis/epic/epic_circ.html, last accessed November 2008.

Wallach, 2002, The presence, characteristics and earthquake implications of the St. Lawrence fault zone within and near Lake Ontario (Canada–USA), J.L. Wallach, Tectonophysics 353 (2002) pp. 45– 74

Weichert, 1980. Estimation of the earthquake recurrence parameters for unequal observation periods for different magnitudes, D. H. Weichert, Bulletin of the Seismological Society of America, Volume 70, pp. 1337-1356, 1980.

Weston, 2008, www.bc.edu/research/westonobservatory, last accessed November 2008.

Youngs, 1985. Implications of Fault Slip Rates and Earthquake Recurrence Models to Probabilistic Seismic Hazard Estimates, Bulletin of the Seismological Society of America, R.R. Youngs and K.J. Coppersmith, Volume 75, Number 4, pp 939-964, 1985.}

Table 2.5-62a										
2002-2007 Events In 500 Mile (805 km) Radius										
m_b	Longitude (degree)	Latitude (degree)	Depth (km)	Year	Month	Day	Hour	Minute	Second	Catalog reference
3.80	-73.46	46.06	10	2002	2	11	11	41	37	**USGS (PDE)**
3.10	-75.17	45.29	18	2002	2	24	21	38	33	**USGS (PDE)**
3.04	-69.33	41.62	1	2002	3	12	7	13	24	**ANSS**
5.30	-73.70	44.51	11	2002	4	20	10	50	47	**ANSS**
3.60	-73.68	44.50	10	2002	5	24	23	46	0	**USGS (PDE)**
3.40	-76.62	45.63	18	2002	5	28	9	15	38	**USGS (PDE)**
3.17	-68.98	44.99	27.93	2002	6	5	20	18	44	**ANSS**
3.20	-73.86	45.59	18	2002	6	1	11	35	29	**USGS (PDE)**
3.40	-73.70	44.50	9	2002	6	25	13	40	28	**USGS (PDE)**
3.70	-76.29	46.96	18	2002	9	7	21	27	45	**USGS (PDE)**
3.00	-77.43	44.05	18	2002	11	7	16	55	6	**USGS (PDE)**
3.30	-73.79	44.56	14	2002	12	25	18	25	19	**USGS (PDE)**
3.30	-75.20	46.51	18	2003	2	9	16	18	3	**ANSS**
3.50	-82.89	44.69	5	2003	3	18	6	4	24	**ANSS**
3.70	-74.34	44.62	10	2003	4	8	15	6	14	**USGS (PDE)**
3.90	-78.07	37.76	5	2003	5	5	16	32	32	**USGS (PDE)**
3.60	-81.20	41.80	4	2003	6	30	19	21	17	**USGS (PDE)**

Table 2.5-62a 2002-2007 Events In 500 Mile (805 km) Radius										
m_b	Longitude (degree)	Latitude (degree)	Depth (km)	Year	Month	Day	Hour	Minute	Second	Catalog reference
3.60	-70.02	42.77	11	2003	7	22	11	41	15	**USGS (PDE)**
3.50	-74.95	46.01	18	2003	8	20	1	58	17	**USGS (PDE)**
3.80	-75.11	40.61	3	2003	8	26	18	24	18	**USGS (PDE)**
4.50	-76.37	47.01	18	2003	10	12	8	26	7	**ANSS**
4.50	-77.90	37.59	5	2003	12	9	20	59	14	**USGS (PDE)**
3.30	-81.08	41.78	5	2004	6	30	4	3	14	**USGS (PDE)**
3.20	-78.25	43.69	5	2004	8	4	23	55	26	**USGS (PDE)**
3.30	-77.97	48.05	19.68	2005	1	30	18	6	45	**ANSS**
3.50	-74.20	45.06	18	2005	3	3	2	22	1	**USGS (PDE)**
3.60	-80.98	46.54	18	2005	3	13	17	8	14	**USGS (PDE)**
3.40	-75.64	46.28	18	2005	3	31	15	13	8	**USGS (PDE)**
3.40	-73.45	46.26	18	2005	4	8	4	32	38	**USGS (PDE)**
3.27	-75.61	46.29	5	2005	5	25	19	22	13	**ANSS**
3.30	-76.89	46.24	13.4	2005	7	4	11	47	14	**ANSS**
3.00	-75.13	47.06	10	2005	7	23	2	48	20	**ANSS**
3.60	-75.29	46.27	18	2005	9	6	14	10	51	**USGS (PDE)**
3.10	-76.52	46.63	12.88	2005	10	1	7	1	46	**ANSS**
4.20	-80.48	44.68	11	2005	10	20	21	16	28	**USGS (PDE)**

Table 2.5-62a 2002-2007 Events In 500 Mile (805 km) Radius										
m_b	Longitude (degree)	Latitude (degree)	Depth (km)	Year	Month	Day	Hour	Minute	Second	Catalog reference
3.70	-73.90	45.03	12.69	2006	1	9	15	35	40	**ANSS**
4.50	-75.23	45.66	18	2006	2	25	1	39	22	**USGS (PDE)**
3.20	-74.71	45.55	18	2006	2	26	4	9	22	**USGS (PDE)**
3.10	-81.39	41.78	5	2006	3	11	12	27	15	**USGS (PDE)**
3.10	-76.62	46.83	18	2006	4	7	12	44	26	**USGS (PDE)**
3.10	-72.68	46.27	18	2006	5	11	6	35	38	**USGS (PDE)**
3.50	-81.23	41.84	5	2006	6	20	20	11	18	**USGS (PDE)**
3.40	-68.19	44.35	7	2006	9	22	10	39	21	**USGS (PDE)**
3.40	-79.58	34.55	5	2006	9	22	11	22	0	**USGS (PDE)**
3.70	-79.88	34.75	5	2006	9	25	5	44	25	**USGS (PDE)**
4.17	-68.14	44.35	10.83	2006	10	3	0	7	38	**ANSS**
4.30	-81.92	37.20	1	2006	11	2	17	53	2	**USGS (PDE)**
4.30	-81.97	37.16	0	2006	11	23	10	42	57	**USGS (PDE)**
4.10	-81.17	46.48	1	2006	11	29	7	22	55	**USGS (PDE)**
3.20	-68.17	44.35	8	2006	12	29	21	21	10	**USGS (PDE)**
3.30	-76.23	47.03	18	2007	1	6	4	8	44	**USGS (PDE)**
3.70	-81.38	41.28	5	2007	3	12	23	18	16	**USGS**

Table 2.5-62a										
2002-2007 Events In 500 Mile (805 km) Radius										
m_b	Longitude (degree)	Latitude (degree)	Depth (km)	Year	Month	Day	Hour	Minute	Second	Catalog reference
										(PDE)
3.20	-76.09	46.71	18	2007	5	11	5	55	22	**USGS (PDE)**
3.00	-72.89	46.99	18	2007	5	31	1	57	44	**USGS (PDE)**
3.00	-74.96	46.09	14.64	2007	6	2	2	19	54	**ANSS**
3.10	-78.17	43.71	5	2007	7	19	17	7	58	**USGS (PDE)**
3.10	-74.12	42.60	15	2007	7	24	1	56	48	**USGS (PDE)**
3.20	-74.36	44.32	2	2007	8	30	3	47	45	**USGS (PDE)**
3.90	-76.52	46.88	13	2007	9	30	17	35	35	**USGS (PDE)**
4.10	-76.88	47.08	18	2007	10	1	16	42	8	**USGS (PDE)**
3.50	-75.13	46.53	11	2007	10	13	5	53	31	**USGS (PDE)**
3.40	-81.42	41.75	5	2007	10	17	20	4	9	**USGS (PDE)**
3.53	-77.14	46.52	3.41	2007	10	28	9	47	18	**ANSS**
3.00	-75.12	46.31	18	2007	12	12	15	51	20	**USGS (PDE)**
3.00	-76.96	45.79	18	2007	12	20	12	16	41	**USGS (PDE)**
3.60	**-77.32**	**46.26**	**18**	**2007**	**12**	**23**	**23**	**48**	**34**	**USGS (PDE)**

Table 2.5-62b

Uniform Hazard Response Spectra Comparison of 500-mi Sensitivity Analysis

Spectral frequency (Hz)	Probability of Exceedance Levels: 2002 Catalog with 2002-2007 Update (500 miles) Spectral Value (g)			2002 Catalog (Base Case) Spectral Value (g)			Difference (%)		
	10^{-4}	10^{-5}	10^{-6}	10^{-4}	10^{-5}	10^{-6}	10^{-4}	10^{-5}	10^{-6}
0.5	0.0355	0.1100	0.2430	0.0357	0.1103	0.2437	-0.5%	-0.3%	-0.3%
1.0	0.0450	0.1175	0.2582	0.0454	0.1183	0.2606	-0.8%	-0.7%	-0.9%
2.5	0.0795	0.2166	0.5464	0.0807	0.2202	0.5565	-1.5%	-1.7%	-1.8%
5.0	0.1279	0.3978	1.0866	0.1307	0.4068	1.1081	-2.1%	-2.2%	-1.9%
10.0	0.1840	0.6314	1.7888	0.1888	0.6474	1.8252	-2.5%	-2.5%	-2.0%
25.0	0.2729	0.9777	3.0327	0.2802	1.0043	3.1000	-2.6%	-2.6%	-2.2%
100.0	0.0947	0.3512	1.0692	0.0973	0.3611	1.0914	-2.6%	-2.7%	-2.0%

Table 2.5-62c

Uniform Hazard Response Spectra Comparison for the 625 mile (1006 km) Charlevoix Sensitivity Analysis Case 1

Spectral frequency (Hz)	Probability of Exceedance Levels: Modified Charlevoix Approach Case 1 Spectral Value (g)			Base Case Spectral Value (g)			Difference (%)		
	10^{-4}	10^{-5}	10^{-6}	10^{-4}	10^{-5}	10^{-6}	10^{-4}	10^{-5}	10^{-6}
0.5	0.0356	0.1101	0.2432	0.0357	0.1103	0.2437	-0.3%	-0.2%	-0.2%
1.0	0.0451	0.1176	0.2585	0.0454	0.1183	0.2606	-0.7%	-0.6%	-0.8%
2.5	0.0796	0.2169	0.5474	0.0807	0.2202	0.5565	-1.4%	-1.5%	-1.6%
5.0	0.1281	0.3986	1.0888	0.1307	0.4068	1.1081	-2.0%	-2.0%	-1.7%
10.0	0.1844	0.6329	1.7924	0.1888	0.6474	1.8252	-2.3%	-2.2%	-1.8%
25.0	0.2734	0.9801	3.0392	0.2802	1.0043	3.1000	-2.4%	-2.4%	-2.0%
100.0	0.0949	0.3521	1.0714	0.0973	0.3611	1.0914	-2.4%	-2.5%	-1.8%

Table 2.5-62d

Maximum Magnitude Distribution used for the for the 625 mile (1006 km) Charlevoix Sensitivity Analyses

Maximum Magnitude	Weight
5.9	0.33
6.3	0.34
6.7	0.33

Table 2. 5-62e

Uniform Hazard Response Spectra Comparison for the 625 mile (1006 km) Charlevoix Sensitivity Analysis Case 2

Spectral frequency (Hz)	Probability of Exceedance Levels								
	Modified Charlevoix Approach Case 2 Spectral Value (g)			Base Case Spectral Value (g)			Difference (%)		
	10^{-4}	10^{-5}	10^{-6}	10^{-4}	10^{-5}	10^{-6}	10^{-4}	10^{-5}	10^{-6}
0.5	0.0357	0.1102	0.2433	0.0357	0.1103	0.2437	0.0%	-0.1%	-0.1%
1.0	0.0452	0.1177	0.2587	0.0454	0.1183	0.2606	-0.4%	-0.5%	-0.7%
2.5	0.0797	0.2170	0.5475	0.0807	0.2202	0.5565	-1.3%	-1.5%	-1.6%
5.0	0.1282	0.3986	1.0888	0.1307	0.4068	1.1081	-1.9%	-2.0%	-1.7%
10.0	0.1844	0.6329	1.7924	0.1888	0.6474	1.8252	-2.3%	-2.2%	-1.8%
25.0	0.2735	0.9801	3.0392	0.2802	1.0043	3.1000	-2.4%	-2.4%	-2.0%
100.0	0.0949	0.3521	1.0714	0.0973	0.3611	1.0914	-2.4%	-2.5%	-1.8%

Table 2.5-62f

Maximum Magnitude Distribution for the RSZ EST Zones

EST	Zone(s) encompassing RSZ	Mmax Distribution		Mean Mmax
		Mmax	Weight	
Bechtel	Zone 13	5.4	0.1	5.82
		5.7	0.4	
		6.0	0.4	
		6.6	0.1	
	BZ5	5.7	0.1	6.15
		6.0	0.4	
		6.3	0.4	
		6.6	0.1	
Dames & Moore	Zone 41	6.1	0.8	6.32
		7.2	0.2	
	Zone 42	6.3	0.75	6.52
		7.2	0.25	
Law	Zone 17	5.7	0.2	6.58
		6.8	0.8	
Rondout	Zone 31	5.8	0.15	6.47
		6.5	0.60	
		6.8	0.25	
WCC	Zone 21	5.3	0.33	6.23
		6.5	0.34	
		6.9	0.33	
Weston	Zone 21	5.4	0.62	5.68
		6.0	0.29	
		6.6	0.09	

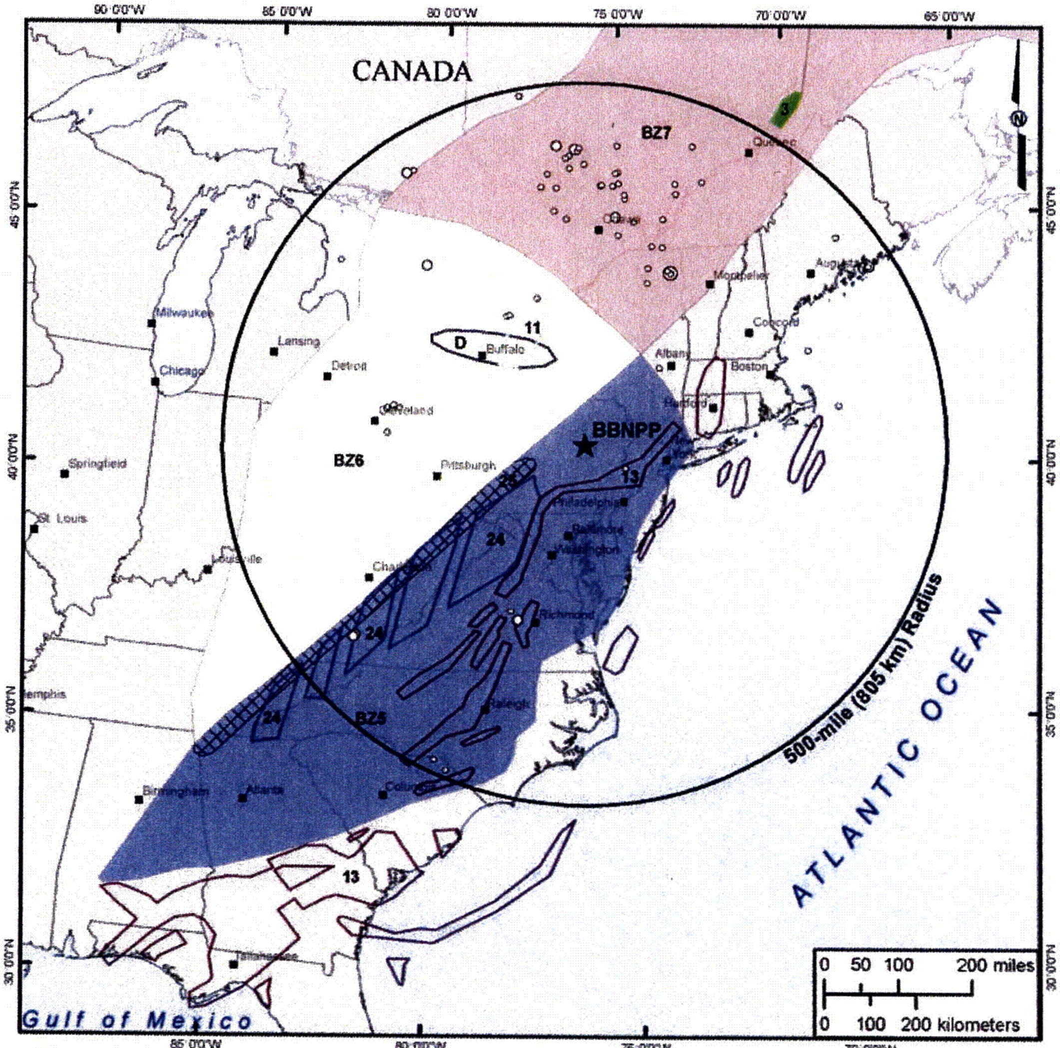

LEGEND

★ Center Point of Proposed Bell Bend NPP (BBNPP)
▪ City
○ NPP Reactor 500-mile (805 km) Radius

Earthquakes by Magnitude, mb (SEE NOTE)

USGS 2002 to 2007

- 3.0 - 3.9
- 4.0 - 4.9
- 5.0 - 5.9

Bechtel Group Sources contributing to 99% of BBNPP Site Hazard

- 3 La Malbaie/Charlevoix
- 11 Clarendon-Linden
- 13 Mesozoic Basins
- 24 Bristol Block
- 26 NY-AL Lineament
- BZ5 Southern Appalachians Background
- BZ6 Southern Eastern Craton Background
- BZ7 Northern Eastern Craton Background
- D Niagara Area

REFERENCES:
- ESRI, 2007.
- USGS 2007.
- ANSS, 2007.
- EPRI Volume IX: Bechtel Group, 1986

NOTE: The 2002 to 2007 seismicity shown in 500-mile (805 km) radius.

Figure 2.5-86a

Bechtel EPRI Source Zones and 2002-2007 events in 500-mile radius

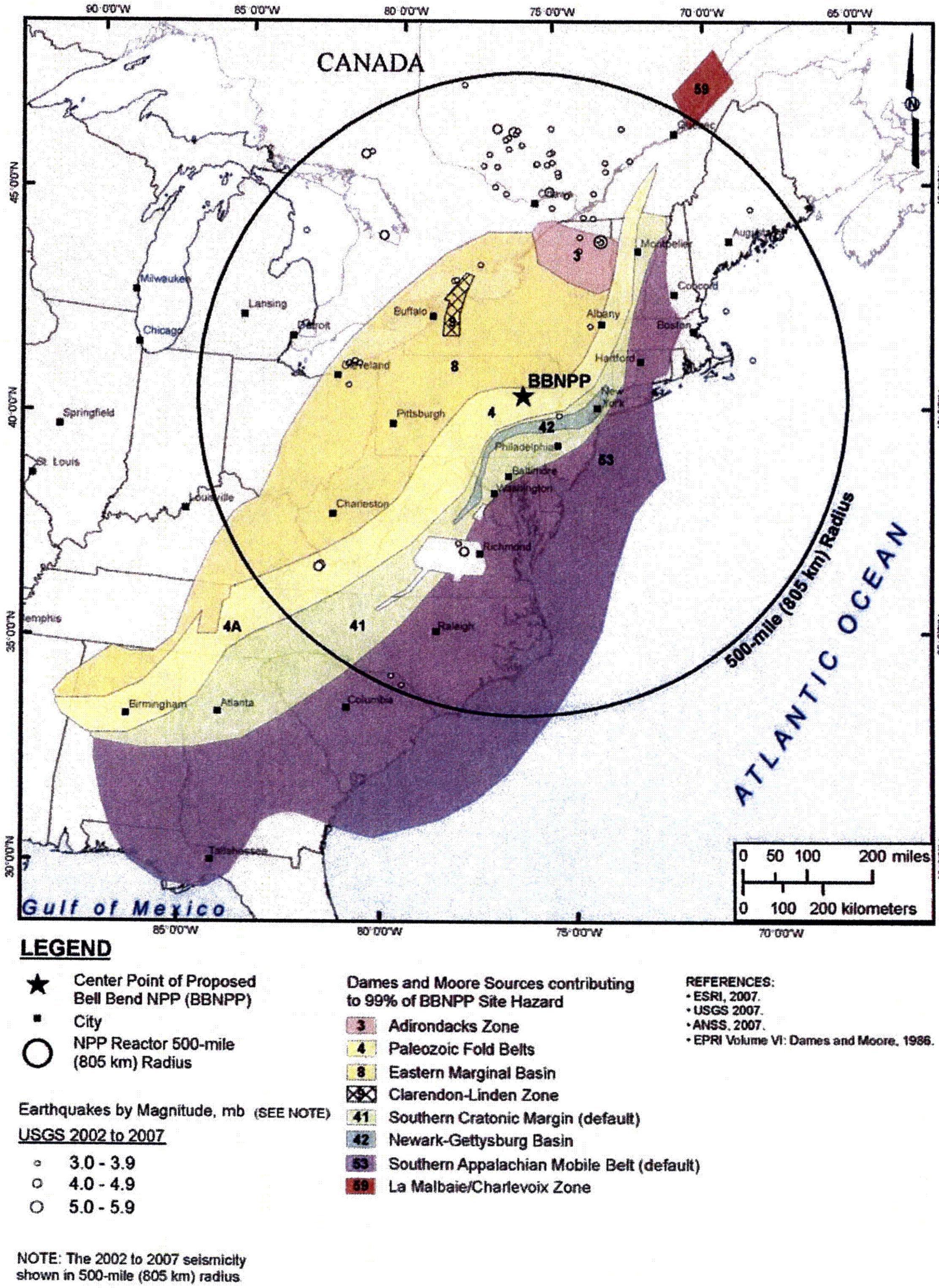

Figure 2.5-86b

Dames and Moore EPRI Source Zones and 2002-2007 events in 500-mile radius

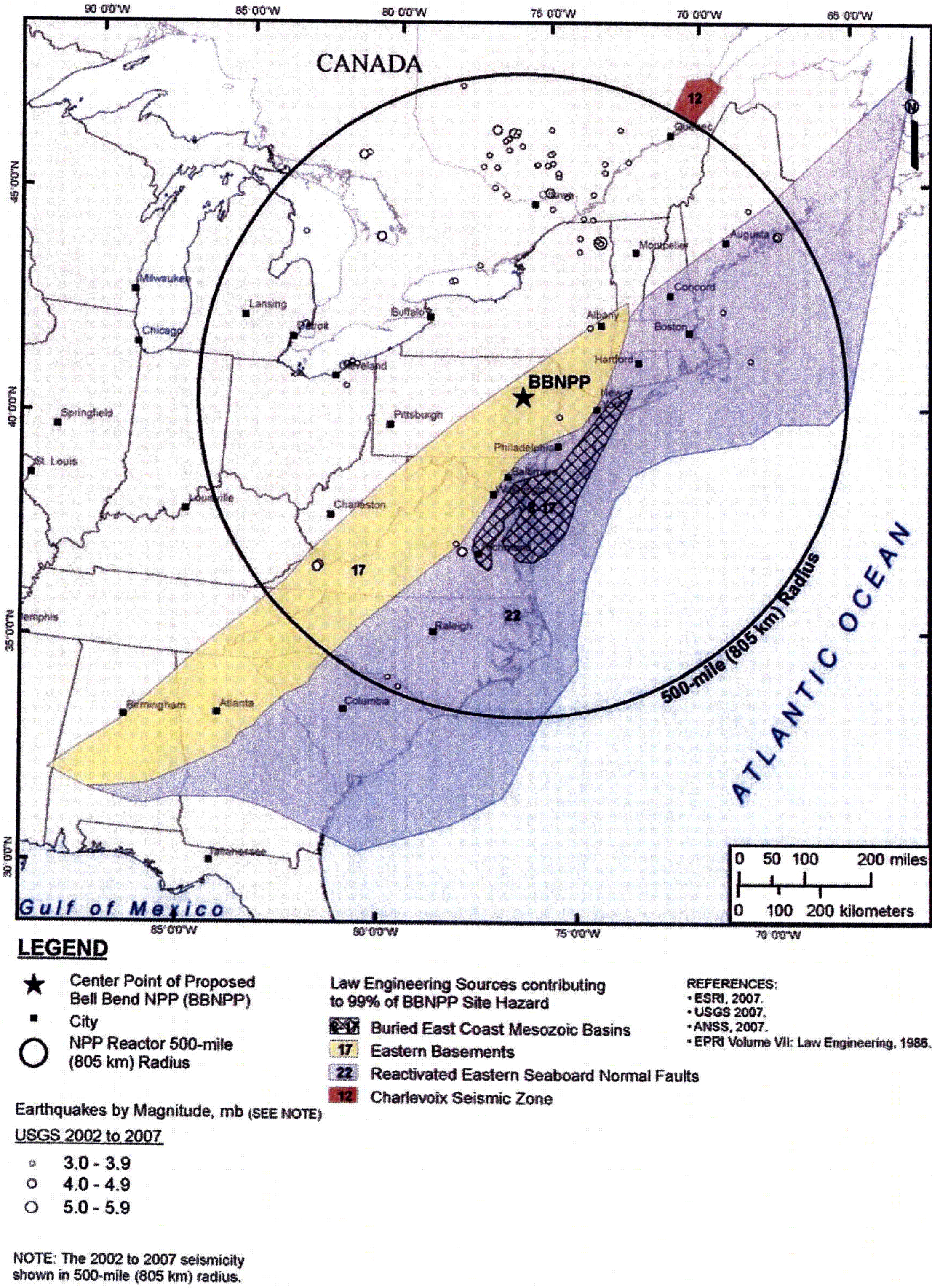

Figure 2.5-86c

Law Engineering EPRI Source Zones and 2002-2007 events in 500-mile radius

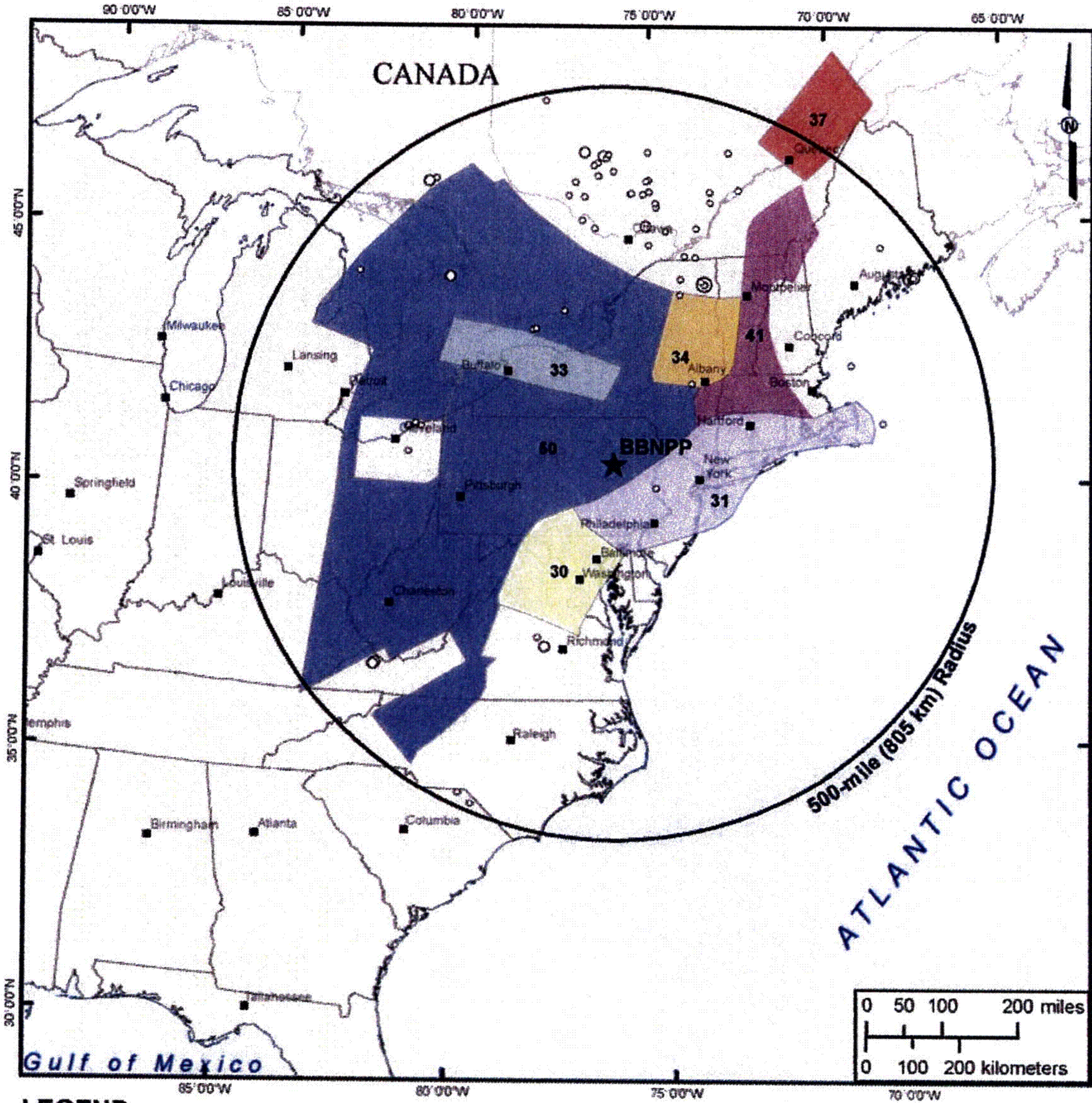

LEGEND

★ Center Point of Proposed Bell Bend NPP (BBNPP)

■ City

○ NPP Reactor 500-mile (805 km) Radius

Earthquakes by Magnitude, mb (SEE NOTE)

USGS 2002 to 2007

- 3.0 - 3.9
- 4.0 - 4.9
- 5.0 - 5.9

NOTE: The 2002 to 2007 seismicity shown in 500-mile (805 km) radius.

Rondout Associates Sources contributing to 99% of BBNPP Site Hazard

- 30 Shenandoah
- 31 Quakers
- 33 Niagara
- 34 Nessmuk
- 37 La Malbaie (Charlevoix) Seismic Zone
- 41 Vermont
- 50 Grenville (Background)

REFERENCES:
- ESRI, 2007.
- USGS 2007.
- ANSS, 2007.
- EPRI Volume X: Rondout Associates, 1986.

Figure 2.5-86d

Rondout Associates EPRI Source Zones and 2002-2007 events in 500-mile radius

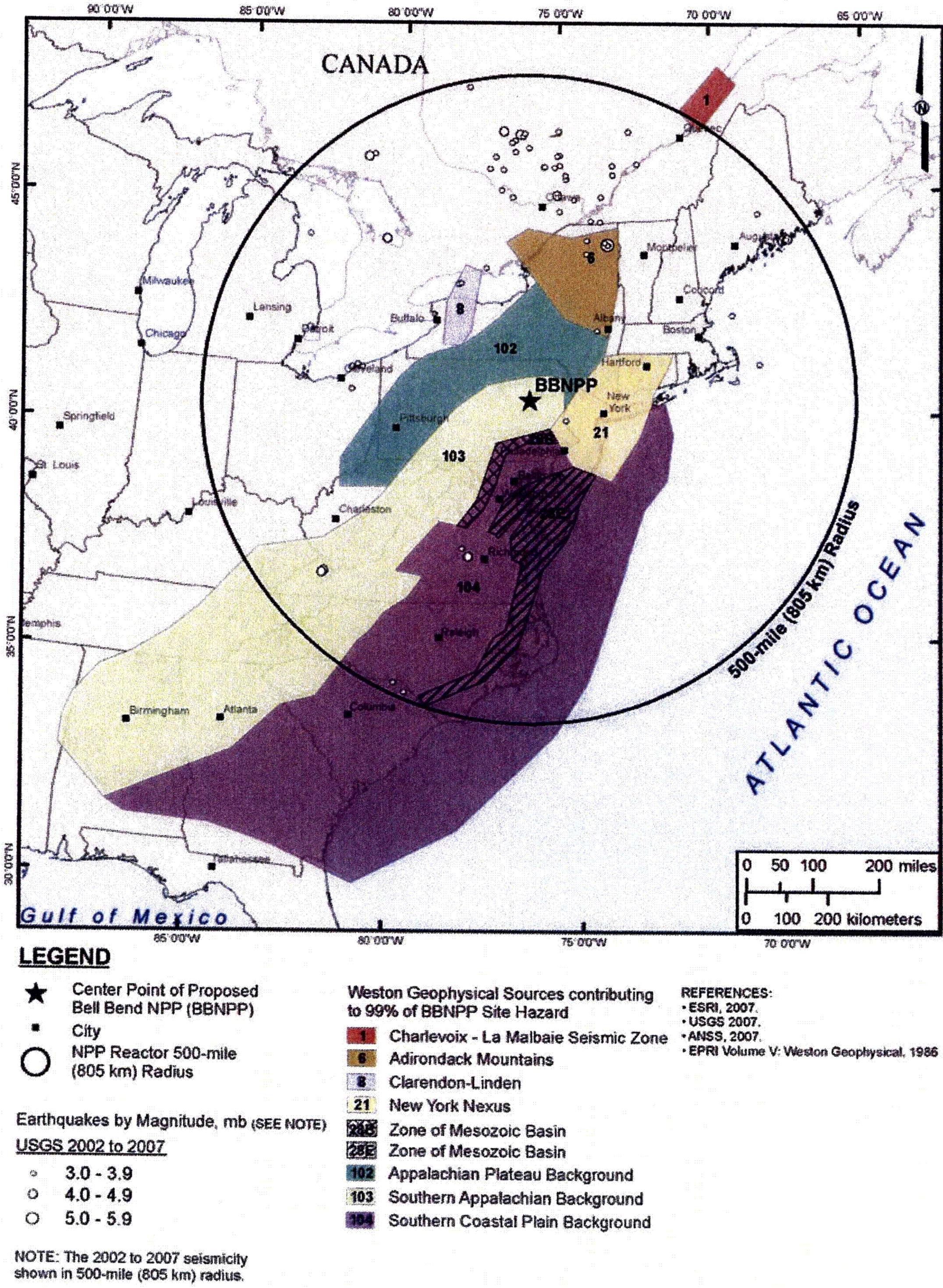

Figure 2.5-86e

Weston Geophysical EPRI Source Zones and 2002-2007 events in 500-mile radius

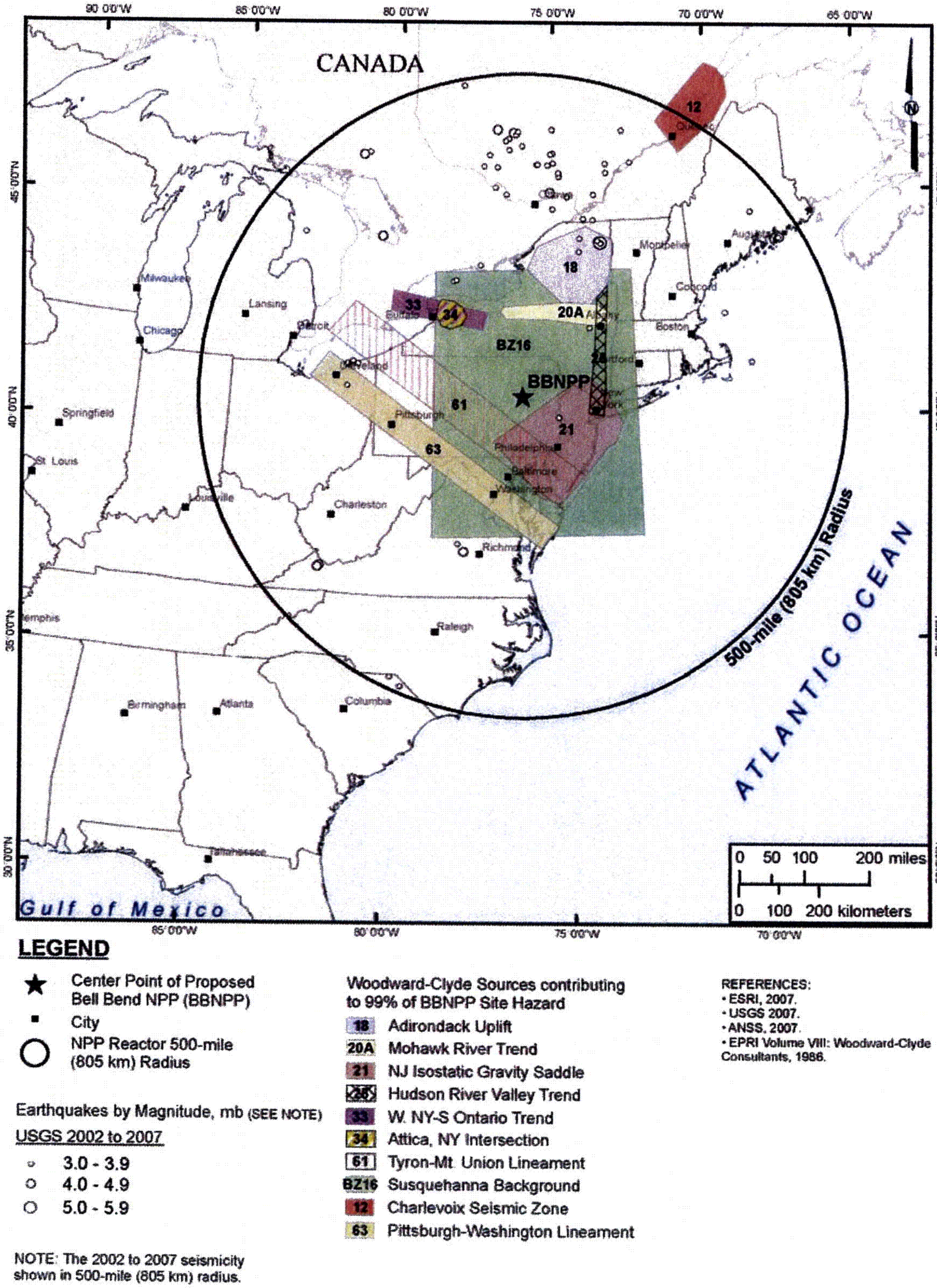

Figure 2.5-86f

Woodward-Clyde EPRI Source Zones and 2002-2007 events in 500-mile radius

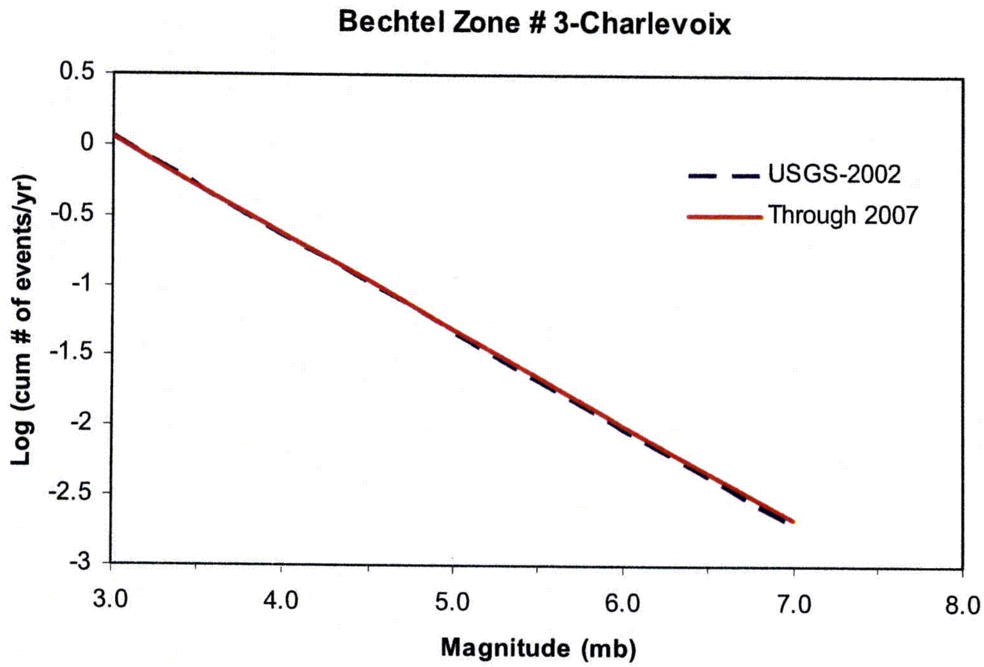

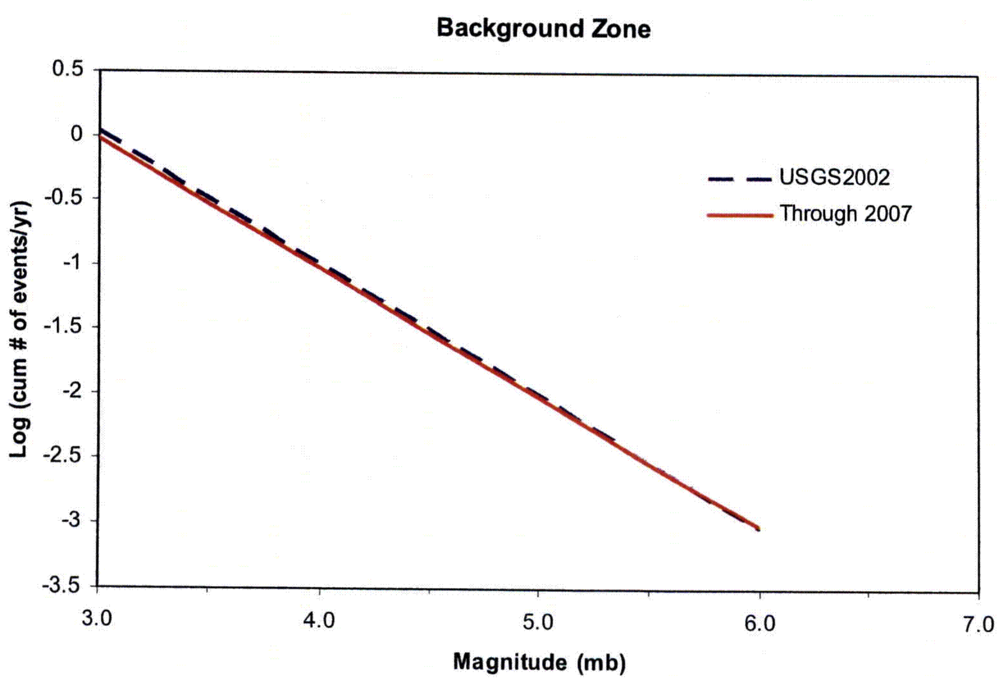

Figure 2.5-86g

Comparison of seismicity rates

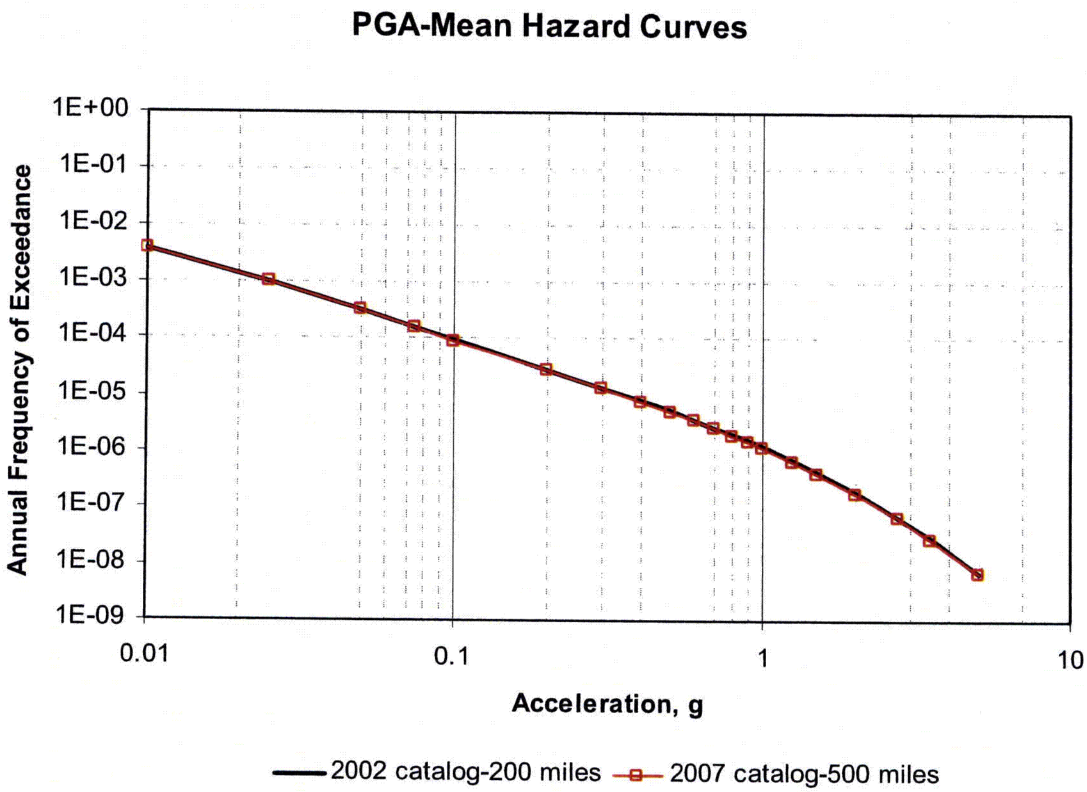

Figure 2.5-86h

Comparison of PGA-Mean Hazard Curves

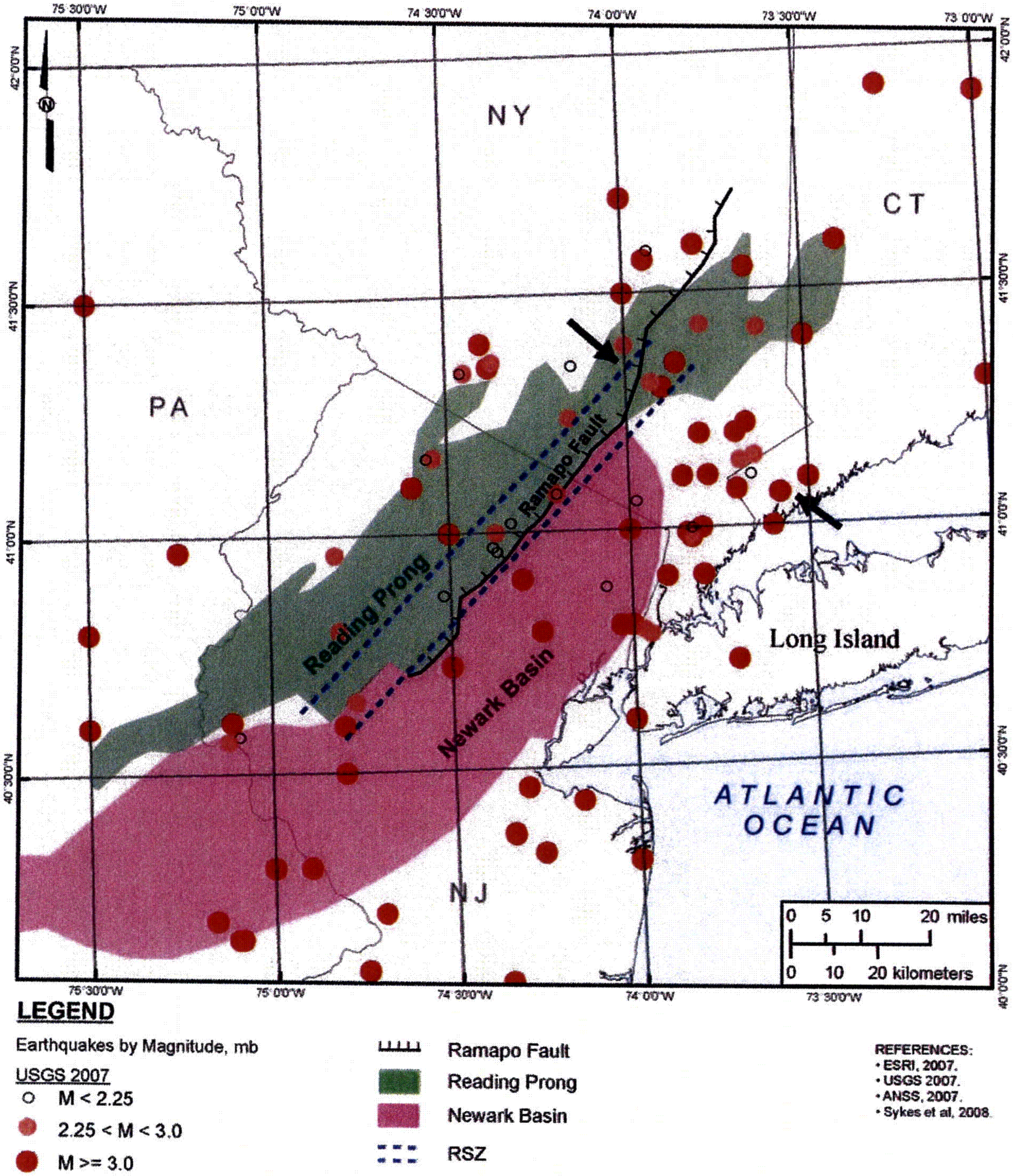

Figure 2.5-86i

Seismicity of New York-Philadelphia area (Sykes et al., 2008)

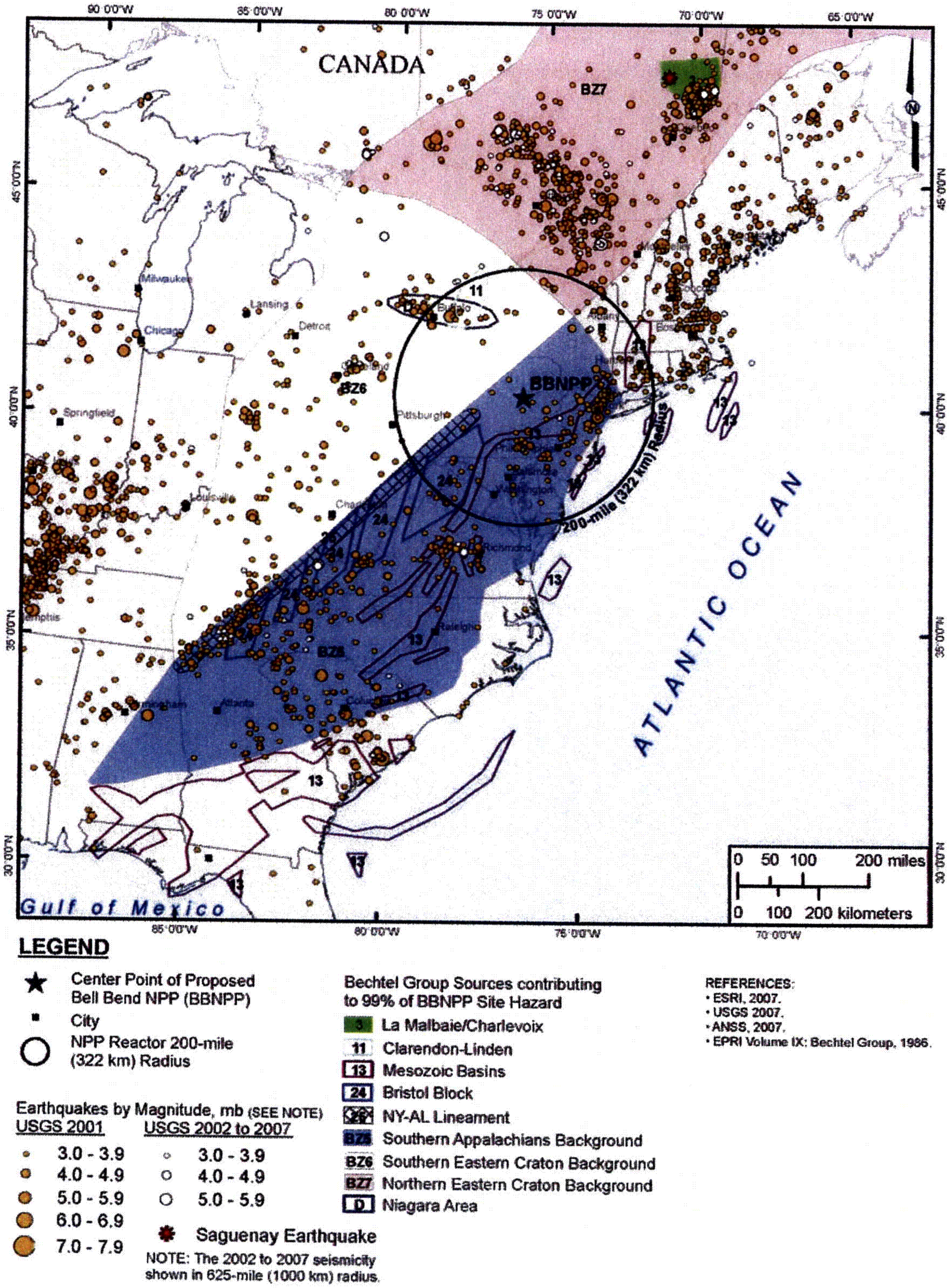

Figure 2.5-86j

Bechtel EPRI Source Zones for Charlevoix Sensitivity Analysis Case 1

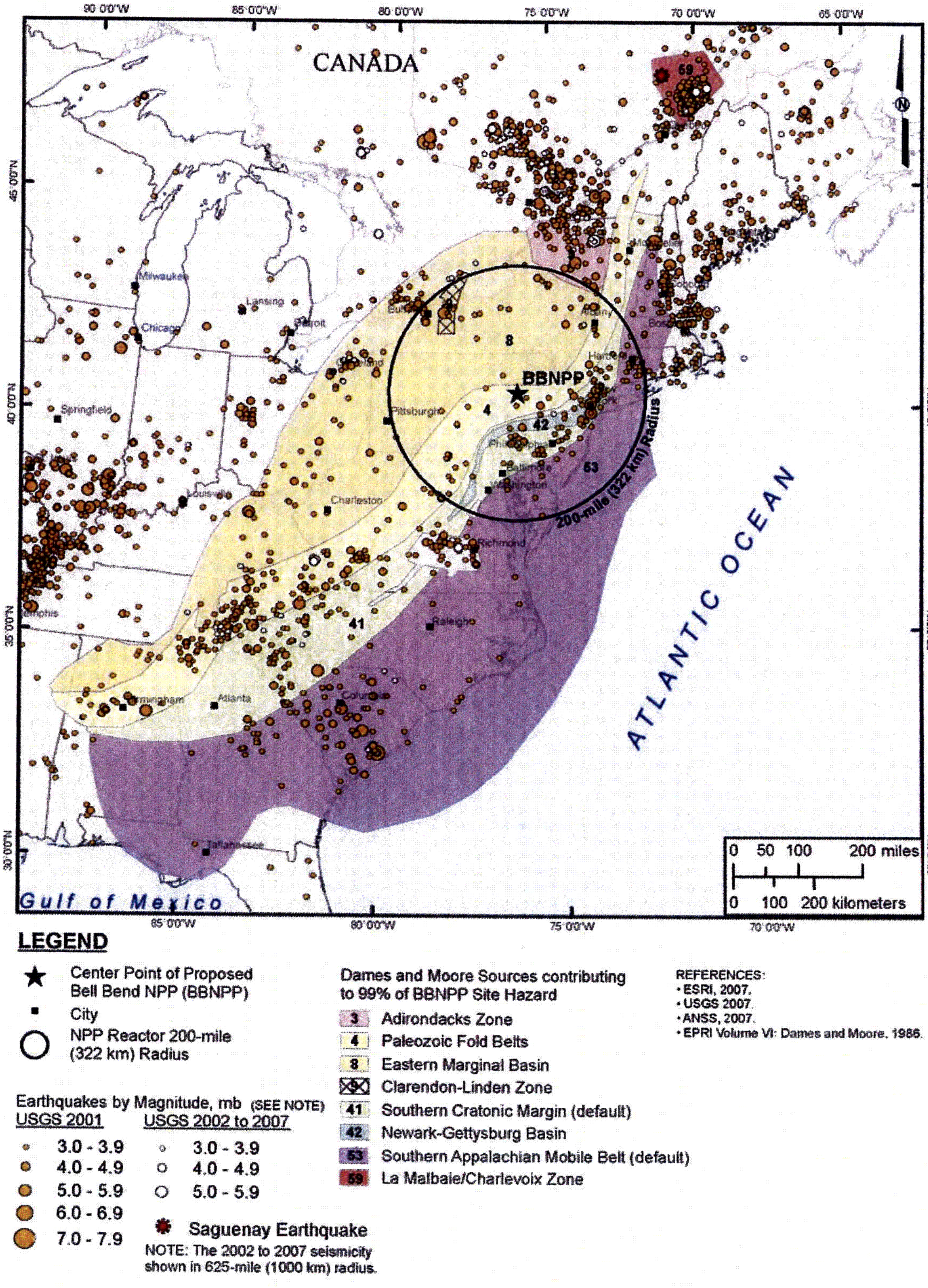

Figure 2.5-86k

Dames and Moore EPRI Source Zones for Charlevoix Sensitivity Analysis Case 1

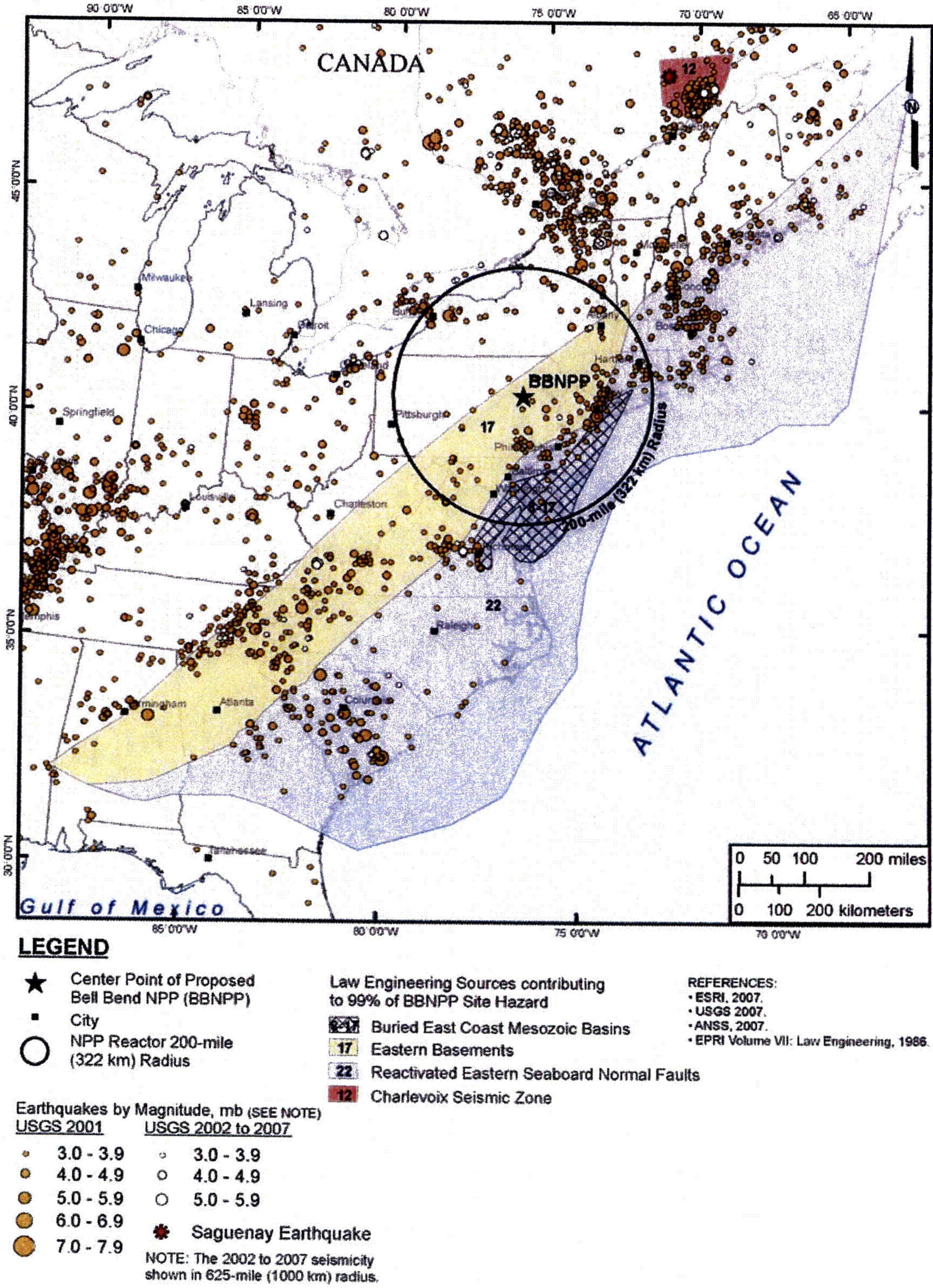

Figure 2.5-86l

Law Engineering EPRI Source Zones for Charlevoix Sensitivity Analysis Case 1

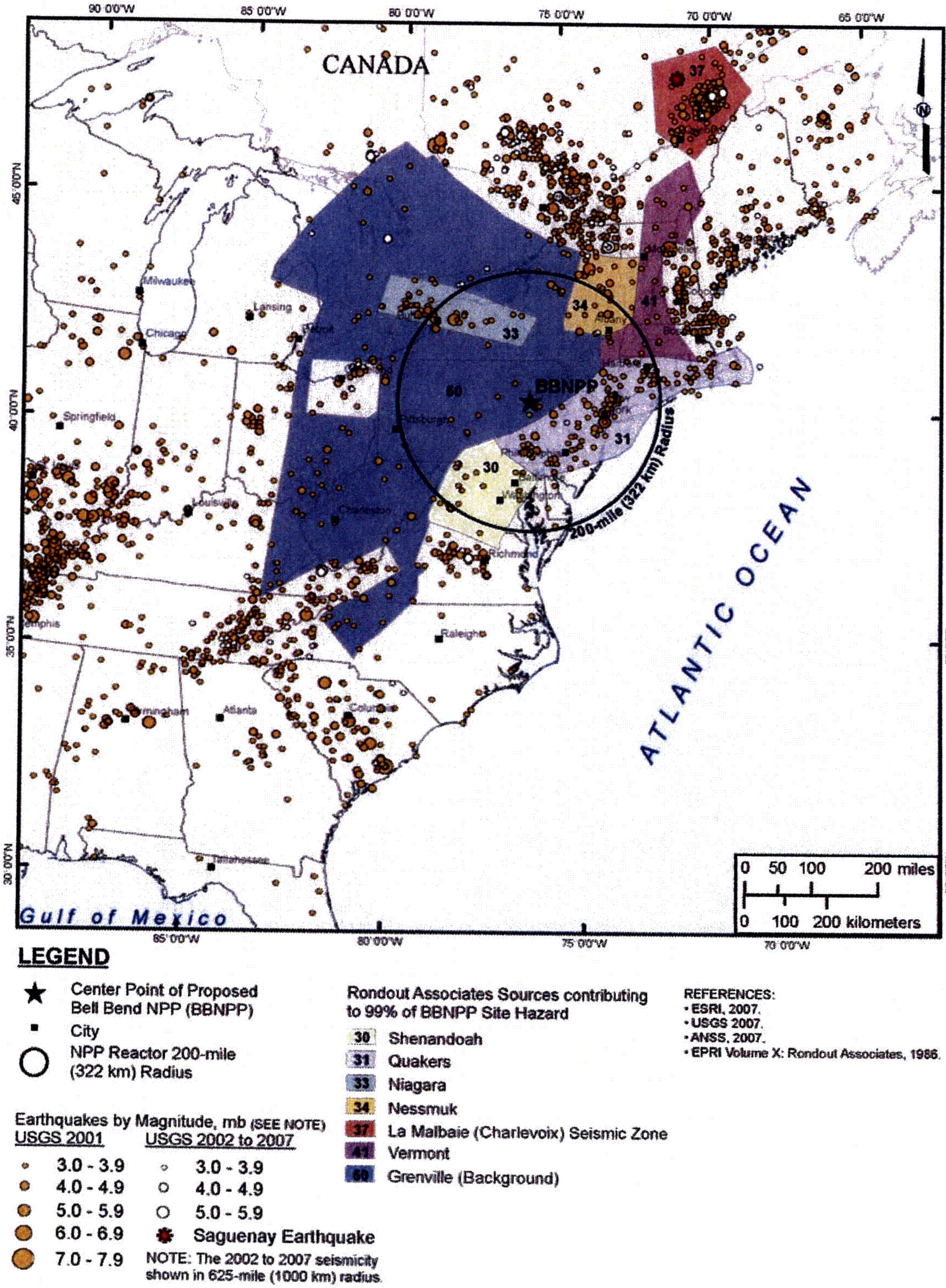

Figure 2.5-86m

Rondout Associates EPRI Source Zones for Charlevoix Sensitivity Analysis Case 1

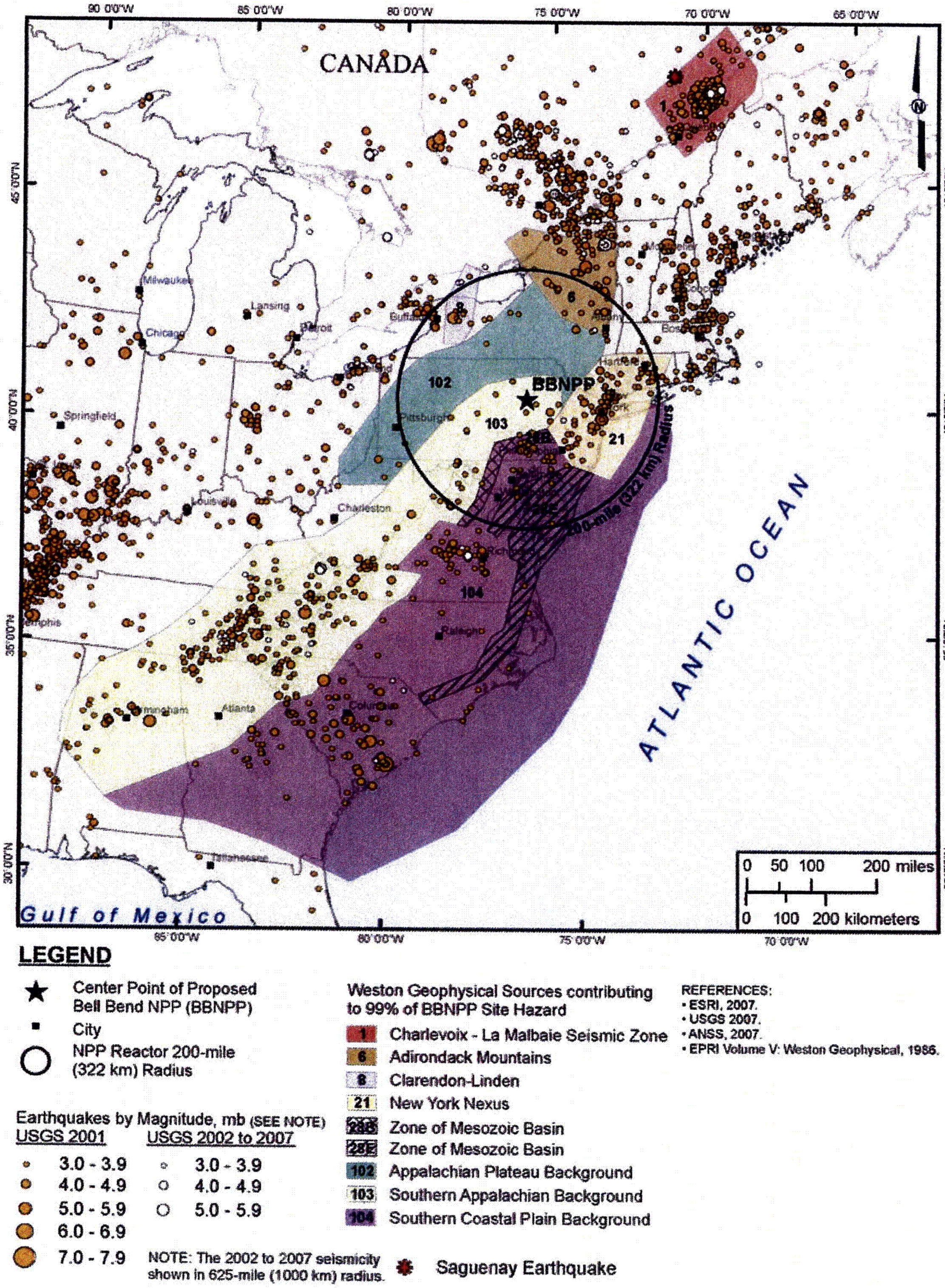

Figure 2.5-86n

Weston Geophysical EPRI Source Zones for Charlevoix Sensitivity Analysis Case 1

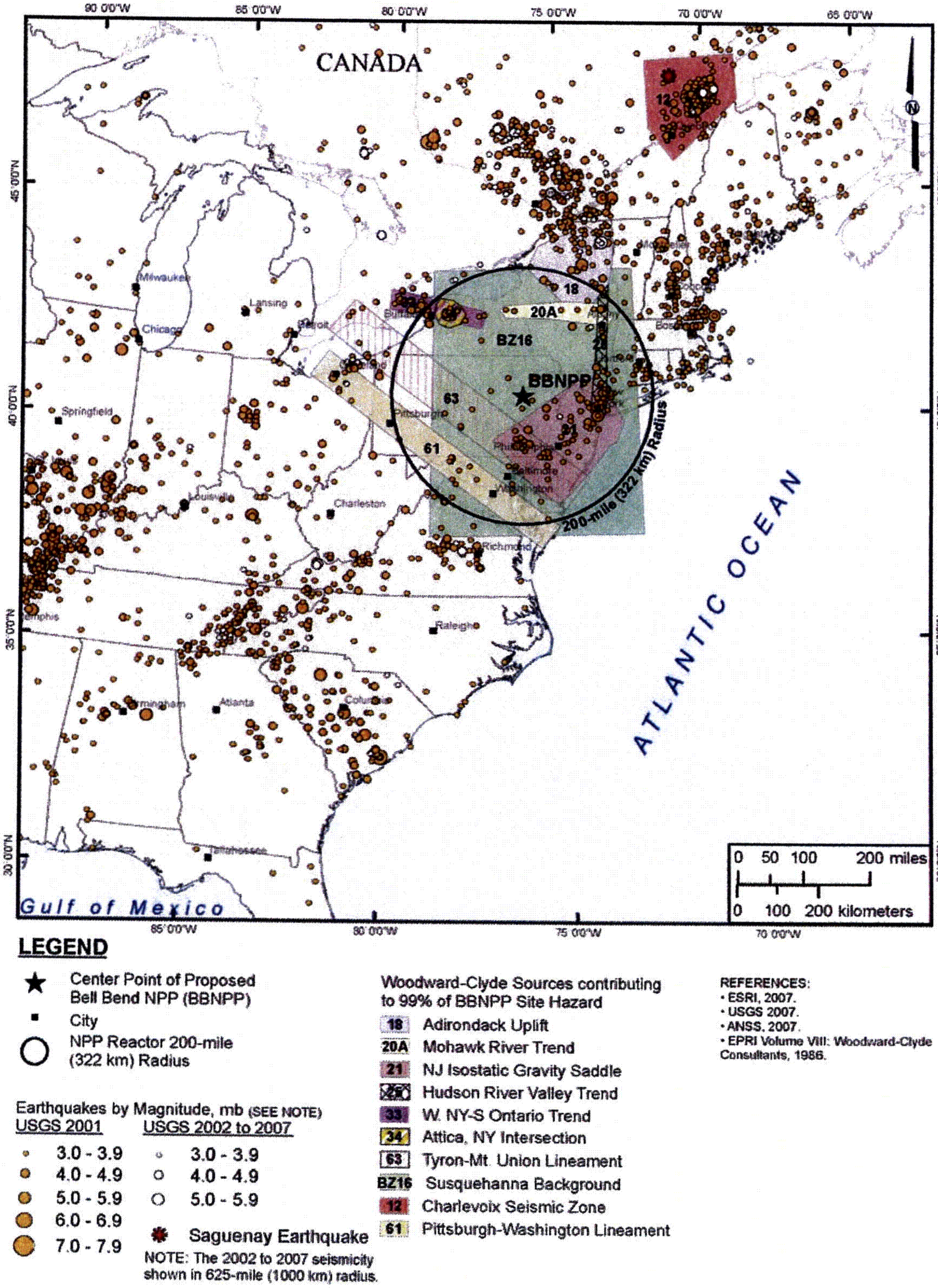

Figure 2.5-86o

Woodward-Clyde EPRI Source Zones for Charlevoix Sensitivity Analysis Case 1

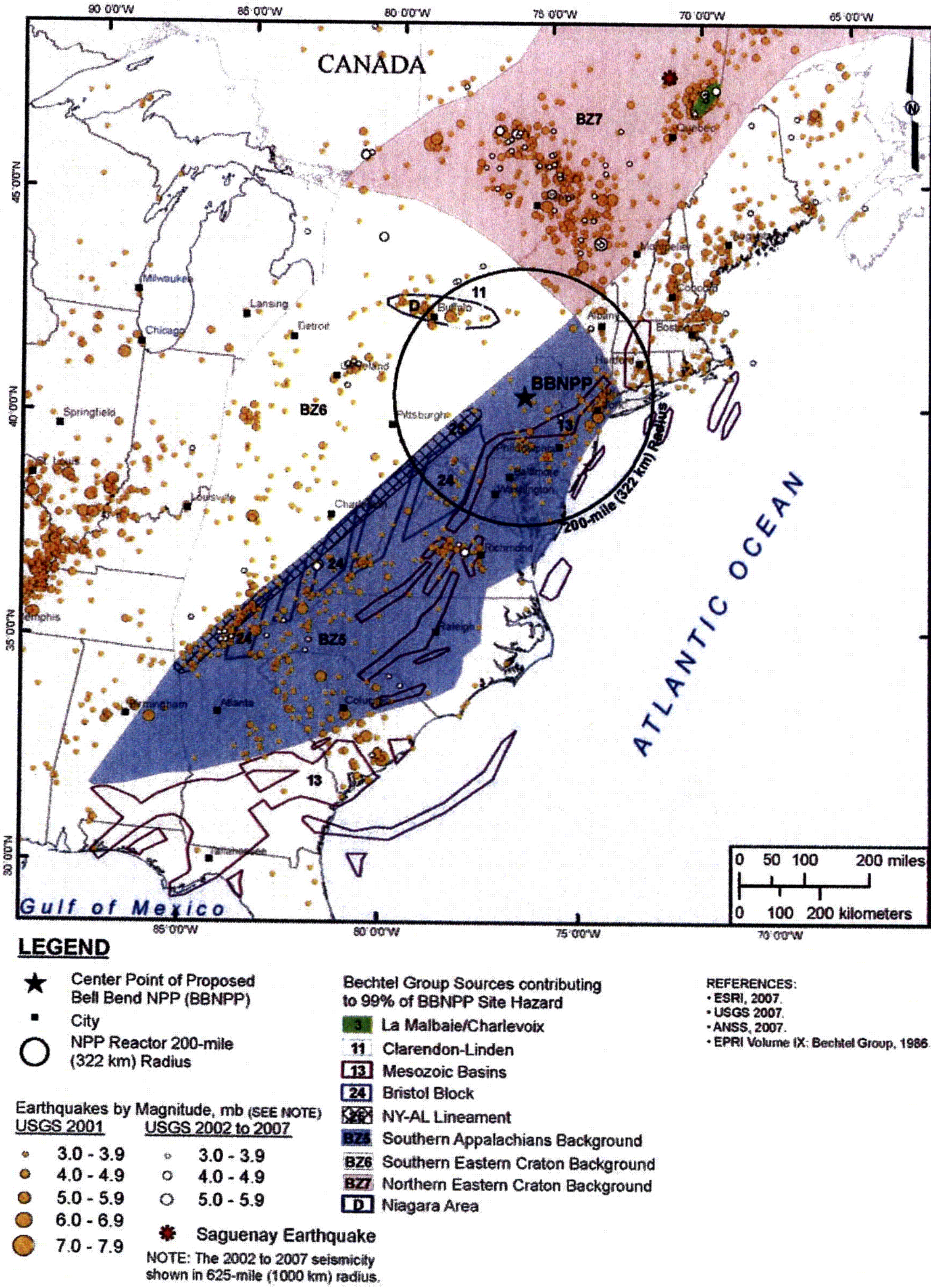

Figure 2.5-86p

Bechtel EPRI Source Zones for Charlevoix Sensitivity Analysis Case 2

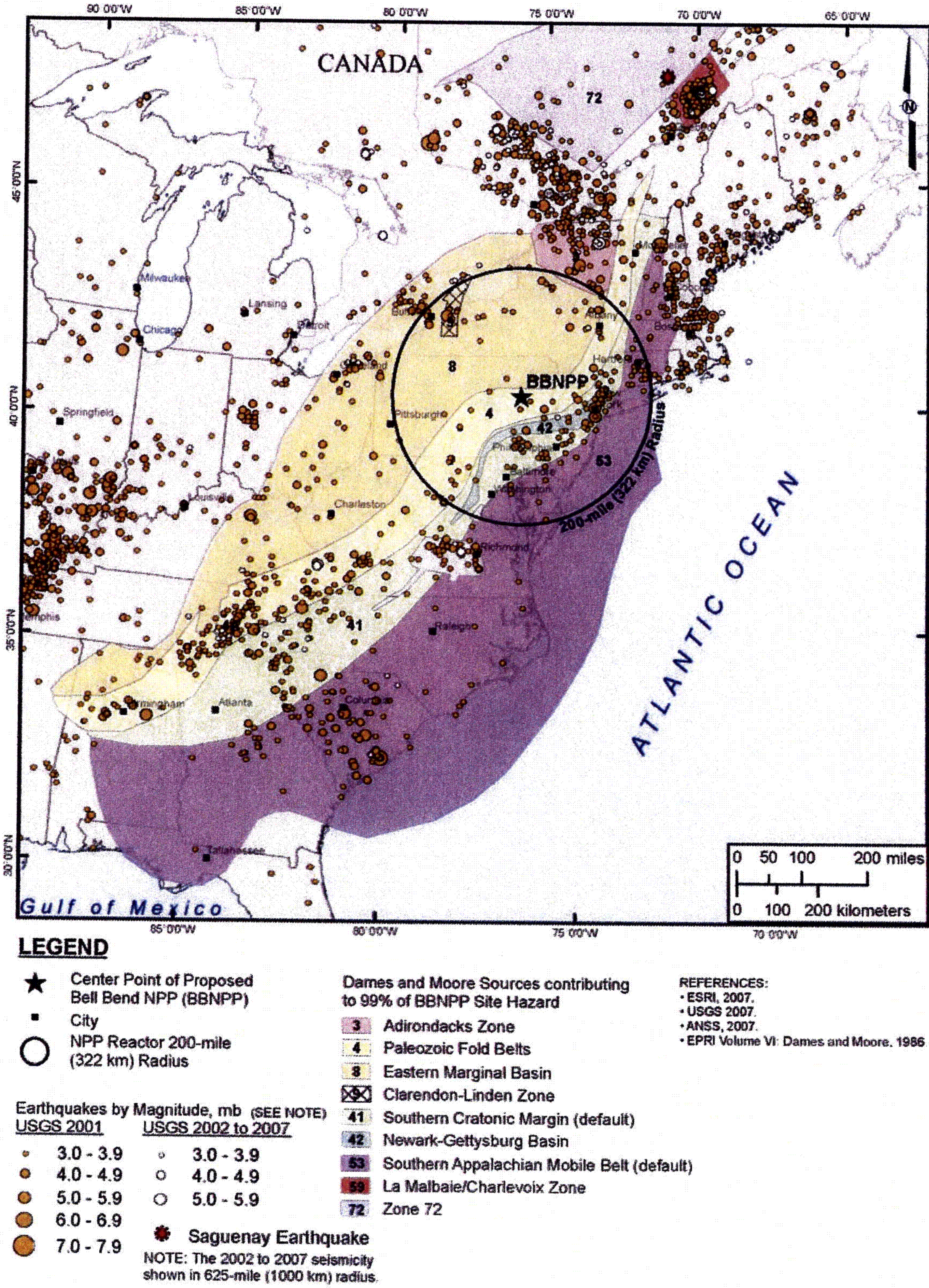

Figure 2.5-86q

Dames and Moore EPRI Source Zones for Charlevoix Sensitivity Analysis Case 2

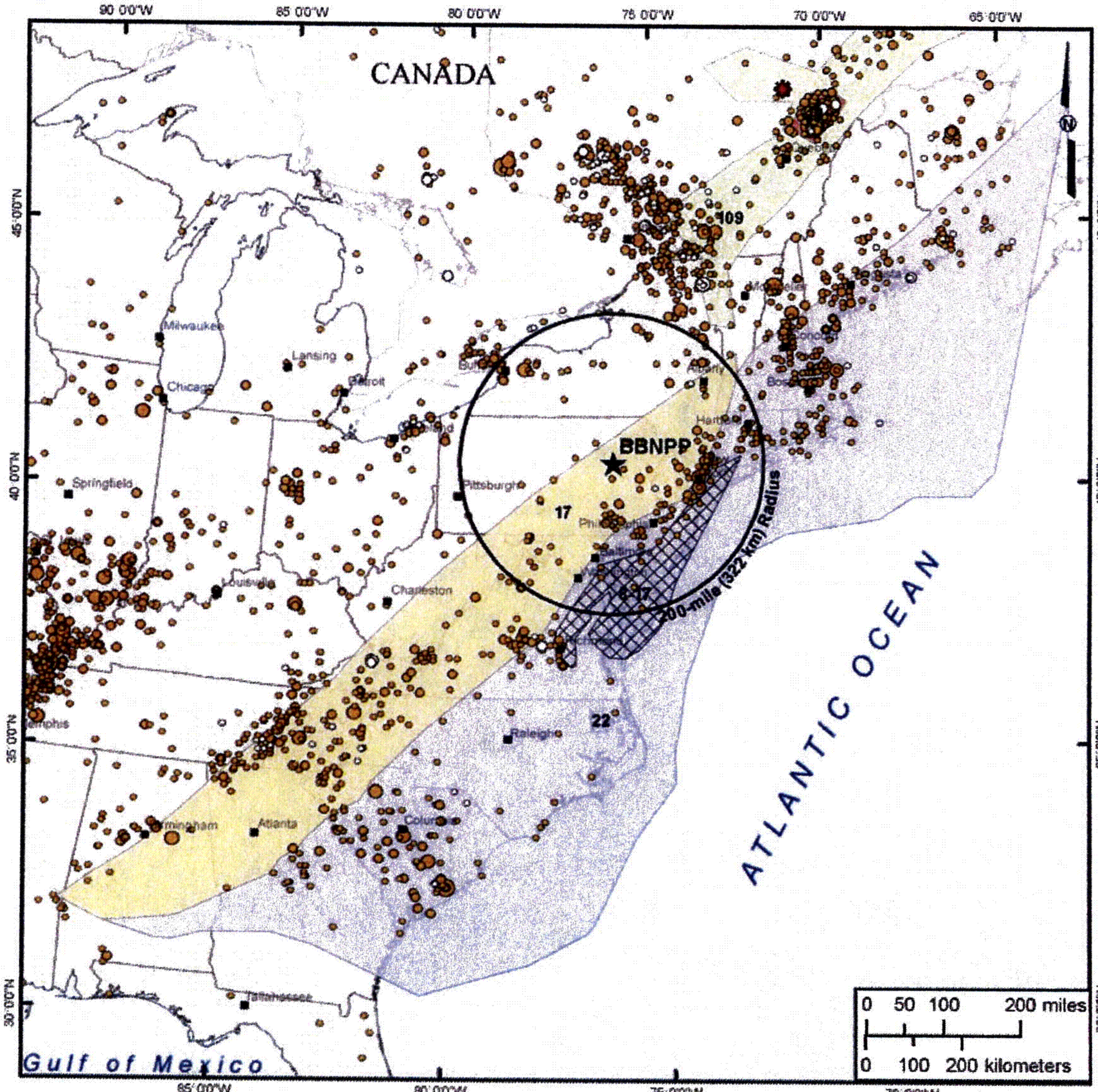

LEGEND

- ★ Center Point of Proposed Bell Bend NPP (BBNPP)
- ▪ City
- ○ NPP Reactor 200-mile (322 km) Radius

Earthquakes by Magnitude, mb (SEE NOTE)

USGS 2001	USGS 2002 to 2007
3.0 - 3.9	3.0 - 3.9
4.0 - 4.9	4.0 - 4.9
5.0 - 5.9	5.0 - 5.9
6.0 - 6.9	Saguenay Earthquake
7.0 - 7.9	

NOTE: The 2002 to 2007 seismicity shown in 625-mile (1000 km) radius.

Law Engineering Sources contributing to 99% of BBNPP Site Hazard

- 8-17 Buried East Coast Mesozoic Basins
- 17 Eastern Basements
- 22 Reactivated Eastern Seaboard Normal Faults
- 12 Charlevoix Seismic Zone
- 109 Zone 109

REFERENCES:
- ESRI, 2007.
- USGS 2007.
- ANSS, 2007.
- EPRI Volume VII: Law Engineering, 1986.

Figure 2.5-86r

Law Engineering EPRI Source Zones for Charlevoix Sensitivity Analysis Case 2

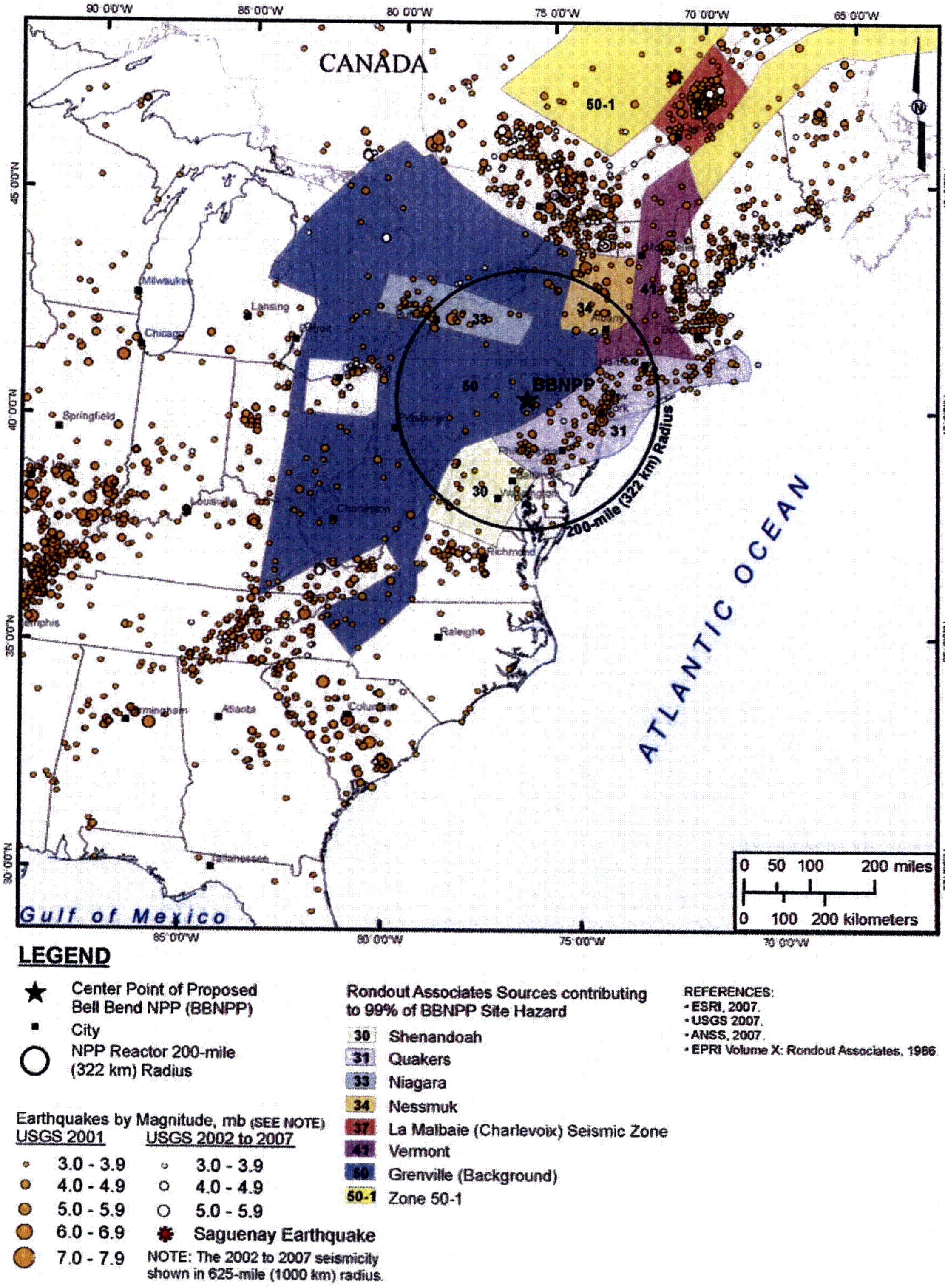

Figure 2.5-86s

Rondout Associates EPRI Source Zones for Charlevoix Sensitivity Analysis Case 2

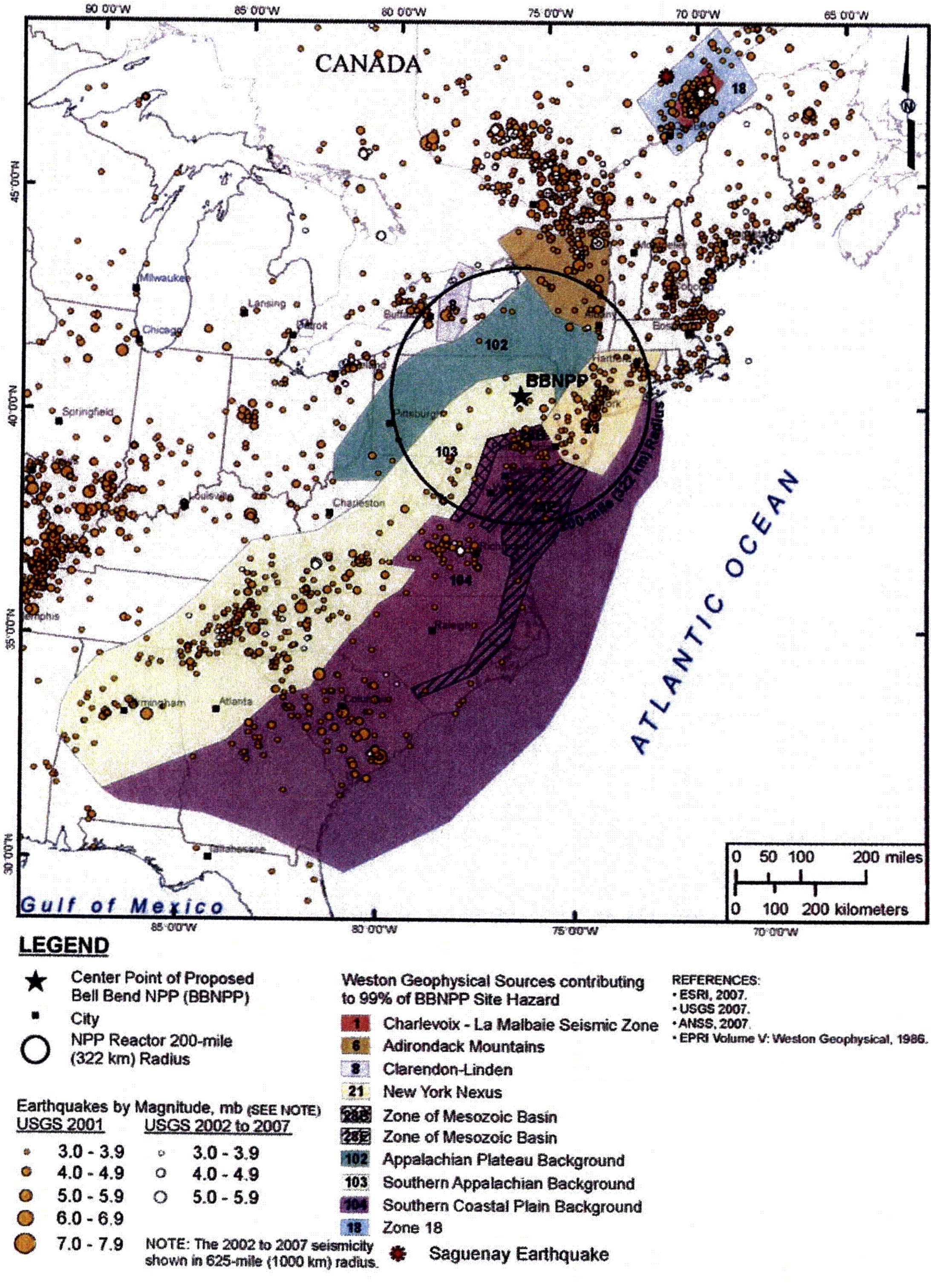

Figure 2.5-86t

Weston Geophysical EPRI Source Zones for Charlevoix Sensitivity Analysis Case 2

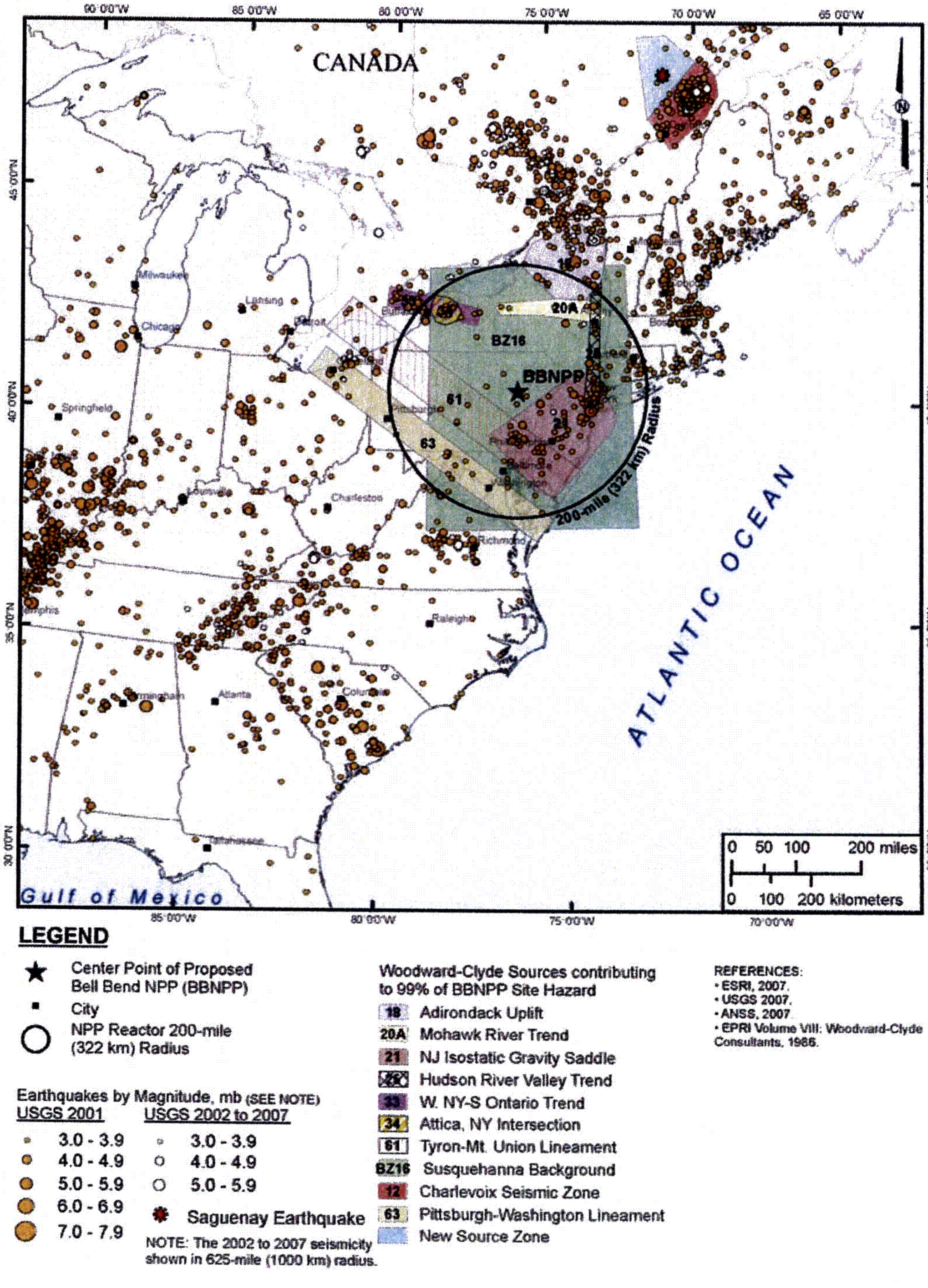

Figure 2.5-86u

Woodward-Clyde EPRI Source Zones for Charlevoix Sensitivity Analysis Case 2

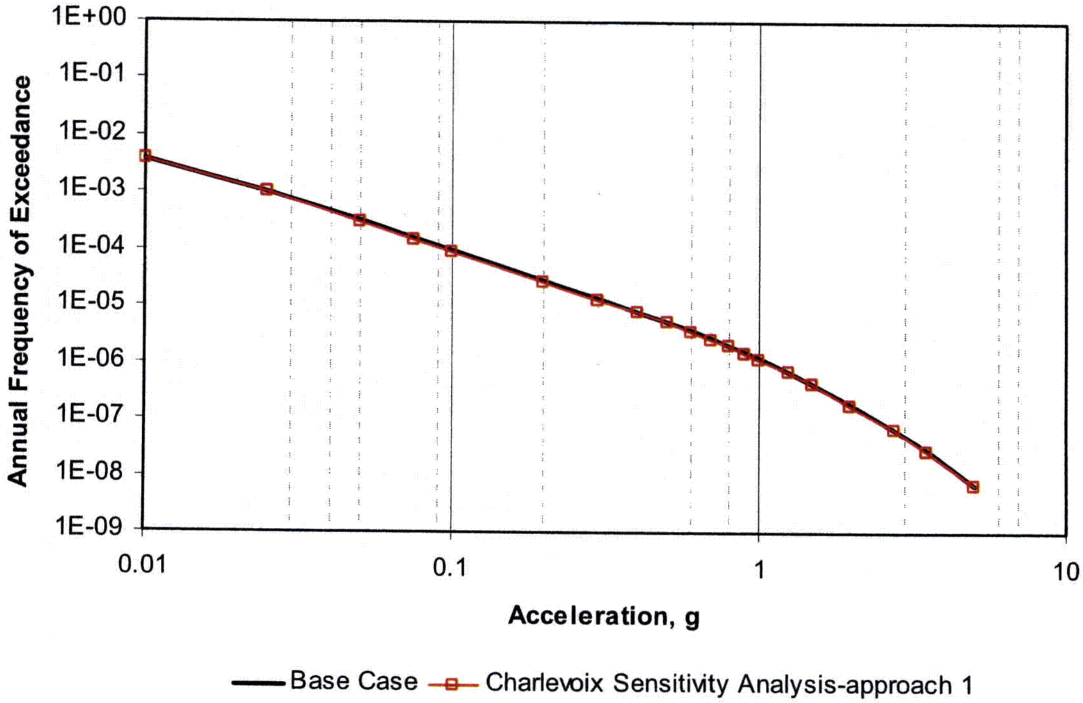

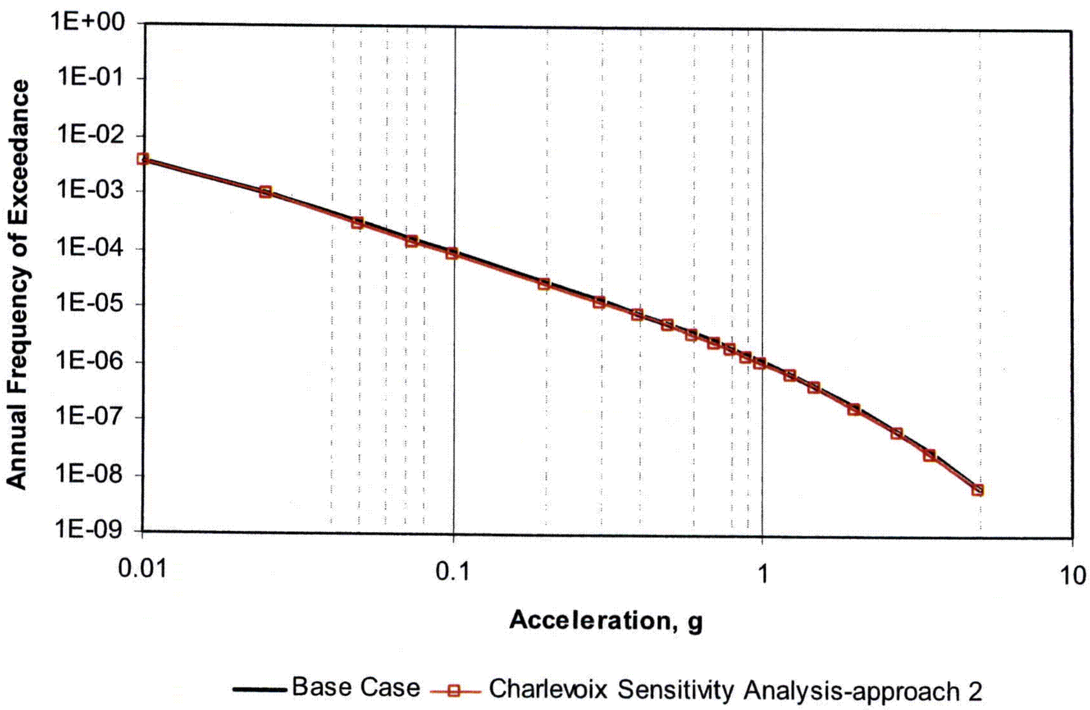

Figure 2.5-86v

Comparison of PGA mean hazard curves for Charlevoix Sensitivity Analysis

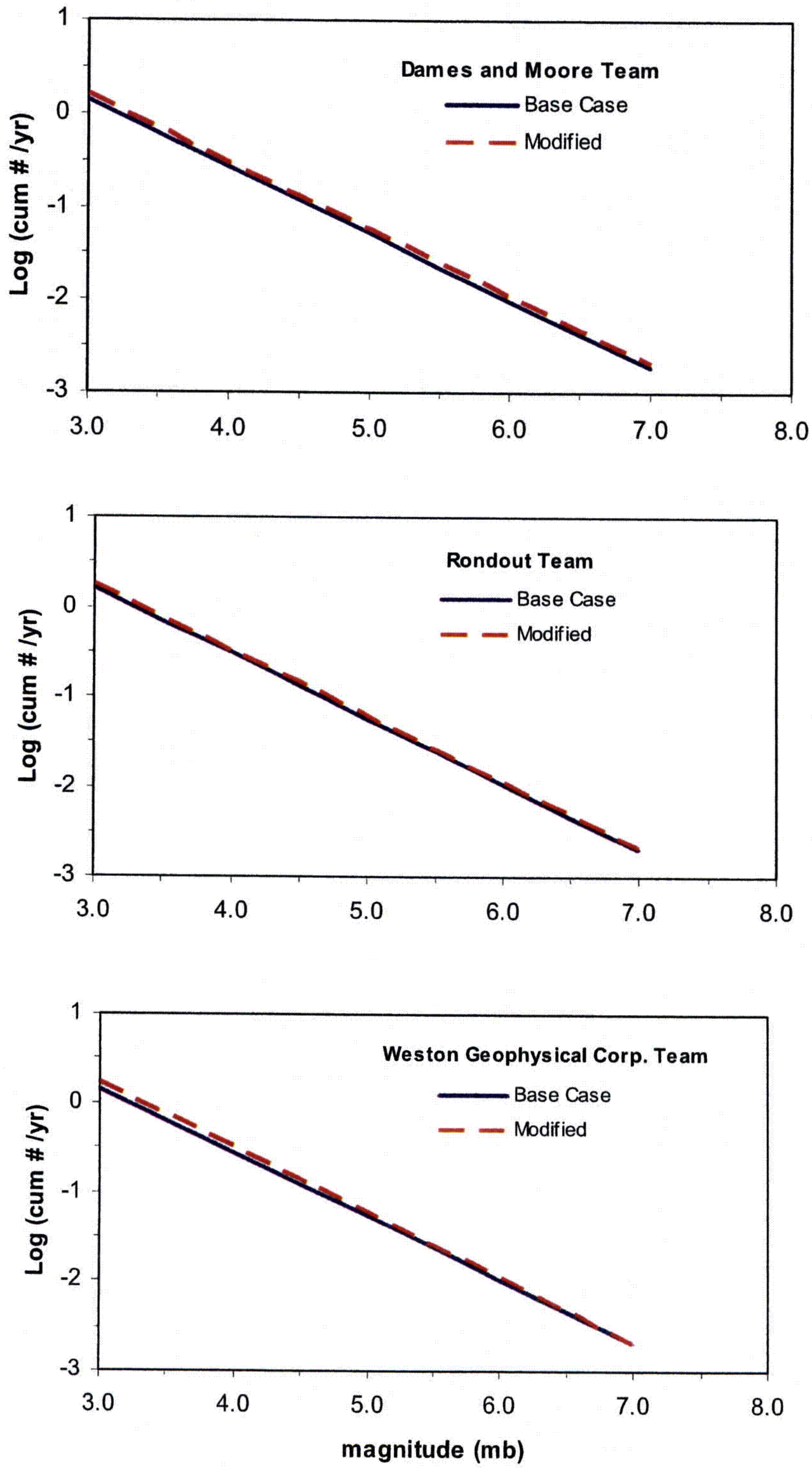

Figure 2.5-86w

Seismicity Rates Charlevoix Sensitivity Analysis

PGA

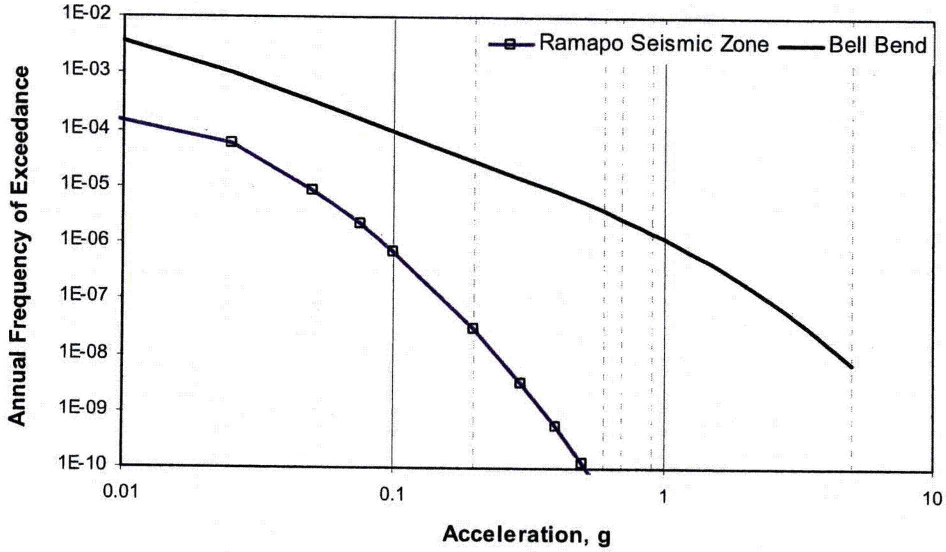

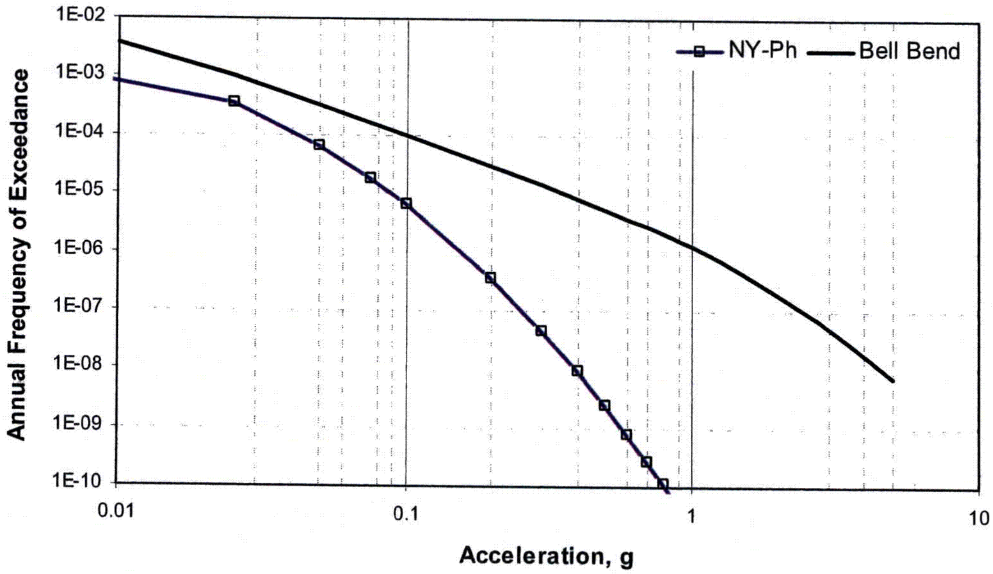

Figure 2.5-86x

Hazard Curves Sensitivity Study of the Ramapo Fault System

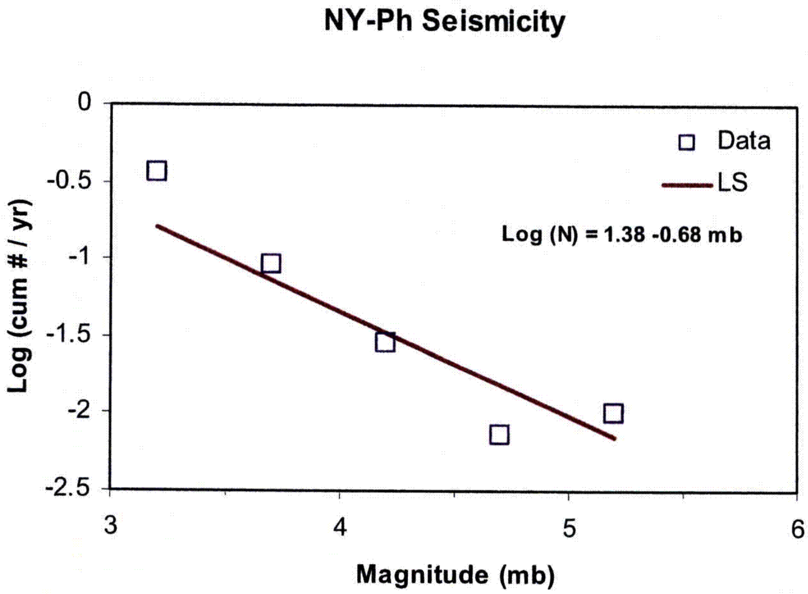

Figure 2.5-86y

Seismicity Rates of the Ramapo Fault System